

Michelle Teixeira de Almeida

Reação inflamatória induzida por duas SVMPS
isoladas do veneno de *Bothrops atrox* e por
fragmentos peptídicos gerados da hidrólise de
componentes da membrana basal por estas enzimas

Tese apresentada ao Programa de Pós-
Graduação em Ciências - Toxinologia do
Instituto Butantan para obtenção do título
de Doutora em Ciências.

São Paulo

2020

Michelle Teixeira de Almeida

Reação inflamatória induzida por duas SVMPS
isoladas do veneno de *Bothrops atrox* e por
fragmentos peptídicos gerados da hidrólise de
componentes da membrana basal por estas enzimas

Tese apresentada ao Programa de Pós-
Graduação em Ciências - Toxinologia do
Instituto Butantan para obtenção do título
de Doutora em Ciências.

Orientadora: Ana Maria Moura da Silva

São Paulo

2020

Dados internacionais de catalogação-na-publicação

Almeida, Michelle Teixeira de

Reação inflamatória induzida por duas SVMPs isoladas do veneno de *Bothrops atrox* e por fragmentos peptídicos gerados da hidrólise de componentes da membrana basal por estas enzimas / Michelle Teixeira de Almeida ; orientadora Ana Maria Moura da Silva. – São Paulo, 2020.

81 f. : il. color.

Tese (doutorado) – Instituto Butantan, Programa de Pós-Graduação em Ciências - Toxinologia. Linha de pesquisa: Toxinas e sistemas biológicos

1. Atividades biológicas. 2. Inflamação. 3. Venenos de Serpentes. 4. Peptídeos. 5. Membrana basal. 6. Toxinas e sistemas biológicos. I. Moura-da-Silva, Ana Maria. II. Instituto Butantan. III. Programa de Pós-Graduação em Ciências - Toxinologia. IV. Título.

Ficha catalográfica elaborada pela Biblioteca do Instituto Butantan

AUTORIZAÇÃO PARA REPRODUÇÃO DO TRABALHO

Eu, Michelle Teixeira de Almeida, aluna de doutorado do Programa de Pós-Graduação em Ciências - Toxinologia do Instituto Butantan, autorizo a divulgação de minha tese por mídia impressa, eletrônica ou qualquer outra, assim como a reprodução total desta tese após publicação, para fins acadêmicos desde que citada a fonte.

Prazo de liberação da divulgação da tese após a data da defesa:

- Imediato
 06 meses
 12 meses
 Não autorizo a divulgação

Justifique:

São Paulo, 29 de Junho de 2020 .

Michelle T. Almeida

.....
Aluna: Michelle Teixeira de Almeida

Ana Maria Moura da Silva

De acordo:
Orientadora: Ana Maria Moura da Silva

**PÓS-GRADUAÇÃO EM CIÊNCIAS-TOXINOLOGIA
INSTITUTO BUTANTAN**

RESULTADO DA DEFESA DE TESE

DOUTORADO

NOME DA ALUNA: MICHELLE TEIXEIRA DE ALMEIDA

DATA DO EXAME: 31/08/2020

BANCA EXAMINADORA: Profs. Drs.

NOME	Assinatura	Aprovada	Reprovada
Ana Maria Moura da Silva (Presidente)		(X)	()
Fernanda C. Vieira Portaro		(X)	()
Luís Roberto C. Gonçalves		(X)	()
Vanessa Moreira		(X)	()
Daiana da Silva Lopes		(X)	()

DECISÃO FINAL: APROVADO (X)

REPROVADO ()

Comentários da Banca (opcional):

PARECER DE COMISSÕES INSTITUCIONAIS REGULATÓRIAS

ib butantan

*Comissão de Ética no
Uso de Animais*

São Paulo, 16 de maio de 2018
CEUA N 6708040817

Ilmo(a). Sr(a).
Responsável: Ana Maria Moura Da Silva
Área: Imunopatologia

Título da proposta: "Caracterização da ação pró-inflamatória induzida pela SVMP Atoxilisina-Ia e dos produtos derivados de sua degradação sobre componentes da matriz extracelular".

Parecer Consubstanciado da Comissão de Ética no Uso de Animais IB (ID 001155)

A Comissão de Ética no Uso de Animais do Instituto Butantan, no cumprimento das suas atribuições, analisou e **APROVOU** a Emenda (versão de 04/maio/2018) da proposta acima referenciada.

Resumo apresentado pelo pesquisador: "SOLICITAÇÃO DE ADITIVO - CEUAIB Camundongos Isogênicos Linhagem: Balb/C Sexo: Machos Idade: 4 a 6 semanas Quantidade: 582 Venho por meio deste pedido, solicitar a adição no número de animais para a realização do projeto acima, que visa avaliar a atividade pró-inflamatória da toxina Atoxilisina I-a e dos produtos derivados de sua degradação sobre componentes da matriz extracelular. Iniciamos o projeto utilizando o modelo de inflamação em pata com camundongos Swiss. Como previsto no projeto, realizamos os testes de indução de edema. Entretanto, para a realização dos testes de indução de infiltrado inflamatório, este modelo mostrou-se bastante dificultoso ao ser reproduzido, com a obtenção de exsudatos ricos em debris e alta variabilidade em todos os testes realizados. Com o objetivo de melhorarmos os resultados obtidos inicialmente, passamos então a utilizar colagenase para a melhor ressuspensão das células livres dos tecidos, e tampão de lise para a remoção de hemácias. Ainda assim, obtivemos uma altíssima variabilidade entre os animais, o que dificultou a obtenção de resultados significativos após o tratamento estatístico das amostras. Realizamos então, testes preliminares em modelo de inflamação em peritônio, que mostrou-se mais satisfatório, com a obtenção do exsudato livre de debris ou contaminantes. Entretanto, a variabilidade entre os animais continua sendo observada, sugerindo que a utilização de camundongos Swiss não seja a mais adequada para esse tipo de experimento. Um outro fator novo no projeto foi a inclusão em nossos testes da toxina Batroxragina, uma SVMP de classe P-III isolada do veneno de Bothrops atrox, que ainda não foi caracterizada quanto à inflamação e sua análise comparativa com a Atoxilisina I-a, uma SVMP de classe P-I isolada do mesmo veneno, será muito importante para estabelecermos relações entre estrutura/atividade dessas classes de toxinas. Em razão das dificuldades acima descritas, utilizamos um número maior que o previsto na elaboração original do projeto, justificando esta solicitação de aditivo. Soma-se a isso a inclusão da nova toxina nos protocolos. Por este motivo, estamos solicitando a adição de camundongos isogênicos da linhagem Balb/C com o objetivo de concluirmos o projeto utilizando o modelo do peritônio, já padronizado, com as duas toxinas isoladas do veneno de B. atrox, e com níveis reduzidos de variabilidade entre os animais devido a isogenia. "

Comentário da CEUA: "".

Maria Leonor Sarno de Oliveira
Coordenador da Comissão de Ética no Uso de Animais
Instituto Butantan

Nancy Oguiura
Vice-Coordenadora da Comissão de Ética no Uso de Animais
Instituto Butantan

Dedico este trabalho à minha mãe Antonia e ao meu marido Odair, pelo apoio e incentivo durante a trajetória acadêmica. Vocês foram peças fundamentais para a realização deste trabalho.

AGRADECIMENTOS

Agradeço a Deus por me dar forças todos os dias para continuar.

Agradeço à minha orientadora Ana Maria Moura da Silva pela referência como cientista e profissional, por sua contribuição acadêmica e pela oportunidade.

Ao Instituto Butantan pelo suporte e acolhimento desde 2012 quando teve início o meu aprimoramento profissional (PAP) nesta instituição.

Agradeço os professores da pós-graduação pelas aulas e conhecimento passado.

Agradeço a todos da coordenação e secretaria do Programa de Pós-graduação em Ciências – Toxinologia pelo auxílio na condução deste trabalho. Meu agradecimento em especial à Dra. Roxane Piazza, Rosana Coelho e Kimie Simokomaki (que fez muita falta neste último ano de pós-graduação). Agradeço também a Débora pelo suporte nestes últimos meses.

A todos os alunos e pesquisadores do Laboratório de Imunopatologia do Instituto Butantan, especialmente a Dra. Eliana Faquim pelo auxílio no início do projeto.

Meu agradecimento a todos os companheiros de laboratório, em especial a Dra. Luciana Sousa por sua proatividade, altruísmo, e pela força em momentos difíceis. À mestre Valéria Alvarenga pelas conversas, conselhos e amizade durante momentos difíceis na etapa final do doutorado. Ao Dr. José Antonio Portes Júnior pela contribuição especialmente durante o PAP e Mestrado, e às doutoras Monica Colombini e Sarah Gimenes pela contribuição na parte experimental deste projeto.

Agradeço o Laboratório de Fisiopatologia do Instituto Butantan, em especial a Dra. Ida Sigueko Sano Martins pelas orientações como docente de acompanhamento, e pelo auxílio junto ao Dr. Luis Roberto nas técnicas de contagem diferencial de leucócitos.

Agradeço o Laboratório de Toxinologia Aplicada, do Centro de Toxinas, Resposta-Imune e Sinalização Celular (CETICs) do Instituto Butantan, especialmente a Dra. Solange Serrano e Dr. Eduardo Kitano pelas análises de espectrometria de massas.

Agradeço o Dr. Luis Roberto Sardinha do Setor de equipamentos multi-usuários do Instituto Butantan pelo auxílio durante os testes de Citometria de Fluxo.

Agradeço o Laboratório de Farmacologia do Instituto Butantan, em especial a Dra. Cristina Maria Fernandes pela colaboração e conhecimentos passados durante o projeto piloto realizado no início do doutorado.

Agradeço os técnicos e funcionários do laboratório de Imunopatologia: D. Josefa, Cris, Daniele, Bianca e Chiquinho que auxiliaram de forma direta ou indiretamente na realização desse trabalho. Meu agradecimento especial à secretária Cleusa, por seu carinho, atenção e prestatividade. Meu agradecimento também à Cris Caporrino (*in memoriam*) por sua disposição e ajuda no Laboratório de Biologia Molecular durante minha formação, pelas risadas, histórias sobre seus gatos, e companhia nas manifestações. Agora o outro plano partilha da sua inteligência, alegria e brilho! Saudades mulher!

Aos membros da banca de qualificação: Dra. Nancy Starobinas, Dra. Renata Giorgi e Dr. Luis Roberto por terem aceito o convite, e pelas sugestões propostas para a finalização e publicação do trabalho.

Ao Comitê de Ética do Instituto Butantan pela concessão no uso de animais durante a vigência do projeto.

Minha gratidão e respeito a todos os animais utilizados nos ensaios biológicos deste trabalho.

Agradeço ao Laboratório de Herpetologia do Instituto Butantan por conceder o veneno de *Bothrops atrox*.

À todos da família Almeida, especialmente minha mãe Antonia e meu marido Odair pelo amor, amizade e apoio em todas as minhas escolhas. Obrigada por acreditar em mim e por não me deixar esmorecer. Meu agradecimento ao Ozzy, filho de quatro patas, que me mostra todos os dias que a vida pode ser mais leve e descomplicada. Amo muito vocês e sou muito grata por tê-los em minha vida!

Agradeço a Coordenação de Aperfeiçoamento de Pessoal de Nível Superior (CAPES) pelo apoio financeiro concedido durante todo o período de doutorado (processo nº 88887.163372/2018-00).

“Toda a nossa ciência, comparada com a realidade, é primitiva e infantil e, no entanto, é a coisa mais preciosa que temos”.

Albert Einstein

RESUMO

ALMEIDA, Michelle Teixeira. **Reação inflamatória induzida por duas SVMPs isoladas do veneno de *Bothrops atrox* e por fragmentos peptídicos gerados da hidrólise de componentes da membrana basal por estas enzimas.** 2020. 81 f. Tese (Doutorado em Ciências - Toxinologia) – Instituto Butantan, São Paulo, 2020.

Metaloproteases do veneno de serpentes (SVMPs) são toxinas chave nos efeitos locais e sistêmicos observados em vítimas de acidentes ofídicos. Os mecanismos envolvidos na ação das SVMPs estão relacionados à hidrólise dos componentes da membrana basal (MB) dos vasos sanguíneos, bem como à sua ação direta sobre plaquetas, receptores de células endoteliais e inflamatórias, e fatores de coagulação. Algumas evidências sugerem que fatores endógenos derivados da hidrólise de MB aumentam os efeitos locais induzidos pelas SVMPs e, conseqüentemente, a gravidade dos acidentes ofídicos. Neste trabalho avaliamos o papel de duas SVMPs de classe P-I e P-III nomeadas Atroxlisina-Ia (ATXL) e Batroxragina (BATXH), respectivamente, isoladas do veneno de *Bothrops atrox*, e seus produtos de hidrólise sobre o Matrigel em modelos experimentais de inflamação. As duas toxinas induziram reação inflamatória em modelos murinos. O edema formado nas patas de camundongos após a injeção de diferentes doses das SVMPs não indicou diferença estatística entre as doses testadas nem entre as toxinas. As lesões foram semelhantes apesar da ATXL possuir massa molecular menor que BATXH. Nos testes de cinética do edema e acúmulo de leucócitos peritoneais foi utilizada a dose de 2 µg/animal. Ambas as toxinas induziram a formação de um pico de edema entre 30 min e 1 h, com aumento de 70% no tamanho das patas. ATXL e BATXH induziram aumento do influxo leucocitário a partir de 4 h após injeção intraperitoneal. Para a avaliação de possíveis mediadores inflamatórios envolvidos nestas reações, estimulamos Células Aderentes Peritoneais Murinas (MPACs) com 40 µg/mL das SVMPs ou veneno de *B. atrox* em diferentes períodos de tempo. A citocina TNF-α foi identificada no sobrenadante de células estimuladas com BATXH ou com veneno de *B. atrox*. O veneno atingiu um pico entre 2 h e 6 h com níveis de 800 pg/mL, e BATXH induziu secreção de 200 pg/mL em 4 h. O mesmo não foi observado com ATXL. Para testar a hipótese de que os peptídeos resultantes da hidrólise de MB pelas SVMPs poderiam participar do processo inflamatório, Matrigel foi incubado com as toxinas

durante 1 h a 37 °C, e os produtos de hidrólise foram identificados por LC-MS/MS. Paralelamente, peptídeos resultantes desta incubação foram isolados em filtros centrífugos com corte de 10 kDa. A reação gerou diferentes fragmentos, principalmente peptídeos da Laminina. Peptídeos isolados por filtração induziram a formação de edema com aumento no tamanho das patas de 30%, e promoveram o acúmulo leucocitário na cavidade peritoneal ($4-5 \times 10^6$ células/mL). Assim, os resultados sugerem que ATXL e BATXH, juntamente com peptídeos resultantes da hidrólise do Matrigel por essas proteases desempenham um papel importante na reação inflamatória observada no envenenamento por *B. atrox*. Geralmente, o envenenamento causa lesões locais irreversíveis, mesmo após a administração do antiveneneno. Neste contexto, apresentamos testes com dois inibidores derivados do pró-domínio da Jararagina que foram capazes de neutralizar a atividade catalítica, fibrinolítica e hemorrágica induzidas pela SVMP, indicando um possível tratamento complementar com soro antiofídico.

Palavras-chave: Atividades biológicas. Inflamação. Venenos de Serpentes. Membrana basal. Peptídeos.

ABSTRACT

ALMEIDA, Michelle Teixeira. **Inflammatory reaction induced by two metalloproteinases isolated from *Bothrops atrox* venom and by fragments generated from the hydrolysis of basement membrane components**. 2020. 81 p. Doctoral dissertation (Doctorate degree in Sciences - Toxinology) – Instituto Butantan, São Paulo, 2020.

Snake venom metalloproteases (SVMPs) are key toxins in local and systemic effects observed in victims of snakebites. The mechanisms involved in SVMPs action are related to the hydrolysis of blood vessels basement membrane components (BM), well as their direct action on platelets, endothelial and inflammatory cell receptors, and coagulation factors. Some evidence suggests that endogenous factors derived from BM hydrolysis increase the local effects induced by SVMPs and, consequently, the severity of snakebites. In this study we evaluated the role of two SVMPs of class P-I and P-III named Atroxlysin-Ia (ATXL) and Batroxrhagin (BATXH), respectively, isolated from the *Bothrops atrox* venom, and its hydrolysis products on Matrigel in experimental models of inflammation. Both toxins induced inflammatory reactions in mice models. The edema formed in the mice paws after the injection of different doses of SVMPs did not indicate a statistical difference between the tested doses or between the toxins. The lesions were similar despite the ATXL having a lower molecular mass than BATXH. In the kinetics tests of edema and accumulation of peritoneal leukocytes, a dose of 2 µg / animal was used. Both toxins induced the formation of an edema peak between 30 min and 1 h, with a 70% increase in the size of the paws. ATXL and BATXH induced an increase in leukocyte influx 4 h after intraperitoneal injection. For the evaluation of possible inflammatory mediators involved in these reactions, we stimulated Murine Peritoneal Adherent Cells (MPACs) with 40 µg / mL of the SVMPs or *B. atrox* venom in different time's period. The cytokine TNF-α was identified in the supernatant of cells stimulated with BATXH or with *B. atrox*. The venom peaked between 2 h and 6 h with levels of 800 pg/mL, and BATXH induces secretion of 200 pg/mL in 4 h. The same was not observed with ATXL. To test the hypothesis that peptides resulting from MB hydrolysis by SVMPs could participate in the inflammatory process, Matrigel was incubated with the toxins for 1 h at 37 ° C, and the hydrolysis products were identified by LC-MS/MS. In parallel, peptides resulting from this incubation were isolated on centrifugal filters with a 10 kDa cut off. The reaction

generated different fragments, mainly Laminin peptides. Isolated peptides in the filters induced the formation of edema with a 30% increase in the size of the paws and promoted leukocyte accumulation in the peritoneal cavity ($4-5 \times 10^6$ cells/mL). Thus, the results suggest that ATXL and BATXH, together with peptides resulting from Matrigel's hydrolysis, play an important role in inflammatory reaction observed in envenoming by *B. atrox*. Generally, envenoming causes irreversible local injuries, even after the administration of antivenom. In this context, we present tests with two inhibitors derived from the Jararhagin pro-domain that were able to neutralize the catalytic, fibrinolytic and hemorrhagic activity induced by SVMP, indicating a possible complementary treatment with antivenom serum.

Keywords: Biological activities. Inflammation. Snake venoms. Basal membrane. Peptides.

SUMÁRIO

1 INTRODUÇÃO GERAL	17
1.1 Epidemiologia dos acidentes ofídicos e espécies de interesse médico.....	17
1.2 Aspectos clínicos dos envenenamentos por serpentes do gênero <i>Bothrops</i> e Tratamento.....	18
1.3 Composição do veneno de <i>Bothrops atrox</i>	21
1.4 SVMPs.....	23
1.5 Mecanismos de ação.....	24
1.6 Atroxlisina e Batroxragina.....	25
1.7 Justificativa e Objetivos.....	26
1.8 Descrição dos artigos publicados.....	28
2 DISCUSSÃO	29
3 CONCLUSÕES	33
REFERÊNCIAS	34
APÊNDICE A - Inflammatory reaction induced by two metalloproteinases isolated from <i>Bothrops atrox</i> venom and by fragments generated from the hydrolysis of basement membrane components.....	41
APÊNDICE B - Processing of Snake Venom Metalloproteinases: generation of toxin diversity and enzyme inactivation.....	61
ANEXOS	77

1 INTRODUÇÃO GERAL

1.1 Epidemiologia dos acidentes ofídicos e espécies de interesse médico

De acordo com a Organização Mundial da Saúde (OMS) em todo o mundo são registrados anualmente entre 1,2 e 5,5 milhões de acidentes ofídicos, onde a mortalidade chega a atingir de 81.000 a 138.000 pessoas (WILLIAMS *et al.*, 2019) alcançando um índice de sobrevivência de cerca de 400.000 pessoas que apresentam sequelas permanentes, sejam elas físicas ou psicológicas (GUTIÉRREZ *et al.*, 2015; WILLIAMS *et al.*, 2019). Destes, os indivíduos com faixa etária entre 10 e 45 anos são os que apresentam a maior taxa de morbidade e mortalidade neste tipo de acidente (HARRISON; GUTIÉRREZ, 2016; CHIPPAUX, 2017).

A maioria dos casos descritos ocorre em países subdesenvolvidos e politicamente marginalizados do continente africano, asiático, americano (América Latina), e em algumas regiões da Oceania (GUTIÉRREZ *et al.*, 2015; WILLIAMS *et al.*, 2019), geralmente em regiões remotas e providas de pouca ou nenhuma infraestrutura, o que leva os acidentados a percorrerem grandes distâncias para serem atendidos em unidades de saúde muitas vezes deficientes de profissionais e de materiais importantes para um tratamento efetivo, o que resulta muitas vezes na busca por tratamentos alternativos baseados na cultura popular (HARRISON; GUTIÉRREZ, 2016).

No Brasil, serpentes da família Viperidae e Elapidae são as principais causadoras de acidentes ofídicos, os quais estão classificados em ordem decrescente em relação aos casos notificados (MINISTÉRIO DA SAÚDE, 2017): entre os anos de 2003 a 2012 foram notificados 86,6% de acidentes causados pelo gênero *Bothrops*, com o gênero *Crotalus* logo em seguida totalizando 8,9% dos acidentes, e por fim, os gêneros *Lachesis* e *Micrurus* com 3,5% e 0,8% de envenenamentos, respectivamente. Ainda com relação ao mesmo período, foi observado que estes acidentes ocorreram em grande parte nos biomas de Mata Atlântica e Amazônia (MATOS; IGNOTTI, 2020).

O gênero *Bothrops* é o responsável pelo maior número de acidentes, que ocorrem principalmente devido a sua ampla distribuição geográfica, tal como *B. atrox* na região Norte, *B. erythromelas* no Nordeste, *B. moojeni* nas regiões Centro-Oeste e Sudeste

e *B. jararaca* nas regiões Sul, Sudeste e Centro-Oeste (CARDOSO; YAMAGUCHI; MOURA-DA-SILVA *et al.*, 2009).

De acordo com a última atualização do Ministério da Saúde, no ano de 2019 foram notificados 20.897 acidentes causados por esse gênero no país, dos quais 8.465 ocorreram na região Norte do Brasil (SINAN, 2020). Estes acidentes acometem principalmente indivíduos jovens, do sexo masculino, trabalhadores ou moradores de regiões rurais (CHIPPAUX, 2017).

A espécie *Bothrops atrox* tem ampla distribuição, podendo ser encontrada em vários países da América do Sul como Colômbia, Venezuela, Bolívia, Peru, e na região amazônica do Brasil, onde essa espécie é responsável pela maior parte dos acidentes ofídicos registrados (WALDEZ; VOGT, 2009; MONTEIRO, *et al.*, 2020). Dados indicam que os hábitos alimentares generalistas dessa espécie tenham relação com a sua ampla distribuição e adaptação a diferentes habitats (SOUSA *et al.*, 2017).

1.2 Aspectos clínicos dos envenenamentos por serpentes do gênero *Bothrops* e Tratamento

O quadro clínico dos envenenamentos por serpentes do gênero *Bothrops* são caracterizados por manifestações locais e sistêmicas. Estas manifestações são desencadeadas pela ação proteolítica, coagulante e hemorrágica dos venenos botrópicos (ALBUQUERQUE *et al.*, 2013).

O acidente ofídico pode ser classificado como leve, moderado ou grave. Para classificar o envenenamento como grave são observadas as manifestações locais, sistêmicas, e tempo de coagulação (ALBUQUERQUE *et al.*, 2013).

Os efeitos locais frequentemente incluem dor, edema, sangramento no local da picada, equimose, necrose e ampla reação inflamatória (TEIXEIRA *et al.*, 2005; MALAQUE; GUTIÉRREZ, 2015; MONTEIRO *et al.*, 2020). Estes efeitos são correlacionados com a ação de proteases, hialuronidases, fosfolipases e mediadores inflamatórios (ALBUQUERQUE *et al.*, 2013). Em alguns casos, infecções secundárias causadas por bactérias presentes na saliva das serpentes podem evoluir para a formação de abscessos, assim como a utilização de torniquetes ou tratamentos

alternativos baseados na cultura popular podem evoluir para casos mais graves de necrose, podendo comprometer o membro afetado (MONTEIRO *et al.*, 2020).

Os efeitos sistêmicos mais comuns como a hemorragia, incoagulabilidade do sangue, gengivorragia e hematúria, estão associados a distúrbios de coagulação causados pela ativação do fator X e o consumo de fatores da coagulação (ALBUQUERQUE *et al.*, 2013). O consumo de fatores da coagulação e sangramentos podem ou não estar associados a alterações hemodinâmicas e danos locais (ESCALANTE *et al.*, 2011; RUCAVADO *et al.*, 2008).

A insuficiência renal aguda é a principal causa de óbito entre os acidentados (ALBUQUERQUE *et al.*, 2013). Ribeiro; Gádia; Jorge (2008) analisaram prontuários de pacientes maiores de vinte anos atendidos no Hospital Vital Brazil do Instituto Butantan, no período entre 1981 a 1992, e observaram que a possibilidade dos idosos apresentarem necrose ou das manifestações clínicas evoluírem para insuficiência renal aguda e óbito, foi maior que a dos pacientes jovens que receberam a mesma dose de soro antiofídico.

Outra pesquisa realizada anos mais tarde também no Hospital Vital Brazil do Instituto Butantan, analisou todos os casos de picadas, inclusive as denominadas “picadas secas” causadas por *Bothrops jararaca* no período entre 1990 a 2004. Os dados foram coletados através de prontuários médicos. Neste estudo, foi identificada a ocorrência dos efeitos locais nas primeiras seis horas após a picada, e o aparecimento dos efeitos sistêmicos após esse período de tempo, indicando que quanto maior o tempo entre a picada e o tratamento, maiores são as possibilidades do paciente apresentar reações mais graves. Outro dado interessante foi que em acidentes causados por serpentes adultas, a necrose foi mais frequente quando comparado aos envenenamentos causados por filhotes (NICOLETI *et al.*, 2013).

De acordo com Silva de Oliveira *et al.* (2019), os efeitos sistêmicos mais comuns observados em pacientes tratados no hospital da Fundação de Medicina Tropical Dr. Heitor Vieira Dourado, no estado do Amazonas, entre Jan/2016 a Dez/2017 foram a incoagulabilidade sanguínea, hemorragias sistêmicas e trombocitopenia, seguidos por gengivorragia, hematúria e equimose.

A gravidade dos sintomas vai depender da idade do paciente, local da picada, quantidade de veneno inoculado, presença de comorbidades pré-existentes, e do tempo entre o acidente e a administração do antiveneno (OLIVEIRA *et al.*, 2010).

A soroterapia é a forma mais eficaz de tratamento dos sintomas induzidos pelo envenenamento botrópico (MONTEIRO *et al.*, 2020).

Serpentes da espécie *Bothrops atrox* possuem grande importância na região amazônica. Entretanto, o veneno dessa serpente não faz parte do pool usado na produção do soro comercial que é produzido no Brasil (FURTADO *et al.*, 2010).

O Soro Antibotrópico (SAB) comercial é preparado a partir do soro hiperimune de cavalos, imunizados com um pool contendo 50 % de veneno de *Bothrops jararaca* e o restante com um mesmo percentual (12,5 %) dos venenos de *Bothrops alternatus*, *Bothrops jararacussu*, *Bothrops moojeni* e *Bothrops neuwiedi* (CARDOSO; YAMAGUCHI; MOURA-DA-SILVA *et al.*, 2009).

No Brasil, os principais centros de produção do antiveneno são o Instituto Butantan (IB), Instituto Vital Brazil (IVB), a Fundação Ezequiel Dias (FUNED) e o Centro de Pesquisa e Produção de Imunobiológicos (CPPI) (DA GRAÇA SALOMÃO; DE OLIVEIRA LUNA; MACHADO, 2018).

A produção do soro antibotrópico consiste inicialmente na imunização de cavalos com um pool de venenos que induz uma resposta imunológica, resultando na produção de anticorpos presentes no plasma. Depois, o tratamento e purificação deste material pode ocorrer por duas vias: (a) pela precipitação de fragmentos de imunoglobulinas através da adição de ácido caprílico, para a obtenção somente da IgG inteira; (b) o plasma é submetido à digestão enzimática, precipitação por sulfato de amônia e à etapas de cromatografia para a obtenção da porção F(ab')₂ (GUTIÉRREZ *et al.*, 2005; CASTRO *et al.*, 2014).

Testes experimentais demonstraram a eficácia do SAB nas principais atividades tóxicas induzidas pelo veneno. E dentre várias espécies do gênero *Bothrops*, como *Bothrops jararaca*, *neuwiedi* e *atrox*, as SVMPs foram os antígenos de maior reconhecimento dentro da peçonha, indicando uma maior eficácia do SAB em solucionar grande parte dos danos induzidos especialmente pelas SVMPs de classe P-III, que são as mais abundantes no veneno de *B. atrox* e também as que apresentam maior potencial imunogênico com relação às proteínas de classe P-I, que apresentam baixa reatividade ao uso do antiveneno (SOUSA *et al.*, 2013).

O fato das SVMPs P-I e também das PLA₂ serem pouco imunogênicas ao soro, pode esclarecer questões acerca da baixa eficiência do SAB na resolução dos danos teciduais provocados pela ação destas duas toxinas (MONTEIRO *et al.*, 2020), o que não exclui o fato de que quanto menor o tempo entre o acidente e a administração do

soro, maiores são as possibilidades de obter um tratamento mais eficaz (NICOLETI *et al.*, 2013).

Recentemente Moura-da-Silva *et al.*, (2020) correlacionaram os aspectos clínicos do envenenamento por *B. atrox* com a composição do veneno das serpentes responsáveis por cada acidente. A maioria dos pacientes que foram avaliados de janeiro a dezembro de 2017, apresentou edema, dor e sangramento local. Um paciente apresentou bolhas, três apresentaram abscesso e dois indivíduos tiveram necrose. Testes de cromatografia com os venenos obtidos revelou diferentes perfis em cada amostra, permitindo a identificação de variabilidade individual na composição de cada veneno. Nos ensaios de análise proteômica foram identificadas 11 famílias de proteínas mais abundantes em todos os venenos, e, considerando este fato, as SVMPs aparecem como as principais toxinas envolvidas com distúrbios hemorrágicos e edema. Isoformas individuais de SVMP, CTL e SVSP analisadas apresentaram correlação com os distúrbios hemorrágicos, edema, equimose e formação de bolhas, demonstrando que a variabilidade nos componentes do veneno pode exercer influência sobre as manifestações clínicas observadas nas vítimas de envenenamento, assim como na eficácia do tratamento pelo soro antiofídico.

Este fato juntamente com a baixa reatividade de algumas toxinas do veneno ao soro, levanta questões sobre a inclusão da metaloprotease e fosfolipase recombinantes no protocolo de imunização, ou sobre a inclusão de anticorpos monoclonais no tratamento. Outra sugestão levantada seria a utilização de um tratamento complementar à soroterapia, com o uso de compostos peptidomiméticos ou fragmentos gerados no processamento natural das toxinas como inibidores seletivos para as SVMPs ou fosfolipases (MONTEIRO *et al.*, 2020; MOURA-DA-SILVA *et al.*, 2020).

1.3 Composição do veneno de *Bothrops atrox*

O veneno de *B. atrox* é composto por uma mistura de toxinas onde se destacam diferentes isoformas de PLA₂ (*Fosfolipases A₂*), SVSP (*Serino proteases do veneno de serpentes*), CTLs (*Lectinas do tipo C*), e as SVMPs (*Metaloproteases do veneno de serpentes*) (SOUSA *et al.*, 2013).

PLA₂s são enzimas geralmente envolvidas nos danos locais, que induzem miotoxicidade local, hiperalgesia, formação de edema e secreção de citocinas pró-inflamatórias (LOMONTE; ANGULO; CALDERÓN, 2003). As SVSPs são proteases associadas a distúrbios da coagulação, por meio de sua ação sobre os sistemas fibrinolítico, caliceína-cinina e em componentes da cascata da coagulação (SERRANO, 2013). CTLs estão envolvidas em distúrbios da hemostasia, através de sua ação sobre fatores de coagulação e receptores de integrinas (ARLINGHAUS; EBLE, 2012). As SVMPs são proteases capazes de atuar em diferentes vias, causando distúrbios na coagulação, hidrólise de proteínas constituintes da matriz extracelular presente na microvasculatura, morte de células endoteliais por apoptose, e indução de reação inflamatória com a ativação e influxo de leucócitos, atuando diretamente sobre receptores celulares e induzindo resposta das células que secretam mediadores pró-inflamatórios (MOURA-DA-SILVA; BUTERA; TANJONI, 2007).

Entre as toxinas que constituem o veneno de *B. atrox*, se destacam as SVMPs, que constituem mais de 50% do total de proteínas presentes no veneno. No entanto, diferenças de filogenia, idade, sexo e distribuição geográfica podem contribuir sobre a variabilidade na composição dos venenos, alterando o percentual de expressão de cada toxina (SOUSA *et al.*, 2013).

Dados recentes obtidos por análise proteômica do veneno de espécimes de *B. atrox* envolvidas em acidentes na região amazônica, revelaram a presença de 15 isoformas para ATXL e 28 isoformas para BATXH, apresentando diferentes níveis de expressão entre os venenos (MOURA-DA-SILVA *et al.*, 2020).

O percentual de expressão de isoformas de determinadas toxinas pode refletir em alterações funcionais dos venenos, conforme dados obtidos por Moretto Del-Rei *et al.* (2019), que ao utilizar pools de venenos obtidos a partir de serpentes *B. atrox* originárias de três regiões distintas e separadas pelo rio Amazonas, mas nascidas e mantidas sob cativeiro em mesmas condições, observou maior atividade dermonecrotica no veneno das serpentes da região ao norte do rio, em comparação ao veneno obtido das serpentes originárias da região ao sul do rio, que apresentou maior letalidade. Estas diferenças, segundo os autores, podem ocorrer devido a uma expressão maior ou menor de isoformas, como SVMPs de classe P-I ou P-III, que podem variar dependendo da distribuição geográfica e acesso às presas.

1.4 SVMPS

SVMPS fazem parte da família das Metzincinas, que são metaloproteases com atividade catalítica dependente de íons metálicos de zinco. Essas enzimas são compostas essencialmente por um pró-domínio presente na região N-terminal que confere a latência das enzimas, e um domínio catalítico com o motivo ligante de zinco e uma estrutura do tipo “*met-turn*” na região C-terminal (GOMIS-RÜTH, 2009).

Elas são classificadas em três classes: a classe P-I composta pelos domínios pré, pró e metaloproteinase; classe P-II composta pelos domínios da classe P-I mais o domínio desintegrina; e classe P-III composta por pré, pró, metaloproteinase, tipo desintegrina e domínio rico em cisteína (MOURA-DA-SILVA; BUTERA; TANJONI, 2007).

As SVMPS de classe P-I e de classe P-III podem causar hemorragias através da clivagem de proteínas de membrana basal e integrinas envolvidas na ligação celular à matriz extracelular e nos contatos entre as células, afetando a adesão focal que resulta na morte celular por apoptose e consequente enfraquecimento do endotélio. Proteínas das três classes podem interferir na agregação plaquetária, onde o domínio desintegrina das P-II pode inibir a ligação do fibrinogênio ao receptor de integrina $\alpha_2\beta_3$; SVMPS de classe P-I podem hidrolisar o vWF (Fator de Von Willebrand); e as P-III interferir na ativação plaquetária dependente do colágeno e vWF. Além do mais, estas proteases também podem induzir reação inflamatória nos acidentados, atuando no extravasamento leucocitário através de duas vias: digerindo a membrana basal dos vasos como é observado com MMPs (*Metaloproteases de Matriz*) endógenas, ou então, atuando diretamente sobre macrófagos que secretam os mediadores IL-6 (Interleucina-6) e IL-1 β (Interleucina-1 β) que favorecem o extravasamento e o influxo celular. Também podem clivar o pró-TNF- α (pró-Fator- α de necrose tumoral) liberando a sua forma ativa, e podem atuar sobre fibroblastos que como consequência expressam as quimiocinas IL-8 (Interleucina-8) e CXCL-2 (GRO β), ou então ativam o sistema complemento gerando o componente quimiotático C5a (MOURA-DA-SILVA; BUTERA; TANJONI, 2007; MOURA-DA-SILVA *et al.*, 2009).

1.5 Mecanismos de ação

SVMPs são proteases envolvidas nos efeitos locais representados por hemorragia, formação de bolhas, hidrólise de componentes da matriz extracelular, dermonecrose e inflamação (GUTIÉRREZ *et al.*, 2009; MOURA-DA-SILVA; BUTERA; TANJONI, 2007).

Elas atuam sobre a membrana basal de capilares sanguíneos e sobre a matriz extracelular através da hidrólise de seus componentes, tendo como consequência a ocorrência de hemorragia, formação de bolhas e dermonecrose. Também podem induzir a secreção de vários mediadores pró-inflamatórios, e ativar a mobilização de células inflamatórias, associados à formação de edema e na dor (BALDO *et al.*, 2015; GUTIÉRREZ *et al.*, 2009; LOPES *et al.*, 2009; 2012; MOURA-DA-SILVA; BALDO, 2012).

A coagulopatia observada nos envenenamentos é causada pela ação de SVMPs capazes de ativar ou inibir diversos componentes e fatores da coagulação como o fibrinogênio, a protrombina e o fator X (BALDO *et al.*, 2008; HOFMANN; BON, 1987; KAMIGUTI *et al.*, 1994). Além de sua atuação sobre a cascata da coagulação, estas toxinas embora que raramente, também podem atuar como agonistas da agregação plaquetária, ativando metaloproteases plaquetárias endógenas, induzindo a liberação do ectodomínio da GPVI (Glicoproteína VI de membrana plaquetária) (ANDREWS *et al.*, 2001; WIJEYEWICKREMA *et al.*, 2007). As metaloproteases de veneno também podem inibir a agregação plaquetária, através do fator de von Willebrand, do colágeno, ou então, inibindo a função de receptores de integrina presentes na superfície das plaquetas (BALDO *et al.*, 2010; DE QUEIROZ *et al.*, 2017; DELLA-CASA *et al.*, 2011; KAMIGUTI; HAY; ZUZEL, 1996; MOURA-DA-SILVA *et al.*, 2001; SLAGBOOM *et al.*, 2017; TANJONI *et al.*, 2010).

Além dos distúrbios hemostáticos, as SVMPs também são conhecidas por desencadear reações inflamatórias importantes, que podem avançar para a restauração dos tecidos e função, ou então, avançar para o agravamento da inflamação (TEIXEIRA *et al.*, 2019).

Toxinas de classe P-I são capazes de ativar o recrutamento leucocitário (FARSKY; ANTUNES; MELLO, 2005) e o sistema complemento (FARSKY *et al.*, 2000). Também podem ativar a síntese de mediadores inflamatórios como IL-1 β e IL-

6, e aumentar a expressão da metaloprotease endógena MMP-9 (*Metaloprotease de matriz 9*) (RUCAVADO *et al.*, 2002). Também foi demonstrado que esta classe de metaloproteases induz a resposta inflamatória em células MPAC e C2C12, que secretam as citocinas IL-1 β , IL-6 e a quimiocina KC (derivada de queratinócito) após a incubação com a toxina (LOPES *et al.*, 2009).

SVMPs de classe P-III também desempenham um importante papel na reação inflamatória desencadeada pelo veneno, atuando na formação de edema e hiperalgesia, além de agir diretamente sobre células inflamatórias ou seus receptores, induzindo o recrutamento de leucócitos, ativando a fagocitose por macrófagos, a expressão de citocinas IL-1 β , IL-6, TNF- α , assim como as quimiocinas CXCL1 (GRO α), CXCL2, CXCL8 (IL-8), por meio de seu domínio catalítico ou dos domínios tipo disintegrina e rico em cisteína (CLISSA *et al.*, 2001; COSTA *et al.*, 2002; DALE *et al.*, 2004; GALLAGHER *et al.*, 2005; SILVA *et al.*, 2004).

O veneno de *Bothrops atrox* e algumas SVMPs isoladas a partir dele, podem ativar o influxo de células inflamatórias polimorfonucleares e mononucleares para o local da lesão, e induzir a secreção de mediadores pró-inflamatórios como as citocinas TNF- α , IL-1 β , IL-6, a quimiocina MCP-1 (CCL-2), e os eicosanóides PGE₂ (Prostaglandina E₂) e LTB₄ (Leucotrieno B₄) (MENALDO *et al.*, 2017; MOREIRA *et al.*, 2012).

Recentemente, foi demonstrado através de análises proteômicas a presença de fragmentos de Padrões Moleculares Associados a Danos (*DAMPs*) em exsudatos obtidos após a injeção intramuscular do veneno de *B. asper* em camundongos. A presença dos peptídeos foi associada à hidrólise de componentes da matriz extracelular e ao dano celular, indicando a geração de *DAMPs* no envenenamento causado por serpentes e a sua participação nos processos inflamatórios (RUCAVADO *et al.*, 2016).

1.6 Atroxlisina-Ia e Batroxragina

O veneno de *Bothrops atrox* possui em sua composição mais de 50% de metaloproteases (SOUSA *et al.*, 2013). Devido a grande incidência de acidentes ofídicos envolvendo essa serpente na região norte do Brasil, e à alta expressão de

metalo proteases neste veneno, foram isoladas duas SVMPs altamente hemorrágicas nomeadas como Atroxlisina-Ia e Batroxragina (FREITAS-DE-SOUSA *et al.*, 2015; FREITAS-DE-SOUSA *et al.*, 2017). A Atroxlisina-Ia (ATXL) é uma isoforma da toxina de classe P-I Atroxlysin-I, isolada a partir do veneno de serpentes *B. atrox* peruanas (SANCHEZ *et al.*, 2010).

ATXL difere da Atroxlysin-I pela substituição de apenas um aminoácido. Ela foi capaz de induzir uma hemorragia intensa, em níveis comparáveis à SVMP de classe P-III Batroxragina (BATXH), além de apresentar atividade dermonecrótica já nos primeiros 20 minutos após a injeção da toxina (FREITAS-DE-SOUSA *et al.*, 2017).

A Batroxragina é uma SVMP de 52 kDa que apresenta 96% de similaridade com a Jararagina, uma SVMP de mesma classe isolada do veneno de *Bothrops jararaca*. Em ensaios anteriores, esta toxina foi capaz de inibir a agregação plaquetária dependente do colágeno, hidrolisar a fibrina e induzir hemorragia semelhantemente à outras SVMPs de mesma classe (FREITAS-DE-SOUSA *et al.*, 2015).

1.7 Justificativa e Objetivos

Tendo em vista a importância dos eventos pró-inflamatórios causados pelas SVMPs e a ação de alguns peptídeos bioativos gerados pela hidrólise dos componentes da matriz extracelular, neste estudo avaliamos a ação pró-inflamatória induzida pela ATXL e BATXH, bem como pelos produtos derivados da degradação de produtos da membrana basal presentes no Matrigel por essas duas enzimas. Por outro lado, devido a baixa reatividade de algumas toxinas ao SAB e a busca por possíveis tratamentos complementares à soroterapia, destacamos ainda resultados preliminares obtidos por nosso grupo utilizando dois inibidores isolados do pró-domínio da Jararagina, que demonstraram eficácia ao inibir algumas das principais atividades tóxicas induzidas por SVMPs.

Assim, os objetivos específicos do trabalho foram:

- ❖ Caracterização da ação pró-inflamatória da Atroxlisina-Ia e Batroxragina em modelos experimentais de inflamação:

- Avaliação do efeito dose-resposta do edema induzido por diferentes doses das toxinas injetadas via intraplantar em camundongos BALB/c;
- Cinética em diferentes períodos de tempo do edema induzido por uma única dose das duas toxinas;
- Avaliação do efeito dose-resposta do recrutamento leucocitário induzido por diferentes doses das toxinas administradas via intraperitoneal em camundongos BALB/c;
- Cinética em diferentes períodos de tempo do recrutamento leucocitário induzido por uma única dose das duas toxinas;
- Identificação de mediadores inflamatórios gerados em cultura de células MPAC tratadas com as SVMPs e o veneno de *B. atrox*:
 - Tratamento de células MPAC com as SVMPs e veneno em diferentes períodos de tempo;
 - Avaliação de secreção das citocinas TNF- α , IL-6, IL-10 e quimiocina MCP-1 por Citometria de Fluxo, utilizando os sobrenadantes das MPACs estimuladas.
- ❖ Caracterização da ação pró-inflamatória induzida por peptídeos gerados após a hidrólise de proteínas da membrana basal presentes no Matrigel, pelas SVMPs Atroxlisina-Ia e Batroxragina:
 - Análise bioquímica dos produtos de hidrólise em diferentes períodos de tempo:
 - Eletroforese em gel gradiente;
 - Espectrometria de massas (LC-MS-MS);
 - Cinética de diferentes períodos de tempos do edema induzido pelos produtos de hidrólise injetados via intraplantar camundongos BALB/c;
 - Cinética de diferentes períodos de tempo do recrutamento leucocitário induzido pelos produtos de hidrólise injetados via intraperitoneal em camundongos BALB/c.
- ❖ Avaliação a atividade inibitória do pró-domínio recombinante (PD-Jar) e do peptídeo sintético SynPep em ensaios de atividade enzimática e atividades fibrinolítica e hemorrágica induzidas pela Jararagina.

1.8 Descrição dos artigos publicados

Estão descritos no apêndice A os resultados obtidos no trabalho que foi desenvolvido durante o período de doutorado, e publicado no último ano do mesmo na revista *Toxins*, sendo intitulado “Inflammatory reaction induced by two metalloproteinases isolated from *Bothrops atrox* venom and by fragments generated from the hydrolysis of basement membrane components” (ALMEIDA *et al.*, 2020).

O segundo artigo, descrito no apêndice B e intitulado “Processing of Snake Venom Metalloproteinases: Generation of Toxin Diversity and Enzyme Inactivation”, (MOURA-DA-SILVA *et al.*, 2016) trata-se de uma revisão da literatura, o qual foram apresentados resultados obtidos no período de mestrado sobre a inibição pelo pró-domínio recombinante da Jararagina e pelo peptídeo sintético derivado do pró-domínio da Jararagina (SynPep), nas atividades enzimática, fibrinolítica e hemorrágica, induzidas pela SVMP Jararagina (P-III). Este artigo foi escrito por nosso grupo em colaboração com pesquisadores do Instituto Oswaldo Cruz, no Rio de Janeiro.

2 DISCUSSÃO

SVMPs (*Snake Venom Metalloproteinases*) são proteases compostas por um ou mais domínios de acordo com a sua classificação, e que participam ativamente dos sintomas locais e sistêmicos observados nas vítimas de acidentes ofídicos (MOURA-DASILVA; BUTERA; TANJONI, 2007).

Este grupo de enzimas faz parte da família das Metzincinas juntamente com as MMPs (*Matrix Metalloproteinases*) e ADAMs (*A Disintegrin and Metalloproteinases*) sendo esta família composta por endopeptidases dependentes do zinco, um metal necessário para que as proteases possam exercer sua função catalítica sobre substratos específicos (GOMIS-RÜTH, 2009; GRAMS *et al.*, 1993; RAWLINGS *et al.*, 2014).

No Brasil, mais especificamente na região amazônica, há um alto índice de acidentes associados às serpentes *Bothrops atrox*. O veneno dessa espécie é composto principalmente por SVMPs, e os sintomas observados nas vítimas de envenenamento são semelhantes aos sintomas desencadeados pelo veneno de outras serpentes do mesmo gênero (CAMPOS BORGES; SADAHIRO; DOS SANTOS, 1999; SOUSA *et al.*, 2013).

Sabe-se que a dificuldade de acesso a uma unidade de saúde, imposta pela pouca infraestrutura e grandes distâncias enfrentadas pela vítima do acidente, além da falta ou da ineficácia do antiveneno, que por vezes não foi armazenado adequadamente, são importantes agravantes das lesões locais, que normalmente são caracterizadas por hemorragia e uma ampla reação inflamatória no local da picada (HARRISON; GUTIÉRREZ, 2016; KASTURIRATNE *et al.*, 2008; TEIXEIRA *et al.*, 2005).

Assim, devido a importante reação inflamatória observada nos pacientes vítimas desse tipo de envenenamento, e na ineficácia de tratamento rápido e adequado às lesões locais, dados pelas dificuldades listadas acima, se faz necessária a busca por mais informações a respeito desses eventos, resultando posteriormente em possíveis tratamentos. Desta forma, o nosso trabalho teve como objetivo caracterizar a participação de duas SVMPs isoladas do veneno de *B. atrox* (FREITAS-DE-SOUSA *et al.*, 2015) em modelos experimentais de inflamação.

Na literatura há diversos trabalhos apontando a participação de metaloproteases do veneno em eventos inflamatórios, os quais foram observadas a formação de edema, infiltrado leucocitário, presença de aminas vasoativas pela degranulação de mastócitos ativados pelas toxinas, secreção de mediadores inflamatórios como citocinas e quimiocinas IL-6, TNF- α , CCL-2 e também, de prostaglandinas como PGE₂ e LTB₄, além da ativação do sistema complemento (CLISSA *et al.*, 2001; DE TONI *et al.*, 2015; FARSKY *et al.*, 2000; GUTIÉRREZ *et al.*, 1995; MOURA-DA-SILVA; BUTERA; TANJONI, 2007; RUCAVADO *et al.*, 2002; RUCAVADO *et al.*, 1995; TEIXEIRA *et al.*, 2005).

Neste estudo nós pudemos observar que assim como outras SVMPs de classe P-I e P-III já caracterizadas quanto à sua ação inflamatória, ATXL e BATXH foram capazes de induzir uma rápida formação de edema. Contudo, o tempo de duração da lesão mostrou-se maior que o edema causado por outras SVMPs botrópicas (DALE *et al.*, 2004; ESCALANTE *et al.*, 2000). Nos ensaios de inflamação peritoneal, ambas SVMPs induziram a formação de infiltrado leucocitário com a presença de células polimorfonucleares e mononucleares, assim como foi demonstrado com outras enzimas (FERNANDES *et al.*, 2006; MENALDO *et al.*, 2017), apesar de ter sido encontrado um grande número de células mononucleares também nos períodos iniciais, como foi observado em experimentos com o veneno total (MOREIRA *et al.*, 2012). Além disso, o exsudato resultante da injeção de ATXL continha um número de células consideravelmente maior do que a BATXH.

Utilizamos também o sobrenadante de MPACs estimuladas com veneno de *B. atrox* ou com as toxinas para a pesquisa de liberação de citocinas. Em ensaios cinéticos por citometria de fluxo, identificamos a presença da citocina TNF- α nas amostras incubadas com o veneno e BATXH. Os níveis da citocina secretada pelas células estimuladas com a BATXH, foram próximos a níveis obtidos em experimento semelhante com a P-I Neuwiedase (LOPES *et al.*, 2009). ATXL não induziu a secreção de TNF- α , o que nos leva a sugerir duas hipóteses: (1) TNF- α é mais suscetível à atividade catalítica da BATXH, o que acaba favorecendo a clivagem de seu precursor e liberação da forma ativa, assim como foi observado anteriormente com a Jararagina, que é outra P-III isolada do veneno de *B. jararaca* (MOURA-DA-SILVA *et al.*, 1996). (2) os domínios tipo-disintegrina e rico-em-cisteína da BATXH exercem influência sobre receptores celulares como já descrito com outras SVMPs de classe P-III (CLISSA *et al.*, 2006; MENEZES *et al.*, 2008).

A citocina pró-inflamatória IL-6 não foi identificada nos grupos testados, com exceção apenas do grupo LPS que induziu a secreção de todas as citocinas e quimiocinas testadas, comprovando a eficácia do teste.

Trabalhos recentes têm evidenciado a formação de vários fragmentos resultantes da hidrólise de componentes da matriz extracelular, que atuam como DAMPs durante a inflamação aguda. Nestes trabalhos, camundongos injetados com o exsudato do músculo gastrocnêmio de animais que receberam injeção com o veneno de *B. asper*, tiveram aumento da permeabilidade vascular (HERRERA *et al.*, 2016; RUCAVADO *et al.*, 2016). Além disso, as SVMPs de classe P-I e P-III são enzimas que exercem uma importante ação proteolítica nesses componentes, especialmente sobre o colágeno IV e a laminina (BALDO *et al.*, 2010; FREITAS-DE-SOUSA *et al.*, 2017).

Com base nessas evidências, testamos a hipótese de que peptídeos derivados da hidrólise do Matrigel por ATXL e BATXH poderiam induzir reação inflamatória em nossos modelos experimentais.

O Matrigel, nome comercial dado ao composto semelhante à matriz extracelular isolado do Sarcoma murino Engelbreth-Holm-Swarm é um material rico em proteínas de membrana basal, bem como a laminina, colágeno IV, nidogênio, além de vários outros componentes biológicos como fatores de crescimento e metaloproteases endógenas (TALBOT, CAPERNA *et al.*, 2015).

Neste estudo, avaliamos primeiramente a ação proteolítica das SVMPs, e nos experimentos foi observada a hidrólise total da cadeia α da laminina pelas duas SVMPs. ATXL também hidrolisou as cadeias β e γ da laminina, e o colágeno IV. Identificamos por LC-MS/MS a presença de peptídeos derivados de todas as cadeias da laminina em amostras incubadas com ATXL, e apenas da cadeia α nas amostras da BATXH, corroborando nossos achados no teste de eletroforese, e os artigos que descreveram a mesma ação (ESCALANTE *et al.*, 2006; FREITAS-DE-SOUSA *et al.*, 2017).

Além disso, avaliamos a ação desses produtos de hidrólise em ensaios de indução do edema e acúmulo de leucócitos, e foi demonstrado que estes peptídeos também causaram edema e infiltrado de células inflamatórias, embora numa proporção menor que os resultados observados com as toxinas, o que nos leva a propor que os fragmentos resultantes da hidrólise de componentes da matriz

extracelular pela ação das SVMPs, também tenham correlação com a reação inflamatória induzida pelo veneno.

Por fim, pela baixa eficiência dos antivenenos em neutralizar os efeitos locais dos envenenamentos, o desenvolvimento de tratamentos capazes de reverter ou amenizar as lesões locais é de grande importância. Nesse sentido, considerando que a gravidade dos acidentes ofídicos é impulsionada principalmente por proteases presentes no veneno, realizamos testes de inibição das atividades do veneno com potenciais inibidores das SVMPs: o pró-domínio recombinante da jararagina (PD-Jar) desenvolvido em nosso laboratório (PORTES-JUNIOR *et al.*, 2014), e um peptídeo sintético (SynPep) desenvolvido em colaboração com pesquisadores da Fiocruz. Nestes ensaios de inibição, as atividades catalítica, fibrinolítica e hemorrágica induzidas por SVMPs de classe P-I (BnP1 isolada do veneno de *B. neuwiedi*) (dados não publicados) e de classe P-III (Jararagina) foram eficientemente inibidas, ainda que em ensaios preliminares, demonstrando a importância da pesquisa básica no entendimento dos sintomas causados pelo envenenamento ofídico e na sugestão de tratamentos alternativos para os pacientes.

3 CONCLUSÕES

- ATXL e BATXH induzem importante reação inflamatória nos modelos experimentais testados, com a formação de edema, mobilização de células inflamatórias para o local da lesão e secreção da citocina pró-inflamatória TNF- α .
- Ambas SVMPs hidrolisaram os principais componentes da Membrana basal nos ensaios mimetizados pelo Matrigel, embora ATXL tenha apresentado maior atividade catalítica, principalmente sobre as cadeias de colágeno IV e laminina.
- A laminina gerou peptídeos de diferentes tamanhos que foram identificados por LC-MS-MS.
- Nos ensaios experimentais utilizando os produtos de hidrólise do Matrigel pelas toxinas, houve a formação de edema e acúmulo leucocitário significativamente maior que os peptídeos do grupo controle de Matrigel.
- É de suma importância a busca por tratamentos complementares à soroterapia, para o tratamento das lesões locais, utilizando por exemplo, inibidores de SVMPs, como foi demonstrado nos resultados preliminares com o pró-domínio recombinante e o peptídeo sintético SynPep.

REFERÊNCIAS¹

ALBUQUERQUE, P. L.; JACINTO, C. N.; SILVA JUNIOR, G. B.; LIMA, J. B. et al. Acute kidney injury caused by *Crotalus* and *Bothrops* snake venom: a review of epidemiology, clinical manifestations and treatment. **Rev Inst Med Trop Sao Paulo**, v. 55, n. 5, p. 295-301, 2013 Sep-Oct 2013.

ALMEIDA, M. T. et al. Inflammatory reaction induced by two metalloproteinases isolated from *Bothrops atrox* venom and by fragments generated from the hydrolysis of basement membrane components. **Toxins (Basel)**, v. 12, n. 2, Feb 2020.

ANDREWS, R. K.; GARDINER, E. E.; ASAZUMA, N.; BERLANGA, O. et al. A novel viper venom metalloproteinase, alborhagin, is an agonist at the platelet collagen receptor GPVI. **J Biol Chem**, v. 276, n. 30, p. 28092-28097, Jul 2001.

ARLINGHAUS, F. T.; EBLE, J. A. C-type lectin-like proteins from snake venoms. **Toxicon**, v. 60, n. 4, p. 512-519, Sep 2012.

BALDO, C. et al. Mechanisms of vascular damage by hemorrhagic snake venom metalloproteinases: tissue distribution and in situ hydrolysis. **PLoS Negl Trop Dis**, v. 4, n. 6, p. e727, Jun 2010.

BALDO, C. et al. Jararhagin disruption of endothelial cell anchorage is enhanced in collagen enriched matrices. **Toxicon**, v. 108, p. 240-8, Dec 2015.

BALDO, C. et al. BnP1, a novel P-I metalloproteinase from *Bothrops neuwiedi* venom: biological effects benchmarking relatively to jararhagin, a P-III SVMP. **Toxicon**, v. 51, n. 1, p. 54-65, Jan 2008.

CAMPOS BORGES, C.; SADAHIRO, M.; DOS SANTOS, M. C. Epidemiological and clinical aspects of snake bites in the municipalities of the state of Amazonas, Brazil. **Rev Soc Bras Med Trop**, v. 32, n. 6, p. 637-46, Nov-Dec 1999.

CARDOSO, J. L. C.; YAMAGUCHI, I. K.; MOURA-DA-SILVA, A. M. Produção de soros antitoxinas e perspectivas de modernização por técnicas de biologia molecular. In: CARDOSO, J. L. C et al. (Eds.). **Animais Peçonhentos no Brasil**. São Paulo: Sarvier, 2009. p. 419-431.

CASTRO, J. M.; OLIVEIRA, T. S.; SILVEIRA, C. R.; CAPORRINO, M. C. et al. A neutralizing recombinant single chain antibody, scFv, against BaP1, A P-I hemorrhagic metalloproteinase from *Bothrops asper* snake venom. **Toxicon**, v. 87, p. 81-91, Sep 2014.

CHIPPAUX, J. P. Incidence and mortality due to snakebite in the Americas. **PLoS Negl Trop Dis**, v. 11, n. 6, p. 1-39, Jun 2017.

¹ De acordo com: ASSOCIAÇÃO BRASILEIRA DE NORMAS TÉCNICAS. **NBR 6023**: Informação e documentação - referências - elaboração. Rio de Janeiro: ABNT, 2018.

CLISSA, P. B. *et al.* The effect of jararhagin, a metalloproteinase from *Bothrops jararaca* venom, on pro-inflammatory cytokines released by murine peritoneal adherent cells. **Toxicon**, v. 39, n. 10, p. 1567-73, Oct 2001.

CLISSA, P.B. *et al.* Importance of jararhagin disintegrin-like and cysteine-rich domains in the early events of local inflammatory response. **Toxicon**, v. 47, n. 5, p. 591-6, Apr 2006.

COSTA, E. P. *et al.* Importance of metalloproteinases and macrophages in viper snake envenomation-induced local inflammation. **Inflammation**, v. 26, n. 1, p. 13-7, Feb 2002.

DA GRAÇA SALOMÃO, M.; DE OLIVEIRA LUNA, K. P.; MACHADO, C. [Epidemiology of accidents by venomous animals and distribution of antivenon: state of art and world status]. **Rev Salud Publica (Bogota)**, v. 20, n. 4, p. 523-529, 2018 Jul-Aug 2018.

DALE, C. S. *et al.* The C-terminus of murine S100A9 inhibits hyperalgesia and edema induced by jararhagin. **Peptides**, v. 25, n. 1, p. 81-9, Jan 2004.

DELLA-CASA, M. S. *et al.* Insularin, a disintegrin from *Bothrops insularis* venom: inhibition of platelet aggregation and endothelial cell adhesion by the native and recombinant GST-insularin proteins. **Toxicon**, v. 57, n. 1, p. 125-33, Jan 2011.

DE QUEIROZ, M. R. *et al.* The role of platelets in hemostasis and the effects of snake venom toxins on platelet function. **Toxicon**, v. 133, p. 33-47, Jul 2017.

DE TONI, L. G. *et al.* Inflammatory mediators involved in the paw edema and hyperalgesia induced by Batroxase, a metalloproteinase isolated from *Bothrops atrox* snake venom. **Int Immunopharmacol**, v. 28, n. 1, p. 199-207, Sep 2015.

ESCALANTE, T. *et al.* Effectiveness of batimastat, a synthetic inhibitor of matrix metalloproteinases, in neutralizing local tissue damage induced by BaP1, a hemorrhagic metalloproteinase from the venom of the snake *Bothrops asper*. **Biochem Pharmacol**, v. 60, n. 2, p. 269-74, Jul 2000.

ESCALANTE, T. *et al.* Novel insights into capillary vessel basement membrane damage by snake venom hemorrhagic metalloproteinases: a biochemical and immunohistochemical study. **Arch Biochem Biophys**, v. 455, n. 2, p. 144-53, Nov 2006.

ESCALANTE, T. *et al.* Key events in microvascular damage induced by snake venom hemorrhagic metalloproteinases. **J Proteomics**, v. 74, n. 9, p. 1781-94, Aug 2011.

FARSKY, S. H. *et al.* *Bothrops asper* snake venom and its metalloproteinase BaP-1 activate the complement system. Role in leucocyte recruitment. **Mediators Inflamm**, v. 9, n. 5, p. 213-21, Sep 2000.

FARSKY, S. H.; ANTUNES, E.; MELLO, S. B. Pro and antiinflammatory properties of toxins from animal venoms. **Curr Drug Targets Inflamm Allergy**, v. 4, n. 3, p. 401-11, Jun 2005.

FERNANDES, C. M. *et al.* Inflammatory effects of BaP1 a metalloproteinase isolated from *Bothrops asper* snake venom: leukocyte recruitment and release of cytokines. **Toxicon**, v. 47, n. 5, p. 549-59, Apr 2006.

FREITAS-DE-SOUSA, L. A. *et al.* Comparison of venoms from wild and long-term captive *Bothrops atrox* snakes and characterization of Batroxtrotoxin, the predominant class PIII metalloproteinase from the venom of this species. **Biochimie**, v. 118, p. 60-70, Nov 2015.

FREITAS-DE-SOUSA, L. A. *et al.* Insights into the Mechanisms Involved in Strong Hemorrhage and Dermonecrosis Induced by Atroxlysin-Ia, a PI-Class Snake Venom Metalloproteinase. **Toxins (Basel)**, v. 9, n. 8, Aug 2017.

FURTADO, M. E. F. *et al.* Antigenic cross-reactivity and immunogenicity of *Bothrops* venoms from snakes of the Amazon region. **Toxicon**, v. 55, n. 4, p. 881-7, Apr 2010.

GALLAGHER, P. *et al.* Role of the snake venom toxin jararhagin in proinflammatory pathogenesis: in vitro and in vivo gene expression analysis of the effects of the toxin. **Arch Biochem Biophys**, v. 441, n. 1, p. 1-15, Sep 2005.

GOMIS-RÜTH, F. X. Catalytic domain architecture of metzincin metalloproteases. **J Biol Chem**, v. 284, n. 23, p. 15353-7, Jun 2009.

GRAMS, F. *et al.* Activation of snake-venom metalloproteinases by a cysteine switch-like mechanism. **FEBS Letters**, v. 335, n. 1, p. 76-80, Nov 1993.

GUTIÉRREZ, J. M. *et al.* Isolation and characterization of a metalloproteinase with weak hemorrhagic activity from the venom of the snake *Bothrops asper* (terciopelo). **Toxicon**, v. 33, n. 1, p. 19-29, Jan 1995.

GUTIÉRREZ, J. M.; ROJAS, E.; QUESADA, L.; LEÓN, G. *et al.* Pan-African polyspecific antivenom produced by caprylic acid purification of horse IgG: an alternative to the antivenom crisis in Africa. **Trans R Soc Trop Med Hyg**, v. 99, n. 6, p. 468-475, Jun 2005.

GUTIÉRREZ, J. M. *et al.* Experimental pathology of local tissue damage induced by *Bothrops asper* snake venom. **Toxicon**, v. 54, n. 7, p. 958-75, Dec 2009.

GUTIÉRREZ, J. M. *et al.* A Call for Incorporating Social Research in the Global Struggle against Snakebite. **PLoS Negl Trop Dis**, v. 9, n. 9, p. 1-4, Sep 2015.

HARRISON, R. A.; GUTIÉRREZ, J. M. Priority Actions and Progress to Substantially and Sustainably Reduce the Mortality, Morbidity and Socioeconomic Burden of Tropical Snakebite. **Toxins (Basel)**, v. 8, n. 12, p. 1-14, Nov 2016.

HERRERA, C. *et al.* Muscle Tissue Damage Induced by the Venom of *Bothrops asper*: Identification of Early and Late Pathological Events through Proteomic Analysis. **PLoS Negl Trop Dis**, v. 10, n. 4, p. 1-22, Apr 2016.

HOFMANN, H.; BON, C. Blood coagulation induced by the venom of *Bothrops atrox*. 1. Identification, purification, and properties of a prothrombin activator. **Biochemistry**, v. 26, n. 3, p. 772-80, Feb 1987.

KAMIGUTI, A. S. *et al.* Properties of fibrinogen cleaved by Jararhagin, a metalloproteinase from the venom of *Bothrops jararaca*. **Thromb Haemost**, v. 72, n. 2, p. 244-9, Aug 1994.

KAMIGUTI, A. S.; HAY, C. R.; ZUZEL, M. Inhibition of collagen-induced platelet aggregation as the result of cleavage of alpha 2 beta 1-integrin by the snake venom metalloproteinase jararhagin. **Biochem J**, v. 320 (Pt 2), p. 635-41, Dec 1996.

KASTURIRATNE, A. *et al.* The global burden of snakebite: a literature analysis and modelling based on regional estimates of envenoming and deaths. **PLoS Med**, v. 5, n. 11, p. e218, Nov 2008.

LOMONTE, B.; ANGULO, Y.; CALDERÓN, L. An overview of lysine-49 phospholipase A2 myotoxins from crotalid snake venoms and their structural determinants of myotoxic action. **Toxicon**, v. 42, n. 8, p. 885-901, Dec 2003.

LOPES, D. S. *et al.* Characterization of inflammatory reaction induced by neuwiedase, a P-I metalloproteinase isolated from *Bothrops neuwiedi* venom. **Toxicon**, v. 54, n. 1, p. 42-9, Jul 2009.

LOPES, D. S. *et al.* Gene expression of inflammatory mediators induced by jararhagin on endothelial cells. **Toxicon**, v. 60, n. 6, p. 1072-84, Nov 2012.

MALAQUE, C. M. S. A.; GUTIÉRREZ, J. M. Snakebite Envenomation in Central and South America. *In: Brendt et al. (Eds.). Critical Care Toxicology*. Switzerland: Springer International, 2015. p. 1-22.

MATOS, R. R.; IGNOTTI, E. [Incidence of venomous snakebite accidents by snake species in Brazilian biomes]. **Cien Saude Colet**, v. 25, n. 7, p. 2837-2846, Jul 2020.

MENALDO, D. L. *et al.* Immune cells and mediators involved in the inflammatory responses induced by a P-I metalloprotease and a phospholipase A. **Mol Immunol**, v. 85, p. 238-247, May 2017.

MENEZES, M. C. *et al.* Activation of leukocyte rolling by the cysteine-rich domain and the hyper-variable region of HF3, a snake venom hemorrhagic metalloproteinase. **FEBS Lett**, v. 582, n. 28, p. 3915-21, Nov 2008.

MINISTÉRIO DA SAÚDE (Brasil). Acidentes por animais peçonhentos: serpentes. 2017. Available at: <http://www.saude.gov.br/saude-de-a-z/acidentes-por-animais-peconhentos-serpentes>. Cited: 04 abr. 2020.

MONTEIRO, W. M.; CONTRERAS-BERNAL, J. C.; BISNETO, P. F.; SACHETT, J. *et al.* *Bothrops atrox*, the most important snake involved in human envenomings in the amazon: How venomics contributes to the knowledge of snake biology and clinical toxinology. **Toxicon X**, v. 6, p. 1-18, Jun 2020.

MOREIRA, V. *et al.* Local inflammatory events induced by *Bothrops atrox* snake venom and the release of distinct classes of inflammatory mediators. **Toxicon**, v. 60, n. 1, p. 12-20, Jul 2012.

MORETTO DEL-REI, T. H. *et al.* Functional variability of *Bothrops atrox* venoms from three distinct areas across the Brazilian Amazon and consequences for human envenomings. **Toxicon**, v. 164, p. 61-70, Jun 2019.

MOURA-DA-SILVA, A. M.; LAING, G. D.; PAINE, M. J.; DENNISON, J. M. *et al.* Processing of pro-tumor necrosis factor-alpha by venom metalloproteinases: a hypothesis explaining local tissue damage following snake bite. **Eur J Immunol**, v. 26, n. 9, p. 2000-2005, Sep 1996.

MOURA-DA-SILVA, A. M. *et al.* Selective recognition of alpha2beta1 integrin by jararhagin, a Metalloproteinase/disintegrin from *Bothrops jararaca* venom. **Thromb Res**, v. 102, n. 2, p. 153-9, Apr 2001.

MOURA-DA-SILVA, A. M.; BUTERA, D.; TANJONI, I. Importance of snake venom metalloproteinases in cell biology: effects on platelets, inflammatory and endothelial cells. **Curr Pharm Des**, v. 13, n. 28, p. 2893-905, 2007.

MOURA-DA-SILVA A. M. *et al.* Snake venom metalloproteinases: structure, function and effects on snake bite pathology. *In*: LIMA M. E. *et al.* (Eds.). **Animal Toxins**. Minas Gerais: Editora UFMG, 2009. p. 401-422.

MOURA-DA-SILVA, A. M.; BALDO, C. Jararhagin, a hemorrhagic snake venom metalloproteinase from *Bothrops jararaca*. **Toxicon**, v. 60, n. 3, p. 280-9, Sep 2012.

MOURA-DA-SILVA, A. M. *et al.* Processing of Snake Venom Metalloproteinases: Generation of Toxin Diversity and Enzyme Inactivation. **Toxins (Basel)**, v. 8, n. 6, p. 1-15, Jun 2016.

MOURA-DA-SILVA, A. M.; CONTRERAS-BERNAL, J. C.; CIRILO GIMENES, S. N.; FREITAS-DE-SOUSA, L. A. *et al.* The relationship between clinics and the venom of the causative Amazon pit viper (*Bothrops atrox*). **PLoS Negl Trop Dis**, v. 14, n. 6, p. 1-17, Jun 2020.

NICOLETI, A. F.; MEDEIROS, C. R.; DUARTE, M. R.; FRANÇA, F. O. Comparison of *Bothropoides jararaca* bites with and without envenoming treated at the Vital Brazil Hospital of the Butantan Institute, State of São Paulo, Brazil. **Rev Soc Bras Med Trop**, v.43, n. 6, p. 657-661, 2010 Nov-Dec 2010.

OLIVEIRA, F. N.; BRITO, M. T.; MORAIS, I. C.; FOOK, S. M. *et al.* Accidents caused by *Bothrops* and *Bothropoides* in the State of Paraíba: epidemiological and clinical aspects. **Rev Soc Bras Med Trop**, v. 43, n. 6, p. 662-667, 2010 Nov-Dec 2010.

PORTES-JUNIOR, J. A. *et al.* Unraveling the processing and activation of snake venom metalloproteinases. **J Proteome Res**, v. 13, n. 7, p. 3338-48, Jul 2014.

RAWLINGS, N. D. *et al.* MEROPS: the database of proteolytic enzymes, their substrates and inhibitors. **Nucleic Acids Res**, v. 42, Database issue, p. D503-9, 2014.

RIBEIRO, L. A.; GADIA, R.; JORGE, M. T. [Comparison between the epidemiology of accidents and the clinical features of envenoming by snakes of the genus *Bothrops*, among elderly and non-elderly adults]. **Rev Soc Bras Med Trop**, v. 41, n. 1, p. 46-49, 2008 Jan-Feb 2008.

RUCAVADO, A. *et al.* Local tissue damage induced by BaP1, a metalloproteinase isolated from *Bothrops asper* (Terciopelo) snake venom. **Exp Mol Pathol**, v. 63, n. 3, p. 186-99, Dec 1995.

RUCAVADO, A. *et al.* Increments in cytokines and matrix metalloproteinases in skeletal muscle after injection of tissue-damaging toxins from the venom of the snake *Bothrops asper*. **Mediators Inflamm**, v. 11, n. 2, p. 121-8, Apr 2002.

RUCAVADO, A. *et al.* Assessment of metalloproteinase inhibitors clodronate and doxycycline in the neutralization of hemorrhage and coagulopathy induced by *Bothrops asper* snake venom. **Toxicon**, v. 52, n. 7, p. 754-9, Dec 2008.

RUCAVADO, A. *et al.* Viperid Envenomation Wound Exudate Contributes to Increased Vascular Permeability via a DAMPs/TLR-4 Mediated Pathway. **Toxins (Basel)**, v. 8, n. 12, Nov 2016.

SANCHEZ, E. F. *et al.* The novel metalloproteinase atroxlysin-I from Peruvian *Bothrops atrox* (Jergón) snake venom acts both on blood vessel ECM and platelets. **Arch Biochem Biophys**, v. 496, n. 1, p. 9-20, Apr 2010.

SERRANO, S. M. The long road of research on snake venom serine proteinases. **Toxicon**, v. 62, p. 19-26, Feb 2013.

SILVA, C. A. *et al.* Activation of alpha(M)beta(2)-mediated phagocytosis by HF3, a P-III class metalloproteinase isolated from the venom of *Bothrops jararaca*. **Biochem Biophys Res Commun**, v. 322, n. 3, p. 950-6, Sep 2004.

SILVA DE OLIVEIRA, S.; CAMPOS ALVES, E.; DOS SANTOS SANTOS, A.; FREITAS NASCIMENTO, E. *et al.* *Bothrops* snakebites in the Amazon: recovery from hemostatic disorders after Brazilian antivenom therapy. **Clin Toxicol (Phila)**, v. 58, n. 4, p. 266-274, Jul 2019.

SINAN - Sistema de Informação de Agravos de Notificação: acidente por animais peçonhentos. Brasília: Ministério da Saúde. DATASUS. Updated: jan. 2020. Available at: <http://tabnet.datasus.gov.br/cgi/tabcgi.exe?sinannet/cnv/animaisbr.def%20>. Cited: 04 abr. 2020.

SLAGBOOM, J. *et al.* Haemotoxic snake venoms: their functional activity, impact on snakebite victims and pharmaceutical promise. **Br J Haematol**, v. 177, n. 6, p. 947-959, Jun 2017.

SOUSA, L. F. *et al.* Comparison of phylogeny, venom composition and neutralization by antivenom in diverse species of bothrops complex. **PLoS Negl Trop Dis**, v. 7, n. 9, p. 1-16, Sep 2013.

SOUSA, L. F.; PORTES-JUNIOR, J. A.; NICOLAU, C. A.; BERNARDONI, J. L. *et al.* Functional proteomic analyses of *Bothrops atrox* venom reveals phenotypes associated with habitat variation in the Amazon. **J Proteomics**, v. 159, p. 32-46, Apr 2017.

TALBOT, N. C.; CAPERNA, T. J. Proteome array identification of bioactive soluble proteins/peptides in Matrigel: relevance to stem cell responses. **Cytotechnology**, v. 67, n. 5, p. 873-883, Oct 2015.

TANJONI, I. *et al.* Different regions of the class P-III snake venom metalloproteinase jararhagin are involved in binding to alpha2beta1 integrin and collagen. **Toxicon**, v. 55, n. 6, p. 1093-9, Jun 2010.

TEIXEIRA, C. E. F. *et al.* Inflammatory effects of snake venom metalloproteinases. **Mem Inst Oswaldo Cruz**, v. 100 Suppl 1, p. 181-4, Mar 2005.

TEIXEIRA, C. *et al.* Inflammation Induced by Platelet-Activating Viperid Snake Venoms: Perspectives on Thromboinflammation. **Front Immunol**, v. 10, p. 1-13, Sep 2019.

WALDEZ, F.; VOGT, R. C. Aspectos ecológicos e epidemiológicos de acidentes ofídicos em comunidades ribeirinhas do baixo rio Purus, Amazonas, Brasil. **Acta Amazônica**, v. 39, p. 681-692, 2009.



WIJEYEWICKREMA, L. C.; GARDINER, E. E.; MOROI, M.; BERNDT, M. C. *et al.* Snake venom metalloproteinases, crotarhagin and alborhagin, induce ectodomain shedding of the platelet collagen receptor, glycoprotein VI. **Thromb Haemost**, v. 98, n. 6, p. 1285-1290, Dec 2007.

WILLIAMS, D. J. *et al.* Strategy for a globally coordinated response to a priority neglected tropical disease: Snakebite envenoming. **PLoS Negl Trop Dis**, v. 13, n. 2, p. 1-12, Feb 2019.

APÊNDICE A - Inflammatory reaction induced by two metalloproteinases isolated from *Bothrops atrox* venom and by fragments generated from the hydrolysis of basement membrane components.

Article

Inflammatory Reaction Induced by Two Metalloproteinases Isolated from *Bothrops atrox* Venom and by Fragments Generated from the Hydrolysis of Basement Membrane Components

Michelle Teixeira de Almeida ^{1,2}, Luciana Aparecida Freitas-de-Sousa ² , Monica Colombini ², Sarah N. C. Gimenes ², Eduardo S. Kitano ³, Eliana L. Faquim-Mauro ², Solange M. T. Serrano ³ and Ana Maria Moura-da-Silva ^{2,*} 

¹ Programa de Pós-Graduação em Ciências-Toxinologia, Instituto Butantan, São Paulo 05503-900, Brazil; michelle.almeida@butantan.gov.br

² Laboratório de Imunopatologia, Instituto Butantan, São Paulo 05503-900, Brazil; luciana.sousa@butantan.gov.br (L.A.F.-d.-S.); monica.colombini@butantan.gov.br (M.C.); sarah.gimenes@butantan.gov.br (S.N.C.G.); eliana.faquim@butantan.gov.br (E.L.F.-M.)

³ Laboratório de Toxinologia Aplicada, Center of Toxins, Immune-Response and Cell Signalig, CeTICS, Instituto Butantan, São Paulo 05503-900, Brazil; eduardosh.kitano@gmail.com (E.S.K.); solange.serrano@butantan.gov.br (S.M.T.S.)

* Correspondence: ana.moura@butantan.gov.br; Tel.: +55-(11)-2627-9779

Received: 11 December 2019; Accepted: 30 January 2020; Published: 2 February 2020



Abstract: Snake venom metalloproteinases (SVMPs) play an important role in local tissue damage of snakebite patients, mostly by hydrolysis of basement membrane (BM) components. We evaluated the proinflammatory activity of SVMPs Atroxlysin-Ia (ATXL) and Batroxrhagin (BATXH) from *Bothrops atrox* venom and their hydrolysis products of Matrigel. BALB/c mice were injected with SVMPs (2 µg), for assessment of paw edema and peritoneal leukocyte accumulation. Both SVMPs induced edema, representing an increase of ~70% of the paw size. Leukocyte infiltrates reached levels of 6×10^6 with ATXL and 5×10^6 with BATXH. TNF- α was identified in the supernatant of BATXH—or venom-stimulated MPAC cells. Incubation of Matrigel with the SVMPs generated fragments, including peptides from Laminin, identified by LC-MS/MS. The Matrigel hydrolysis peptides caused edema that increased 30% the paw size and promoted leukocyte accumulation ($4\text{--}5 \times 10^6$) to the peritoneal cavity, significantly higher than Matrigel control peptides 1 and 4 h after injection. Our findings suggest that ATXL and BATXH are involved in the inflammatory reaction observed in *B. atrox* envenomings by direct action on inflammatory cells or by releasing proinflammatory peptides from BM proteins that may amplify the direct action of SVMPs through activation of endogenous signaling pathways.

Keywords: *Bothrops atrox*; SVMPs; metalloproteinases; basal membrane; hydrolysis; peptides; inflammation

Key Contribution: PI- and PIII-class SVMPs isolated from *B. atrox* venom induce inflammatory reactions in mice characterized by edema and leukocyte accumulation. One mechanism involved in the toxins' effect is the proinflammatory activity of peptides resulting from hydrolysis of BM components by both SVMPs.

1. Introduction

Snakebites represent a major public health problem and are considered a neglected tropical disease. According to some estimates, there are 1.8 to 2.7 million ophidian envenomings in the world annually, of which about 81,000 to 138,000 result in death [1]. In Brazil, the genus *Bothrops* is responsible for the greatest number of these accidents, which are characterized by several systemic or local effects that can evolve into significant temporary or permanent disabilities. These effects are caused by a wide range of toxins present in the venoms of *Bothrops* snakes, such as serine proteinases, phospholipases A₂ and snake venom metalloproteinases (SVMPs), which participate in different events, including inflammation [2].

Studies with venoms from *Bothrops* snakes have demonstrated their proinflammatory activity, since these venoms are capable of causing increased vascular permeability, formation of edema, recruitment of leukocytes and expression of adhesion molecules, cytokines and chemokines [3]; in such events, SVMPs play important role. SVMPs are zinc-dependent enzymes, classified in three classes, based on their precursors: the PI-class is composed of the pre-, pro- and metalloproteinase domains; PII-class of pre-, pro-, metalloproteinase and disintegrin domains; and PIII-class composed of pre-, pro-, metalloproteinase, disintegrin-like and cysteine-rich domains [4]. The PI- and PIII-classes are widely expressed in viper venoms and well characterized for their proinflammatory action, which is frequently associated with their catalytic activity [5–7] or with the activation of inflammatory cells as macrophages that release proinflammatory mediators [8,9]. Due to their catalytic activity, SVMPs may also have action on endogenous pro-metalloproteinases and pro-cytokines, such as pro-MMPs [10] and pro-TNF- α [11], which, upon cleavage by SVMPs, are released in their active form. However, the proinflammatory activity of these enzymes is not only due to the presence of the catalytic activity, but also to their action on cell receptors through the disintegrin-like and/or cysteine-rich domains, which can induce leukocyte recruitment and cytokine synthesis [12,13].

Bothrops atrox snakes are reported to be the leading cause of ophidian accidents in the Amazon region. Human envenomings are characterized in most cases by consumption coagulopathy and local damages, such as edema, pain, erythema and local hemorrhage, which are not effectively neutralized by *Bothrops* antivenom [14]. In experimental models, *B. atrox* venom displays proinflammatory activity and is capable of causing an increase in vascular permeability and an important influx of leukocytes to the site of injury, characterized by the presence of polymorphonuclear and mononuclear cells, as well as the release of the eicosanoids PGE₂ and LTB₄, and the cytokines TNF- α and IL-6 [15]. However, the knowledge about the contribution of each toxin class to *B. atrox* venom on proinflammatory reaction is still restricted to the isolated PI-class SVMPs. A pool of low-molecular-mass proteinases was able to induce the formation of edema and leukocyte infiltrate [16]. Considering isolated toxins, Batroxase, a PI-class SVMP isolated from the venom of *Bothrops atrox*, was capable of inducing leukocyte migration, as well as the release of proinflammatory mediators, such as IL-1 β , IL-6 and PGE₂, involved in these events [17].

PIII-class SVMPs, such as Jararhagin, isolated from the venom of *B. jararaca* [18], present hemorrhagic activity and trigger different events during the envenoming [19]. They are able to trigger the proinflammatory activity, with increased expression of cytokines, such as IL-6 and TNF- α , which are shortly degraded by the catalytic activity of SVMPs after expression in in vitro assays [12].

Recently, our group isolated two hemorrhagic SVMPs from the venom of *B. atrox* that were named Atroxlysin-Ia [20] and Batroxrhagin [21]. Batroxrhagin (BATXH) is a PIII-class SVMP structurally and functionally similar to Jararhagin, isolated from *B. jararaca* venom [21]. Atroxlysin-Ia (ATXL) is an isoform of the PI-class SVMP Atroxlysin-I, isolated from *B. atrox* Peruvian snakes [22] and is structurally different than Batroxase [23]. However, unlike the previously isolated toxins, ATXL presents a dermonecrotic activity and is capable of inducing an intense hemorrhage, in levels comparable to the PIII-class SVMP. The mechanism suggested for ATXL higher hemorrhagic and dermonecrotic action than other PI-class SVMPs was its higher efficiency to cleave Basement Membrane (BM) components as collagen IV and laminin, important structural elements that guarantees stability to BM [20]. Laminin

is a glycoprotein that plays important roles in cell biology, such as cell adhesion, migration and proliferation, among other biological activities [24]. Some studies have reported different biological activities of peptides obtained from laminin degradation, for example, SIKVAV and AG73, which present the ability to regulate the expression of adhesion, migration, invasion and proteolytic activity molecules in some cell lines of carcinoma [25,26]. Thus, proteolytic hydrolysis of laminin by SVMs could also release bioactive peptides that could interfere in cell adhesion and, consequently, in tissue organization. Rucavado et al. [27] demonstrated, by proteomic analysis, the presence of fragments of Damage Associated Molecular Patterns (DAMPs) in exudates obtained after intramuscular injection of *B. asper* venom in mice. The authors associated the presence of the peptides with the hydrolysis of extracellular matrix components and cell damage, indicating the generation of DAMPs in snakebite envenomation and its participation in inflammatory processes.

Thus, in view of the importance of proinflammatory events caused by SVMs and the action of some bioactive peptides generated by hydrolysis of ECM components, in this study, we evaluated the proinflammatory action induced by the ATXL and BATXH, as well as by the products derived from BM degradation by these two enzymes.

2. Results

2.1. Inflammatory Reaction Induced by SVMs

Our first approach was to evaluate and compare the inflammatory effects induced by the administration of ATXL and BATXH into the mouse foot paw. Edema formation was observed after injections with different doses (0.5, 1, 2 and 5 μg) of ATXL or BATXH (Figure 1). The doses of 1, 2 and 5 μg of both toxins induced edema significantly higher than the control did. The differences among doses from 1 to 5 μg , within and between each toxin group, were not statistically significant, indicating that the two-times-lower molecular mass of ATXL than BATXH would not impact the comparisons in this range of doses. The intermediate dose of 2 $\mu\text{g}/\text{mouse}$ was then selected to evaluate and compare the time course of the edema induced by both toxins, since this dose was capable of inducing edema without causing hemorrhage in the animals [20].

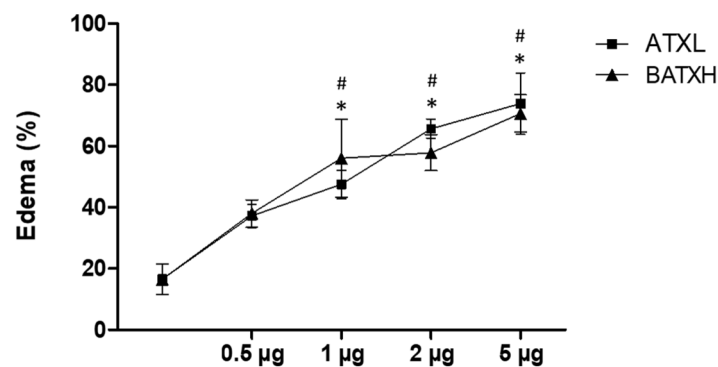


Figure 1. Edema induced by different doses of Atroxlysin-Ia (ATXL) and Batroxrhagin (BATXH). Mice ($n = 6$) were injected on the left paw with different protein doses (0.5, 1, 2 and 5 $\mu\text{g}/\text{animal}$) or with saline as negative control. The results are expressed as the mean \pm S.E. of two independent experiments. Symbols indicate significant differences ($p \leq 0.05$) compared to the negative control for ATXL (*) or BATXH (#) groups.

According to the kinetics experiments, the edema induced by both toxins peaked between 30 min and 1 h after injection (Figure 2). ATXL-induced edema was significantly higher than control within 3 h after the injection. On the other hand, animals injected into the paw with BATXH showed significantly higher peaks of edema between 30 min and 6 h. In this group, the edema remained until 24 h after

injection. Edema reduction occurred progressively until almost reaching the basal level in 48 h, when compared to the control group injected with saline.

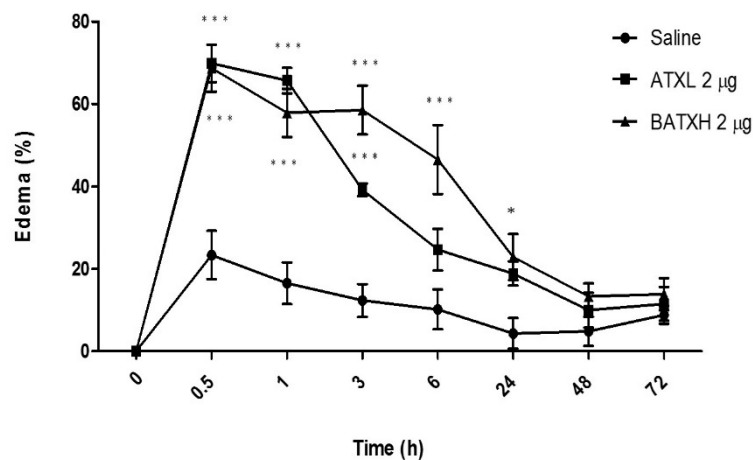


Figure 2. Time course of edema induced by Atrolysin-Ia (ATXL) and Batroxrhagin (BATXH). Mice ($n = 6$) were injected on the left paw with 2 µg/animal or with saline as negative control. The results are expressed as the means \pm S.E. of two independent experiments. * ($p \leq 0.05$), *** ($p \leq 0.001$) compared to the negative control group.

In the following experiment, we compared the leukocyte accumulation induced by intraperitoneal administration of the two SVMPs. In dose-response experiments, doses of 1 and 2 µg of both toxins induced significant leukocyte accumulation, and the differences among 1 and 2 µg doses of both toxin groups were not statistically significant (Figure 3A). The dose of 5 µg/mouse was not tested, as it induced hemorrhage in the previous experiment. The dose of 2 µg/mouse was then selected for the following experiments. In relation to the total number of leukocytes accumulated by the SVMPs in the peritoneum, ATXL induced statistical significant leukocyte influx of 6×10^6 cells/mL at 4, 24 and 48 h after injection, while BATXH showed significant differences from the control after 4 and 48 h, reaching the number of 5×10^6 cells/mL (Figure 3B). In the differential counts, ATXL induced the increase of polymorphonuclear cells in periods of 4, 24 and 48 h after injection, whereas BATXH showed a later response after 24 and 48 h (Figure 3C). Both toxins induced increased influx of mononuclear cells at the periods of 4 and 48 h (Figure 3D).

2.2. Cytokines and Chemokine Quantification

We next carried out kinetics assay of inflammatory mediators secreted by Murine Peritoneal Adherent Cells (MPAC) treated with 40 µg/mL *B. atrox* venom, ATXL and BATXH or 1 µg/mL LPS as positive controls, and culture medium, as negative control. Treatments with whole venom or isolated toxins did not induce cytotoxicity in cultures of MPAC, even in incubation periods as long as 24 h (data not shown). MPAC cultures were then submitted to these different stimuli for 2, 4, 6 and 18 h, and the supernatants were analyzed by flow cytometry by using the CBA kit.

Figure 4A shows that *B. atrox* venom and BATXH stimulated the secretion of the proinflammatory cytokine TNF- α . Venom-induced TNF- α peaked between 2 and 6 h, with levels up to 800 pg/mL; BATXH induced a significant TNF- α secretion of 200 pg/mL at 4 h. ATXL, on the other hand, showed cytokine levels comparable to the negative control. In our analysis, only the positive control (LPS) induced significant increases of IL-6 and IL-10 cytokines or MCP-1 chemokine in the cell culture supernatants (Figure 4B–D, respectively).

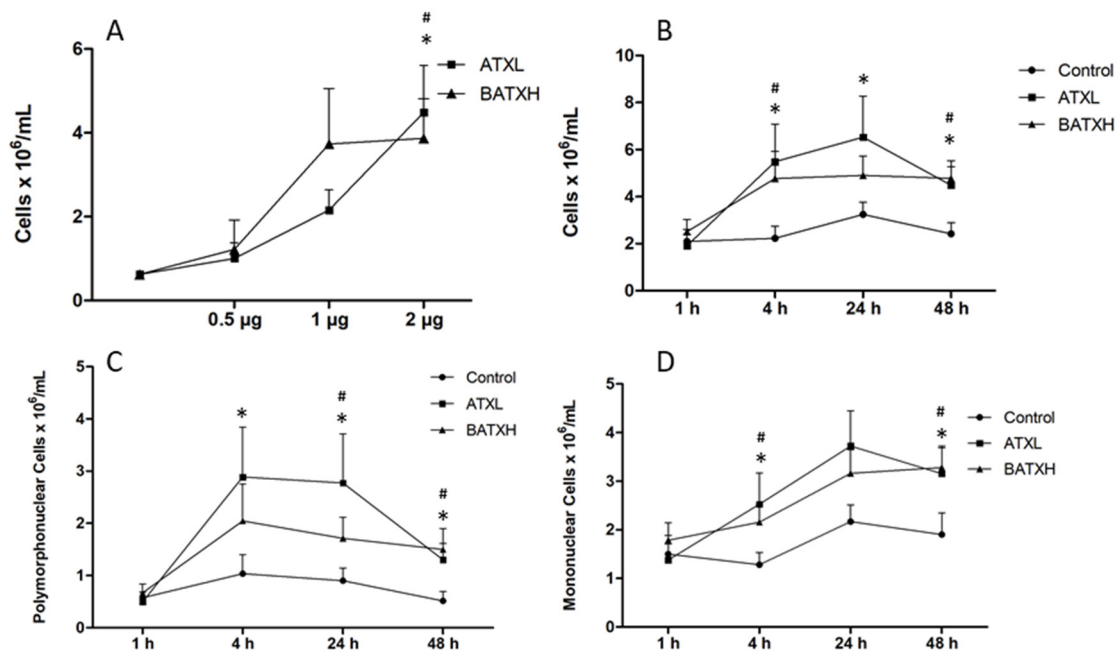


Figure 3. Leukocyte accumulation in the peritoneal cavity induced by Atoxylisin-Ia (ATXL) and Batroxrhagin (BATXH). For dose-response experiments (A), mice were injected intraperitoneally with increasing doses of ATXL, BATXH or saline as a negative control, in a final volume of 500 µL/animal. After 4 h, the animals were sacrificed in CO₂ chamber, for the removal of the peritoneal exudate and the total number of leukocytes counted in Newbauer's chamber. For time-course experiments, 2 µg of ATXL or BATXH was injected, as described above, and the peritoneal exudate was collected at 1, 4, 24 and 48 h. The total number of leukocytes was counted in Newbauer's chamber (B). Cells were differentiated into polymorphonuclear (C) or mononuclear cells (D), under optical microscopy (Amplification: 400×). The results are expressed as the mean ± S.E. ($n = 6-12$) of four independent experiments. Significant differences ($p \leq 0.05$) compared to the negative control for ATXL (*) or BATXH (#) groups.

2.3. Hydrolysis of Matrigel by SVMs

In order to test our hypothesis that BM peptides generated by SVM hydrolysis participate in venom-induced inflammation, our first attempt was to check by SDS-PAGE the hydrolysis of Matrigel components after 30 min, 1 h and 24 h of incubation with ATXL and BATXH. In Figure 5, lane 1, we show the Matrigel control with the two major diffuse bands that may include Laminin α -1 (~400 kDa), β and γ (~250 kDa) chains [28], and Collagen IV α -1 (~210 kDa) and α -2 (~190 kDa) chains [7]. Total hydrolysis of the 400 kDa band occurred in the first 30 min of incubation with ATXL (lanes 2–4) and BATXH (lanes 5–7). The 250 kDa band was digested by ATXL in all incubation times, whereas hydrolysis by BATXH provoked only a reduction in the intensity of this band, though it was more evident in the longer incubation time. In the Matrigel control sample, the ~150 and 110 kDa bands correspond to the molecular masses of Nidogen chains [28]. Both SVMs degraded the 100 kDa band; however, there was no apparent digestion of the 150 kDa band. The highlighted bands of 52 and 25 kDa correspond to ATXL and BATXH, respectively. Interestingly, although the proteinases generated different profiles of Matrigel hydrolysis products, both generated large fragments of 30–220 kDa.

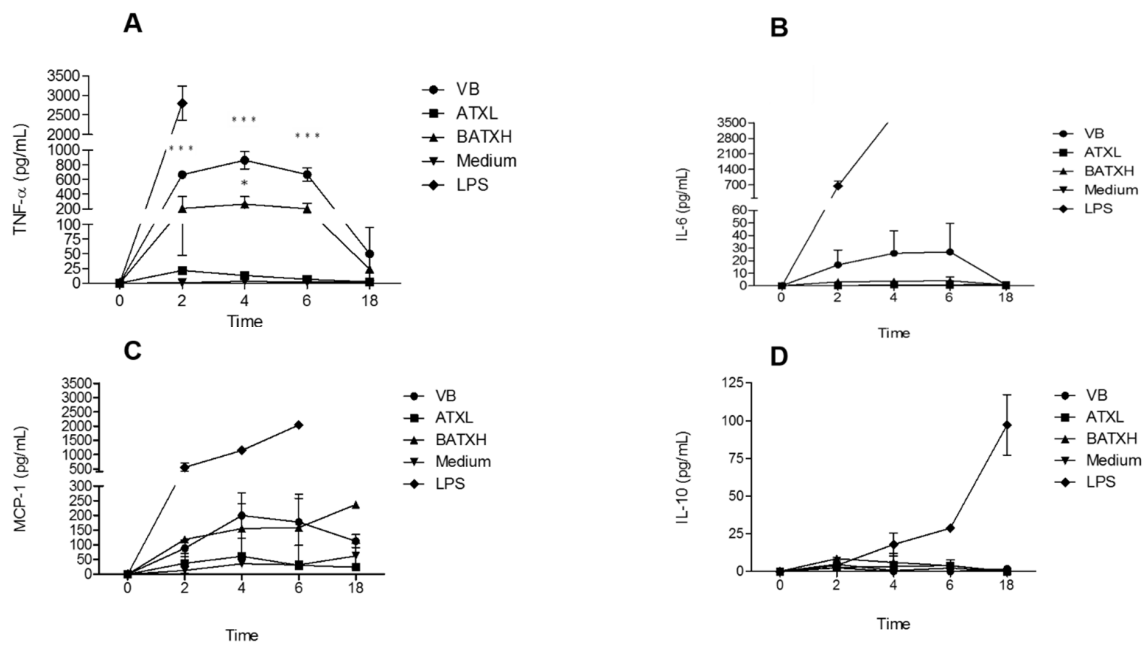


Figure 4. Kinetics of inflammatory mediators secreted by MPACs stimulated with Atroxlysin-Ia (ATXL) or Batroxrhagin (BATXH). MPACs were stimulated with 40 $\mu\text{g/mL}$ of *Bothrops atrox* venom, ATXL, BATXH or LPS (1 $\mu\text{g/mL}$) as positive control, or culture medium as negative control. Supernatants were collected after 2, 4, 6 and 18 h, for analysis of TNF- α (A), IL-6 (B), MCP-1 (C) and IL-10 (D) by the CBA method. The results are expressed as mean \pm S.E. of three independent experiments. * ($p \leq 0.05$), *** ($p \leq 0.001$) compared to the negative control group.

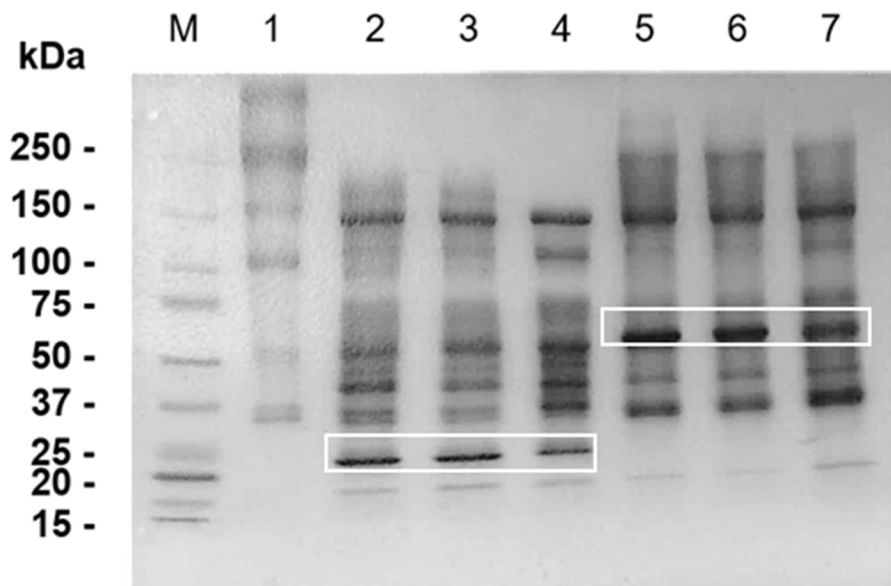


Figure 5. Hydrolysis of Matrigel by Atroxlysin-Ia (ATXL) and Batroxrhagin (BATXH). Matrigel was incubated for different periods of time with the proteinases in the enzyme:substrate ratio of 1:10 (w/w) at 37 $^{\circ}\text{C}$. After incubation, the samples were filtered in centrifugal filter devices (cut off at 10 kDa), and the proteins retained in the molecular filters were submitted to SDS-PAGE (5–15% SDS-polyacrylamide gel), under reducing conditions. After electrophoresis, bands were fixed and stained with Coomassie Blue R-250. M—Molecular mass markers; 1—Matrigel (control); 2—ATXL + Matrigel (30 min); 3—ATXL + Matrigel (1 h); 4—ATXL + Matrigel (24 h); 5—BATXH + Matrigel (30 min); 6—BATXH + Matrigel (1 h); 7—BATXH + Matrigel (24 h). The bands of 24 and 52 kDa, indicated by white rectangles, correspond to ATXL and BATXH, respectively.

To gain further insight into the hydrolysis of Matrigel components by ATXL and BATXH, we identified the resulting peptide fraction by LC–MS/MS (peptidome). Supplementary Table S1 shows the list of peptides identified with Posterior Error Probability ≤ 0.01 in the control and proteinase-incubated Matrigel samples. This analysis showed the presence of peptides from various types of proteins in the Matrigel control sample, including intracellular, extracellular and plasma proteins. Moreover, many peptides present in the control Matrigel samples were not detected in those incubated with the proteinases, indicating that they might have been further degraded by the venom proteinases (Supplementary Table S2). The peptidome data were further filtered to only accept peptides that were detected in both LC–MS/MS runs of products derived from Matrigel incubated with each toxin and were absent in the control Matrigel sample runs (Table 1). Accordingly, a rather low number of peptides (17 peptides for ATXL and 10 for BATXH) were detected as hydrolysis products. Laminin α -1 subunit peptides were detected among the products generated by both ATXL and BATXH, while peptides from Laminin β and γ were identified only in the ATXL samples. The low number of peptides identified is in good agreement with the SDS-PAGE profile that showed various protein bands, indicating that the proteinases interacted with Matrigel components, promoting limited proteolysis rather than unspecific degradation to small peptides. Most peptides generated by the proteinases contain a hydrophobic amino acid residue at the N-terminus, including various peptides that contain N-terminal Leu or Ile, which is in agreement with the preference of SVMPPs for Leu at the P1' position of peptides bonds [29] (Table 1).

Table 1. Peptides generated by the incubation of Matrigel with Atroxlysin-Ia (ATXL) and Batroxrhagin (BATXH).

Proteins *	Uniprot Entry	Identified Peptides *	
		ATXL	BATXH
Laminin subunit alpha-1	P19137	HADIIKGNQ IRSQQDVLGGHRQ LVEHVPGRPVR LINGRPSADDPSP	ALLHAPTGS LWDLGSGSTR LINGRPSADDPSP
Laminin subunit beta-1	P02469	AIKQADEDIQGTQN	
Laminin subunit gamma-1	P02468	IRNTIEETGI	
Tubulin beta-4B chain	P68372	HSLGGGTGSGMGT	
Vimentin	P20152	ANYQDTIGR	
Actin, cytoplasmic 2	P63260	TVLSGGTTMYPGIAD QVITIGNER	
Fibrinogen beta chain	Q8K0E8	LRPAPPISGGGY	
60 kDa heat shock protein, mitochondrial	P63038	VGGTSDVEVNEK	
60S ribosomal protein L30	P62889	IIDPGDSDIIR	
Glyceraldehyde-3-phosphate dehydrogenase	P16858	HSSTFDAGAGIA	IFQERDPTNIK ITIFQERDPTNIK
Heterogeneous nuclear ribonucleoprotein F	Q9Z2X1	SVQRPGPYDRPGTA	
Prolyl 3-hydroxylase 1	Q3V1T4	FSSGTENPHGVKA	
Transcription intermediary factor 1-beta	Q62318	LTEGPGAEGPR	
40S ribosomal protein S3	P62908		IGPKKLPDHSV
40S ribosomal protein S4, X isoform	P62702		TIRYPDPLI
78 kDa glucose-regulated protein	P20029		VAFTPEGER
Hemoglobin subunit beta-1	P02088		LVVYPWTQR
Protein disulfide-isomerase	P09103		ITSNSGVFSK

* Protein group full description, and all data on biological replicates, including criteria to accept peptide identification, are shown in Materials and Methods and Supplementary Tables S1 and S2.

2.4. Characterization of Paw Edema and Leukocyte Accumulation Induced by Matrigel-Derived Peptides

We next evaluated the proinflammatory effect of peptides generated by ATXL or BATXH hydrolysis of Matrigel. For this purpose, ATXL or BATXH were incubated with Matrigel for 1 h, and the peptide fraction was isolated by filtering on 10 kDa cut-off membranes, as described in the Methods section. The doses injected in each mouse corresponded to the total amount of peptides released from Matrigel by 10 µg of SVMs, which is the dose that induced hemorrhage in mice models [20]. Figure 6A,B shows that the products resulting from the hydrolysis of Matrigel by BATXH and ATXL were able to induce edema significantly higher than those of peptides present in Matrigel control samples. The edema was most pronounced in the periods of 30 min to 1 h after injection and reached basal levels around 3 h after injection. Peptides released from Matrigel by ATXL and BATXH caused an increase in the mouse paw of approximately 30–35%, whereas Matrigel peptides induced edema in levels comparable to saline.

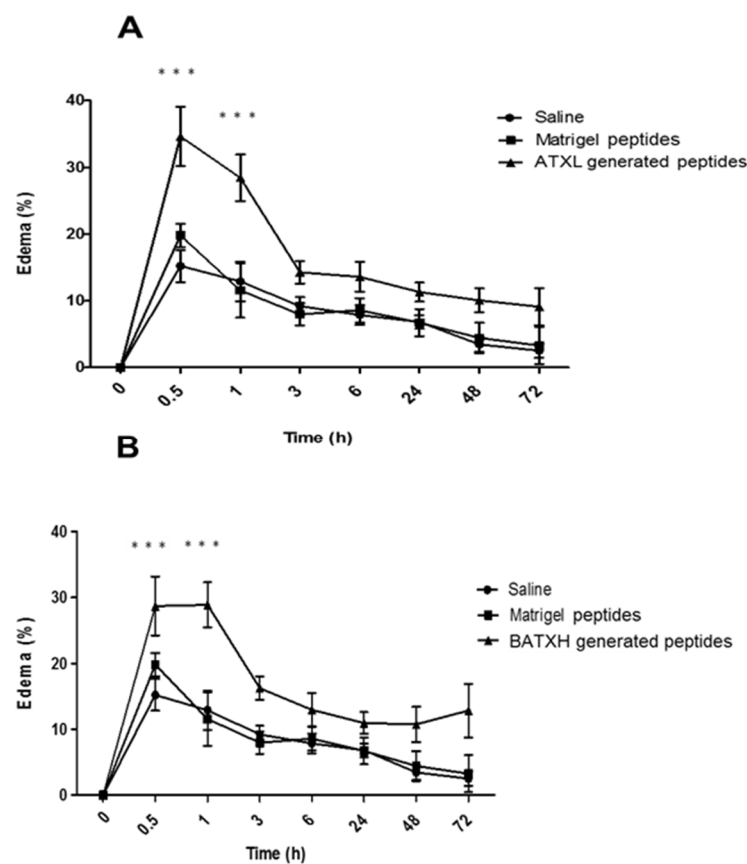


Figure 6. Time course of edema induced by peptides resulting from the hydrolysis of Matrigel by Atroxlysin-Ia (ATXL) (A) and Batroxrhagin (BATXH) (B). Matrigel was incubated with SVMs at an enzyme:substrate ratio of 1:10 (*w/w*) or with no enzyme, for 1 h, at 37 °C. After the incubation period, the samples were filtered, dried and resuspended in saline solution before injection (30 µl) into the left paw of mice (*n* = 6). The filtrate of a Matrigel sample treated under the same conditions, but without the enzymes (Matrigel peptides), was added to the experiments. Results are expressed as mean ± S.E. of two independent experiments. *** (*p* ≤ 0.001) compared to the Matrigel peptide control group.

To test the induction of leukocyte accumulation, mice were injected with peptides, as described for the characterization of the paw edema. In this assay, peptides released by ATXL hydrolysis of Matrigel caused a significantly higher leukocyte accumulation of $4\text{--}5 \times 10^6$ cells/mL, 1 and 4 h after injection, compared to Matrigel control peptides. As for BATXH, a significant increase in the number of leukocytes was observed at 4 h with 4×10^6 cells/mL. In the later periods of 24 and 48 h, Matrigel control peptides induced leukocyte influx of approximately 5×10^6 cell/mL, which is statistically higher

than the control levels observed by saline injection. Peptides released by BATXH hydrolysis of Matrigel induced influx of approximately 6×10^6 cell/mL, at 24 and 48 h periods, statistically higher than the saline control, but with no significant difference to the influx induced by the Matrigel control peptides. Peptides resulted from ATXL hydrolysis of Matrigel-induced leukocyte influx levels similar to saline control and significantly lower than Matrigel control peptides, in periods of 24 and 48 h (Figure 7).

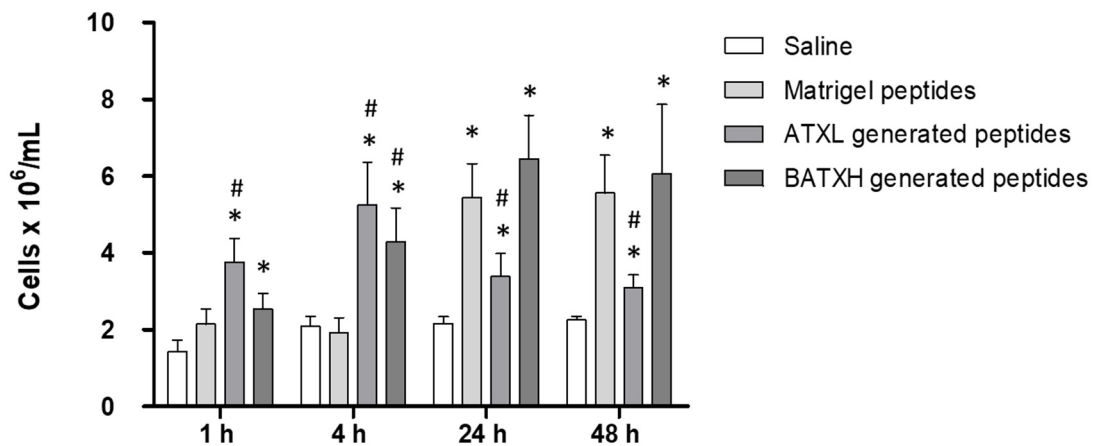


Figure 7. Time course of leukocyte accumulation in the peritoneal cavity induced by peptides released by Atroxlysin-Ia (ATXL) or Batroxrhagin (BATXH) from Matrigel. Mice were injected intraperitoneally with 30 μ L of a filtrate resulted from the hydrolysis of Matrigel by ATXL or BATXH. As controls, we used the same volume of filtrates from Matrigel sample treated under the same conditions (Matrigel peptides), but without the enzymes, or with saline only. After 1, 4, 24 and 48 h, the animals were sacrificed in a CO₂ chamber, for the removal of the peritoneal exudate. The results are expressed as the mean \pm S.E. ($n = 5-6$) of two independent experiments. Symbols indicate significant differences ($p \leq 0.05$) compared to the negative control of saline (*) or Matrigel peptides control group (#).

In differential counts, when comparing to Matrigel control peptides, the peptides resulting from the hydrolysis of Matrigel by ATXL induced a significant increase in the accumulation of polymorphonuclear cells after 1 and 4 h and peptides resulted from BATXH hydrolysis of Matrigel only at 4 h (Figure 8A). In the same periods, increases of mononuclear cells by peptides generated by hydrolysis of Matrigel by both toxins were not statistically significant comparing to Matrigel control peptides (Figure 8B). As observed for total leukocyte countings, in periods of 24 and 48 h, the number of polymorphonuclear cells (PMN) and mononuclear cells (MN) accumulated by injection of peptides from the Matrigel control was higher than saline control or peptides generated by Matrigel hydrolysis by ATXL and similar to peptides generated by BATXH hydrolysis of Matrigel.

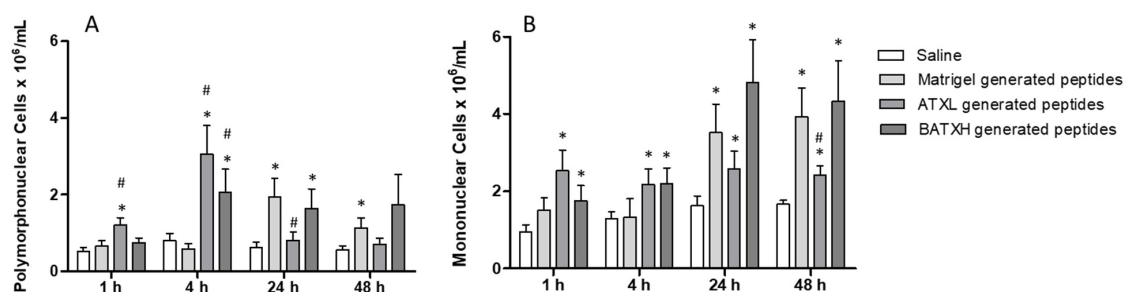


Figure 8. Differential count of leukocytes accumulated in the peritoneal cavity by Atroxlysin-Ia (ATXL) or Batroxrhagin (BATXH). Cells were identified as polymorphonuclear (A) or mononuclear (B) cells under optical microscopy (Amplification: 400 \times). The results are expressed as the mean ($n = 5-6$) of two independent experiments. Symbols indicate significant differences ($p \leq 0.05$) compared to the negative control of saline (*) or Matrigel peptides control group (#).

Thus, we considered as significant only the inflammatory reaction induced 1 and 4 h after injection of peptides released by ATXL and BATXH from Matrigel. Moreover, treatment of MPAC cultures with these peptide fractions did not induce an increase in cytokine or chemokine levels in comparison to the control samples (data not shown).

3. Discussion

SVMPs present in the venoms of *Bothrops* snakes are responsible for several inflammatory responses such as edema formation, leukocyte infiltration and the release of mediators such as cytokines and chemokines, which play an important role in the inflammatory process [17]. To compare the proinflammatory action of SVMPs, we tested the local effects of one representative of PI-class (ATXL) and one of the PIII-class (BATXH) SVMPs, both recently isolated by our group from *B. atrox* venom. Both displayed edematogenic activity at low doses ranging from 1 to 5 µg, peaking from 30 min to 1 h, comparable to the other SVMPs isolated from venoms of *Bothrops* snakes [5,30,31]. The injury time of ATXL was similar to that observed with BaP1 [5]. However, in relation to PIII-class SVMPs Jararhagin and BpirMP, BATXH edema was shown to be more persistent [30,31]. It is known that edema formation is influenced by vasoactive amine histamine and eicosanoids such as prostaglandins, which act on vasodilation and increase in the vascular permeability. In normal tissues, the production of prostaglandins is usually low, but in damaged tissues, a large production occurs that precedes the leukocyte recruitment and the process of infiltration of these cells [32,33]. Recently, De Toni et al. [34] observed that the edema in rats generated by Batroxase is mediated by histamine and LTB₄. In in vitro tests, this metalloproteinase was able to induce degranulation of mast cells, explaining in part the relation of the lesion with the presence of the mediators.

In the leukocyte accumulation induction experiments, we observed an increase in cell infiltrates in the peritoneal cavity induced by the injection of the two selected SVMPs. ATXL induced a slightly larger accumulation compared to BATXH, although not statistically significant. A significant increase of polymorphonuclear cells was observed at 4, 24 and 48 h periods by ATXL, and at 24 and 48 h by BATXH. Curiously, mononuclear cells were also observed a few hours after the induction of the reactions, but the number of mononuclear cells was higher in late periods, such as 24 and 48 h after induction with both toxins. These results are distinct than the tests performed with Batroxase, which demonstrated induction of lower levels of leukocyte influx (2×10^6 cells/mL), with increased influx of polymorphonuclear cells between 2 and 4 h, and increased infiltrate of mononuclear cells in 24 h [17] and data obtained by Fernandes et al. [35] with influx of mononuclear cells only in later periods after injection with BaP1. However, Moreira et al. [15], in agreement with our data, demonstrated the accumulation of mononuclear cells between 1 and 8 h after the induction by *B. atrox* venom, and this accumulation was attributed to the synergistic effect of the different toxins that make up the total venom. The SVMPs used in this study were also able to induce a rapid influx of mononuclear cells that could be explained due to the presence of resident cells, indicating that further analyses are necessary to fully understand the proinflammatory mechanisms of whole venoms and isolated SVMPs.

Interestingly, in spite of the structural differences between ATXL and BATXH, both toxins induced inflammatory signs at the same magnitude. The catalytic domain present on both ATXL and BATXH is involved in the degradation of ECM molecules [7], activation of pro-MMPs [10], processing of cytokines as pro-TNF-α [11] or proteins from the complement system [36]. These effects are responsible for induction or amplification of inflammatory reaction, including the cytokine release, and may be essential mechanisms involved in the proinflammatory reaction of SVMPs. Studies using MMP inhibitors have already confirmed the importance of the catalytic activity for the proinflammatory activity of SVMPs in experimental mice models. Leukocyte infiltrates induced by Jararhagin or BaP1 were reduced by treatments with chelating agents, such as o-phenanthroline or EDTA, respectively [8,35]. Escalante et al. [5] tested the action of Batimastat, a broad-spectrum synthetic inhibitor of MMPs, in local damage induced by BaP1 and observed a reduction in bleeding, dermonecrosis and edema in mouse models. More recently, Preciado et al. [37] demonstrated the efficacy of the synthetic CP 471474

inhibitor in edema induced by Batx-I, isolated from *B. atrox* venom. These observations indicate the relevance of catalytic activity for the proinflammatory activity of SVMPs. However, the importance of disintegrin-like and cysteine-rich domains of PIII-class SVMPs, present only in BATXH, has also been reported. Catalytically inactivated PIII-class SVMPs are still able to induce leukocyte recruitment [8] and mRNA synthesis of proinflammatory cytokines [12], thus implying a direct interaction with different receptors attributed to motifs present on the disintegrin-like [38], cysteine-rich domains [39] or both [13].

It has been demonstrated that the inflammatory response induced by the venom of *B. atrox* activates TLR2, which plays a role in the migration of polymorphonuclear cells [40], such as neutrophils, which are the first cells of the immune system to migrate to the site of inflammation, where they are effective in the elimination of pathogens and the production of cytokines [41]. Thus, in order to better understand the mechanisms involved in ATXL and BATXH induction of inflammation, we performed kinetic assays for the quantification of inflammatory mediators commonly found in these events. Our tests showed that MPAC cells secreted the cytokine Tumor Necrosis Factor alpha (TNF- α) when stimulated with *B. atrox* venom or BATXH, while ATXL did not induce synthesis of this mediator. In similar tests with MPAC cells, Clissa et al. [12] reported that Jararhagin, a PIII-class SVMP, induced TNF- α release, while Rucavado et al. [42] did not identify TNF- α in the culture of cells stimulated with a PI-class SVMP, the BaP1 from *B. asper* venom, indicating that the disintegrin-like and/or cysteine-rich domains present only in the PIII-class SVMPs may be acting directly on cellular receptors, thus explaining the lack of stimuli after incubation with PI-class SVMPs.

Interleukin-6 (IL-6), MCP-1 and IL-10 were not identified in the tests performed with ATXL or BATXH, and levels similar to the negative control were found in the samples incubated with the whole venom. IL-6 plays an important role during inflammation process through activation of polymorphonuclear cells, regulation of adhesion molecules, differentiation of T cells and synthesis of other cytokines [43,44], and it was already shown that different PI- and PIII-class SVMPs are able to stimulate IL-6 secretion [13,31,45]. Thus, the apparent contradiction between our observations with previous reports may be attributed to a proteolytic degradation of secreted IL-6 by the metalloproteinase activity of the enzymes, in the same fashion as previously reported in a study that used similar protocol [12].

It is known that one of the best described mechanisms of action of SVMPs is the hydrolysis of BM components, as demonstrated in in vitro and in vivo assays [46]. Baldo et al. [47] demonstrated that Jararhagin and the Jararhagin-C (devoid of catalytic domain) have an affinity for collagen IV of basal membrane and bind to tissues accumulating around the capillary vessels. Later, using in vitro assays with 2D and 3D culture models of HUVECs, it was observed that Jararhagin co-localized on the surface or was internalized by endothelial cells, and also visualized on the surface of the tubules formed in the 3D cultures [48]. The binding of Jararhagin to different substrates of the extracellular matrix as collagen IV and Matrigel and to $\alpha_2\beta_1$ integrin was also reported [29,47]. The basement membrane is a complex structure that is formed by several molecules, such as collagen IV, laminin and nidogen, among other components, and acts as a network, guaranteeing stability to blood vessels and capillaries. Furthermore, the exacerbated hydrolysis of ECM components generate a large amount of fragments that could have a secondary action on the local lesion that occurs in snakebites [27]. Heparan sulphate proteoglycans (HSPG) are also structural components of ECM that modulate adhesion and transmigration of leukocytes to the injury site [49,50]. It is very likely that the hydrolysis of these components releases small fragments acting on some mechanisms of inflammation. ECM fragments can act as damage-associated molecular patterns (DAMPs) by interacting with pattern recognition receptors (PRRs), such as Toll-like receptors (TLRs), triggering a series of proinflammatory events from the innate immune response, which may subsequently influence the adaptive immune response [51,52]. DAMPs can influence the modulation of proinflammatory mediators, cell activation, differentiation and proliferation, and stimulate regeneration processes [53,54].

Recently, it was demonstrated that the muscular exudate of CD-1 mice injected with 50 µg of *B. asper* venom was able to increase the vascular permeability of other animals injected with this material. A subproteomic analysis of this material revealed the presence of more cytokines and chemokines in the collected material 24 h after venom injection, in detriment to the exudate of 1 h, indicating that, even after venom diffusion, these mediators continue to be produced and may be related to the inflammatory processes caused during the envenoming [27]. Thus, we suggest that ECM fragments released by the proteolytic action of SVMPs from *B. atrox* venom, particularly ATXL and BATXH, could act as DAMPs and trigger endogenous stimuli similar to those occurring in cell death processes. To test this hypothesis, we evaluated whether the products of Matrigel hydrolysis by ATXL or BATXH had proinflammatory effects. Matrigel is mostly composed of collagen IV, laminin, nidogen and heparan sulphate proteoglycan. After incubating it with ATXL and BATXH, we observed complete hydrolysis by both SVMPs of the band of approximately 400 kDa, which may correspond to laminin α -chain [28]. However, only ATXL was able to fully hydrolyze the lower molecular mass band (~250 kDa), which corresponds to the molecular masses of laminin β - and γ -chains and collagen IV [7]. Nidogen [28] was partially degraded by the two SVMPs. In the LC-MS/MS analysis, peptides corresponding to laminin α -, β - and γ -chains were identified in the Matrigel samples incubated with ATXL, while BATXH generated peptides from the laminin α -chain only. Previous reports have already shown differential hydrolysis of BM components by PI- and PIII-class SVMPs. Escalante et al. [28] demonstrated the extensive hydrolysis of laminin α and γ chains by BaPI (PI-class) and in the case of Jararhagin (PIII-class) by most of hydrolysis was of the nidogen and only the α -chain of laminin. In in vivo experiments, Freitas-De-Sousa et al. [20] observed that ATXL and BATXH degraded collagen IV and laminin, with total collagen digestion by ATXL, which would explain the proteinase ability to induce hemorrhage, since these BM components play important role in the stability of capillaries.

The products resulting from the hydrolysis of the Matrigel by ATXL and BATXH were then tested for proinflammatory activity. Both samples induced a fast edema formation and peritoneal cell infiltrates in levels statistically significant when compared to Matrigel control peptides. The leukocytes found in the peritoneum region in these periods/conditions were mostly polymorphonuclear cells. Between 24 and 48 h, the number of cells accumulated by the control Matrigel peptides not exposed to SVMPs hydrolysis was higher than those of the saline control and similar to those of the BATXH-generated peptides, respectively. Commercial Matrigel is widely used in human stem cell cultures by mimicking the extracellular matrix (ECM) [55], and it is known to contain components other than structural ECM proteins, such as growth factors and MMPs 2 and 9 [56], or even intracellular or membrane proteins [55]. Talbot et al. [57] demonstrated by semi-quantitative analyses, with capture antibody arrays, the presence of various secreted or soluble proteins and peptides classified as growth factors, chemokines and other proteins with biological activity in four different lots from commercial Matrigel, including the Vascular Endothelial Growth Factor (VEGF), chemokine MCP-1 and peptide C5a. However, these results did not answer some questions about the biological activity of proteins or peptides present in Matrigel, which could impact experiments in vitro involving cell culture. The presence of these bioactive components in Matrigel may explain the fact that our control sample composed of Matrigel peptide fraction (without enzyme digestion) induced a leukocyte accumulation in the peritoneum of injected animals in periods of 24 and 48 h. However, the opposite was observed in the edema induction tests and in the early phase of the leukocyte accumulation test. In these situations, Matrigel peptides did not evoke any inflammatory activity, and this result leads us to suggest that peptides specifically liberated by incubation with ATXL or BATXH are causing the observed early events of the inflammatory reaction.

Other important aspect to be discussed is that only peptides with molecular masses smaller than 10 kDa were used in our model, to induce inflammatory reaction. According to our results of electrophoresis, hydrolysis products were spotted in bands between 30 and 220 kDa, indicating that the effects of ATXL and BATXH on Matrigel correlate more to limited proteolysis rather than unspecific degradation to small peptides. Herrera et al. [58] identified dozens of fragments derived

from extracellular matrix proteins, including heparan sulphate proteoglycan, collagen IV and nidogen, by means of proteomic analysis of the exudate extracted from the gastrocnemius muscle of mice injected with the *B. asper* venom. Considering that larger BM protein fragments also act as DAMPs and these fragments were not included in our sample, it is reasonable to expect that more evident proinflammatory effects will be observed when we test the intermediate molecular mass fragments. Based on these indications, we suggest that the peptides released after the degradation of the BM components by ATXL and BATXH are stimulating cell-receptors as part of the inflammatory process and acting indirectly on the endogenous metalloproteinases, amplifying the inflammatory response observed in the experiments.

In conclusion, ATXL and BATXH SVMPs isolated from *B. atrox* venom are capable of inducing edema formation and leukocyte recruitment in experimental models; however, they do so with slightly different profiles. ATXL induced a higher leukocyte accumulation throughout the evaluation periods, while BATXH induced MPACs for cytokine release as observed with whole venom, particularly of TNF- α . Both metalloproteinases hydrolyzed major components of Matrigel, generating products of different sizes. Once more, ATXL hydrolysis was more extensive, and all Laminin chains were completely degraded and generated peptides identified by LC-MS/MS. The products resulting from SVMP hydrolysis of Matrigel were capable of inducing edematogenic activity and leukocyte accumulation in levels significantly higher than Matrigel control peptides. These data indicate that proinflammatory action of SVMPs may occur by different a mechanism, including the participation of hydrolysis products generated from their catalytic action on BM components.

4. Materials and Methods

4.1. Toxins

Bothrops atrox venom was provided by the Herpetology Laboratory, Instituto Butantan, collected from the snakes maintained under captivity at the Institute for venom production. Atroxlysin-Ia (ATXL) and Batroxtrogin (BATXH) were isolated from *B. atrox* venom, according to the methodologies described previously [20,21].

4.2. Hydrolysis of Matrigel Components and Isolation of the Resulting Peptides

Matrigel obtained from the Engelbreth-Holm-Swarm murine sarcoma (Sigma-Aldrich, St Louis, MO, USA) was incubated with ATXL or BATXH at an enzyme:substrate ratio of 1:10 (*w/w*) in 10 mM Tris-HCl buffer, pH 7.4, for 30 min, 1 or 24 h, at 37 °C. After the incubation period, the reaction was stopped by adding one additional volume of the same ice-cold buffer, and the samples were processed in two different ways: (1) For mass spectrometry, proteins remaining in the hydrolysis solution (1 μ g enzyme:10 μ g Matrigel in 40 μ L) were precipitated by the addition of 8 volumes of ice cold acetone and 1 volume of ice cold methanol and stored for 12 h, at -20 °C. Then the peptides were recovered from the supernatants, after centrifugation for 10 min, at 14,000 \times *g*, at 4 °C. (2) For electrophoresis and biological assays, after digestion, the hydrolysis mixtures (80 μ g enzyme:800 μ g Matrigel in 1 mL) were placed in centrifugal filter devices (cut off at 10 kDa) (Amicon Ultra-2, Merck, Darmstadt,, Germany) and centrifuged at 1500 \times *g*, for 15 min, at 15 °C, until the volume of 500 μ L. Aliquots of sample retained in the filter were analyzed by electrophoresis in a 5–15% gradient polyacrylamide gel. The filtered solutions (500 μ L) were dried in a SpeedVac concentrator (Thermo Fisher Scientific, Waltham, MA, USA) and suspended in 120 μ L of ice-cold saline. Of these, 30 μ L was injected into each mouse, for in vivo assays. In this way, the amount of peptides injected into each mouse corresponded to the amount of peptides that were expected to be generated by 10 μ g of ATXL or BATXH, which is the dose at which they induce hemorrhage in mice [20].

4.3. Gel Electrophoresis

For the analysis of the material retained on the centrifugal filter devices, SDS-PAGE was performed by using 5–15% acrylamide gradient gel according to the technique described by Laemmli [59], but with some modifications. The fractions were diluted 1:3 in sample buffer (350 mM Tris-HCl, 10% SDS, 30% glycerol and 1.2 mg/mL bromophenol blue), under reducing conditions (DTT-Dithiothreitol 9.3% in sample buffer), boiled for 5 min and applied to a stacking gel with 4% polyacrylamide. Electrophoresis occurred with constant amperage of 35 mA and voltage of 180 V, using run buffer (25 mM Tris; 190 mM Glycine, 0.1% SDS, pH 8.3). The gels were stained with Coomassie R-250 blue 0.25% in 25% methanol and 5% acetic acid) and decolorized with bleach solution (40% methanol + 7% acetic acid). Precision Plus Protein Kaleidoscope molecular mass standard (M.W. 10–250 kDa, BIO-RAD, Hercules, CA, USA) was used.

4.4. Analysis of Generated Peptides by LC–MS/MS

The supernatant containing the peptide fraction obtained from the hydrolysis of Matrigel by ATXL and BATXH, as described in Section 4.2, was dried in a SpeedVac vacuum concentrator and dissolved in 0.1% TFA, for desalting, using Sep-pak C-18 cartridges previously conditioned with methanol and 0.1% TFA (Waters, Milford, MA, USA). Samples were dried and reconstituted in 0.1% formic acid (solution A), and injected in EASY Nano LCII system (Thermo Scientific, Waltham, MA, USA), into a 5 cm of 10 μ m Jupiter C-18 trap column (100 μ m I.D. \times 360 μ m O.D.) coupled to an LTQ-Orbitrap Velos mass spectrometer (Thermo Scientific). Chromatographic separation was performed on a 15 cm long column (75 μ m I.D. \times 360 μ m O.D.). Elution occurred with a linear gradient of 5–40% acetonitrile in 0.1% formic acid (solution B) in 60 min, at 200 nL/min. Spray voltage was set at 2.4 kV, and the mass spectrometer was operated in data-dependent mode, in which one full MS scan was acquired in the m/z range of 400–2000, followed by MS/MS acquisition, using higher energy collision dissociation (HCD) of the ten most intense ions from the MS scan. MS and MS/MS spectra were acquired in the Orbitrap analyzer, at 60,000 and 7500 resolution (at 400 m/z), respectively. The maximum injection time and AGC target were set to 25 ms and 1E6 for full MS, and 250 and 100 ms and 5E4 for MS/MS. The minimum signal threshold to trigger fragmentation event, isolation window and normalized collision energy (NCE) were set to, respectively, 5000 cps, 2 m/z and 40. Dynamic peak exclusion was applied to avoid the same m/z of being selected for the next 90 s. Two independent LC–MS/MS runs were performed for each sample.

Mass spectrometric raw data were analyzed by using MaxQuant software (version 1.5.3.12; Cox and Mann, 2008), using the UniProt protein sequences of *Mus musculus* (16,619 sequences, reviewed; date of fasta file: 8 February 2016). The search parameters were as follows: no enzyme specificity; deamidation of glutamine and asparagine and oxidation of methionine were considered as variable modification; peptide and MS/MS mass tolerances were set to 10 ppm and ± 0.025 Da, respectively. Data from both LC–MS/MS runs were filtered by Posterior Error Probability value ≤ 0.01 for each peptide (Supplementary Table S1). Data were further filtered to only accept peptides that were detected in both technical replicates and were absent in the control samples (Supplementary Table S2).

4.5. Evaluation of the Inflammatory Reaction Induced by ATXL, BATXH and Matrigel Hydrolysis Products

4.5.1. Animals

Male mice of the BALB/c strain (18–20 g) were used in the experiments and kept under controlled temperature and light periods with water and feed ad libitum. All experiments were approved by the Butantan Institute Ethics Committee on Animal Use (Protocol Number: 6708040817), on 22 August 2014.

4.5.2. Paw Edema

The protocols described by Kimura et al. [32] and Távora et al. [60] were used for evaluation of edema induction, but with some modifications. In the tests, mice ($n = 6/\text{group}$) had the left hind paw measured with pachymeter (Starret), prior to injection of the samples (zero time). Subsequently, the concentrations of 0.5, 1, 2 and 5 μg of the toxins diluted in 30 μL of saline or 30 μL of the peptide solution, obtained as described in Section 4.2, were injected into the plantar pad of the same foot. Animals injected with saline were used as control. The injected paws were measured again at different time intervals (30 min, 1, 3, 6, 24, 48 and 72 h), and the results were expressed as the percent of increase between the measurements of the paw at the experimental and zero time. Animals injected with saline or Matrigel treated at the same conditions, but without incubation with SVMPs, were used as control groups.

4.5.3. Leukocyte Recruitment

ATXL and BATXH or filtrates from Matrigel hydrolysis by SVMPs, obtained as described in Section 4.2 (30 μL), were diluted in 500 μL of sterile saline and injected intraperitoneally into groups of 6–12 animals/group. A group injected with saline alone or filtrates obtained from Matrigel, without SVMPs, were used as control. The animals were euthanized in the CO_2 chamber after 1, 4, 24 and 48 h, and the peritoneum was washed with 2 mL of ice-cold saline solution. The peritoneal exudate was centrifuged at $500\times g$ at 4°C for 6 min. After centrifugation, the pellet was resuspended in saline and diluted 1:10 (v/v) in the Turk's solution, with some modifications (600 μL of acetic acid + 2 mg of methyl violet in the final volume of 20 mL distilled water), and cells were counted in Newbauer's chamber. In the differential count, the cells were classified as polymorphonuclear and mononuclear, according to the morphological differences. The total and differential counts were performed under an optical microscope, with increases of $400\times$.

4.6. Production of Inflammatory Mediators

Cytokines and chemokines released by treatment with whole venom or isolated SVMPs were assayed in supernatants of stimulated MPAC cultures extracted from BALB/c mice. Animals were euthanized in a CO_2 chamber, and the peritoneum was washed and massaged with 1.5 mL of RPMI 1640 culture medium (Gibco–Life Technologies, Waltham, MA, USA) supplemented with 10% fetal bovine serum. (Gibco–Life Technologies). The obtained exudate was centrifuged at $1500\times g$ for 10 min at 4°C . The supernatant was discarded, and the cells were suspended in 2 mL of supplemented culture medium. The cells were counted in a Newbauer's chamber and subsequently placed in 96-well plates (6×10^4 cells / well), which were then incubated at 37°C , in the presence of 5% CO_2 , for 24 h. Non-adherent cells were removed by PBS washing, and cells that adhered to the plate were used in the cell viability assay and inflammatory mediator quantitation assay. Cultures were tested for the toxicity by the MTT (3-(4,5-dimethylthiazol-2-yl) 2,5-diphenyl tetrazolium bromide) cleavage assay of mitochondrial-cell enzymes, resulting in the formation of formazan blue. MPAC cells were stimulated with the nontoxic concentrations of 40 $\mu\text{g}/\text{mL}$ of ATXL, BATXH or *B. atrox* venom, LPS (1 $\mu\text{g}/\text{mL}$) (Sigma-Aldrich, St. Louis, MO, USA), or incubated with culture medium only, as negative control. Supernatants were collected at 2, 4, 6 and 18 h after the start of incubation.

TNF- α , IL-10 and IL-6 cytokines levels, and the MCP-1 chemokine in the cell culture supernatant, were quantified on the equipment FACSCantoII (BD Biosciences, Franklin Lakes, NJ, USA), using the Cytometric Bead Array (CBA) Mouse Inflammation Kit (BD Biosciences, USA), according to the manufacturer's recommendations.

4.7. Data Analysis

Student's *t*-test was performed to evaluate differences between two groups. Differences between three or more groups were assessed by ANOVA, followed by Bonferroni's test. The analyses were performed by using the software GraphPad Prism 5.0 (San Diego, CA, USA).

Supplementary Materials: The following are available online at <http://www.mdpi.com/2072-6651/12/2/96/s1>. Table S1. Identification of peptides generated by the incubation of Matrigel with ATXL and BATXH by LC-MS/MS; Table S2. Proteins present in Matrigel and identified as cleaved by ATXL and BATXH by LC-MS/MS.

Author Contributions: Conceptualization, M.T.d.A. and A.M.M.-d.-S.; experimental design, M.T.d.A., L.A.F.-d.-S., M.C., E.L.F.-M., S.M.T.S. and S.N.C.G.; data analysis, M.T.d.A., E.S.K., S.M.T.S., S.N.C.G. and A.M.M.-d.-S.; manuscript writing, M.T.d.A. and A.M.M.-d.-S.; funding acquisition, A.M.M.-d.-S.; manuscript revising, all authors. All authors have read and agreed to the published version of the manuscript.

Funding: This research was funded by Coordination for the Improvement of Higher Level Education Personnel—CAPES (063/2010-Toxinology—AuxPE 1209/2011), São Paulo Research Foundation (FAPESP 2016/50127-5; 2014/26058-8; 2013/07467-1) and the National Council for Scientific and Technological (CNPq: 303958/2018-9 AMMS; 308133/2015-3 SMTS).

Acknowledgments: The authors thank Ida Sigueko Sano Martins and Luis Roberto de Camargo Gonçalves for their support of leukocyte differential counting techniques. They also thank Luiz Roberto Sardinha, from the Butantan Instituto multi-user equipment sector, for his assistance in flow cytometry experiments.

Conflicts of Interest: The authors declare no conflicts of interest.

References

- Williams, D.J.; Faiz, M.A.; Abela-Ridder, B.; Ainsworth, S.; Bulfone, T.C.; Nickerson, A.D.; Habib, A.G.; Junghanss, T.; Fan, H.W.; Turner, M.; et al. Strategy for a globally coordinated response to a priority neglected tropical disease: Snakebite envenoming. *PLoS Negl. Trop. Dis.* **2019**, *13*, e0007059. [CrossRef] [PubMed]
- Teixeira, C.e.F.; Fernandes, C.M.; Zuliani, J.P.; Zamuner, S.F. Inflammatory effects of snake venom metalloproteinases. *Mem Inst. Oswaldo Cruz* **2005**, *100*, 181–184. [CrossRef] [PubMed]
- Zamuner, S.R.; Teixeira, C.F. Cell adhesion molecules involved in the leukocyte recruitment induced by venom of the snake *Bothrops jararaca*. *Mediat. Inflamm.* **2002**, *11*, 351–357. [CrossRef] [PubMed]
- Fox, J.W.; Serrano, S.M. Timeline of key events in snake venom metalloproteinase research. *J. Proteom.* **2009**, *72*, 200–209. [CrossRef]
- Escalante, T.; Franceschi, A.; Rucavado, A.; Gutiérrez, J.M. Effectiveness of batimastat, a synthetic inhibitor of matrix metalloproteinases, in neutralizing local tissue damage induced by BaP1, a hemorrhagic metalloproteinase from the venom of the snake *Bothrops asper*. *Biochem. Pharm.* **2000**, *60*, 269–274. [CrossRef]
- Gay, C.C.; Leiva, L.C.; Maruñak, S.; Teibler, P.; Acosta de Pérez, O. Proteolytic, edematogenic and myotoxic activities of a hemorrhagic metalloproteinase isolated from *Bothrops alternatus* venom. *Toxicon* **2005**, *46*, 546–554. [CrossRef]
- Baramova, E.N.; Shannon, J.D.; Bjarnason, J.B.; Fox, J.W. Degradation of extracellular matrix proteins by hemorrhagic metalloproteinases. *Arch. Biochem. Biophys.* **1989**, *275*, 63–71. [CrossRef]
- Costa, E.P.; Clissa, P.B.; Teixeira, C.F.; Moura-da-Silva, A.M. Importance of metalloproteinases and macrophages in viper snake envenomation-induced local inflammation. *Inflammation* **2002**, *26*, 13–17. [CrossRef]
- Silva, C.A.; Zuliani, J.P.; Assakura, M.T.; Mentele, R.; Camargo, A.C.; Teixeira, C.F.; Serrano, S.M. Activation of alpha(M)beta(2)-mediated phagocytosis by HF3, a P-III class metalloproteinase isolated from the venom of *Bothrops jararaca*. *Biochem. Biophys. Res. Commun.* **2004**, *322*, 950–956. [CrossRef]
- Rucavado, A.; Núñez, J.; Gutiérrez, J.M. Blister formation and skin damage induced by BaP1, a haemorrhagic metalloproteinase from the venom of the snake *Bothrops asper*. *Int. J. Exp. Pathol.* **1998**, *79*, 245–254.
- Moura-da-Silva, A.M.; Laing, G.D.; Paine, M.J.; Dennison, J.M.; Politi, V.; Crampton, J.M.; Theakston, R.D. Processing of pro-tumor necrosis factor-alpha by venom metalloproteinases: A hypothesis explaining local tissue damage following snake bite. *Eur. J. Immunol.* **1996**, *26*, 2000–2005. [CrossRef] [PubMed]

12. Clissa, P.B.; Laing, G.D.; Theakston, R.D.; Mota, I.; Taylor, M.J.; Moura-da-Silva, A.M. The effect of jararhagin, a metalloproteinase from *Bothrops jararaca* venom, on pro-inflammatory cytokines released by murine peritoneal adherent cells. *Toxicon* **2001**, *39*, 1567–1573. [[CrossRef](#)]
13. Clissa, P.B.; Lopes-Ferreira, M.; Della-Casa, M.S.; Farsky, S.H.; Moura-da-Silva, A.M. Importance of jararhagin disintegrin-like and cysteine-rich domains in the early events of local inflammatory response. *Toxicon* **2006**, *47*, 591–596. [[CrossRef](#)] [[PubMed](#)]
14. Campos Borges, C.; Sadahiro, M.; dos Santos, M.C. [Epidemiological and clinical aspects of snake bites in the municipalities of the state of Amazonas, Brazil]. *Rev. Soc. Bras. Med. Trop.* **1999**, *32*, 637–646. [[PubMed](#)]
15. Moreira, V.; Dos-Santos, M.C.; Nascimento, N.G.; Borges da Silva, H.; Fernandes, C.M.; D'Império Lima, M.R.; Teixeira, C. Local inflammatory events induced by *Bothrops atrox* snake venom and the release of distinct classes of inflammatory mediators. *Toxicon* **2012**, *60*, 12–20. [[CrossRef](#)]
16. Rodrigues, F.G.; Petretski, J.H.; Kanashiro, M.M.; Lemos, L.; da Silva, W.D.; Kipnis, T.L. The complement system is involved in acute inflammation but not in the hemorrhage produced by a *Bothrops atrox* snake venom low molecular mass proteinase. *Mol. Immunol.* **2004**, *40*, 1149–1156. [[CrossRef](#)]
17. Menaldo, D.L.; Bernardes, C.P.; Zoccal, K.F.; Jacob-Ferreira, A.L.; Costa, T.R.; Del Lama, M.P.; Naal, R.M.; Frantz, F.G.; Faccioli, L.H.; Sampaio, S.V. Immune cells and mediators involved in the inflammatory responses induced by a P-I metalloprotease and a phospholipase A. *Mol. Immunol.* **2017**, *85*, 238–247. [[CrossRef](#)]
18. Paine, M.J.I.; Desmond, H.P.; Theakston, R.D.G.; Crampton, J.M. Purification, cloning, and molecular characterization of a high-molecular-weight hemorrhagic metalloprotease, jararhagin, from *Bothrops jararaca* venom. Insights into the disintegrin gene family. *J. Biol. Chem.* **1992**, *267*, 22869–22876.
19. Moura-da-Silva, A.M.; Baldo, C. Jararhagin, A hemorrhagic snake venom metalloproteinase from *Bothrops jararaca*. *Toxicon* **2012**, *60*, 280–289. [[CrossRef](#)]
20. Freitas-de-Sousa, L.A.; Colombini, M.; Lopes-Ferreira, M.; Serrano, S.M.T.; Moura-da-Silva, A.M. Insights into the Mechanisms Involved in Strong Hemorrhage and Dermonecrosis Induced by Atroxlysin-Ia, a PI-Class Snake Venom Metalloproteinase. *Toxins* **2017**, *9*, 239. [[CrossRef](#)]
21. Freitas-de-Sousa, L.A.; Amazonas, D.R.; Sousa, L.F.; Sant'Anna, S.S.; Nishiyama, M.Y.; Serrano, S.M.; Junqueira-de-Azevedo, I.L.; Chalkidis, H.M.; Moura-da-Silva, A.M.; Mourão, R.H. Comparison of venoms from wild and long-term captive *Bothrops atrox* snakes and characterization of Batroxrhagin, the predominant class PIII metalloproteinase from the venom of this species. *Biochimie* **2015**, *118*, 60–70. [[CrossRef](#)] [[PubMed](#)]
22. Sanchez, E.F.; Schneider, F.S.; Yarleque, A.; Borges, M.H.; Richardson, M.; Figueiredo, S.G.; Evangelista, K.S.; Eble, J.A. The novel metalloproteinase atroxlysin-I from Peruvian *Bothrops atrox* (Jergón) snake venom acts both on blood vessel ECM and platelets. *Arch. Biochem. Biophys.* **2010**, *496*, 9–20. [[CrossRef](#)] [[PubMed](#)]
23. Cintra, A.C.; De Toni, L.G.; Sartim, M.A.; Franco, J.J.; Caetano, R.C.; Murakami, M.T.; Sampaio, S.V. Batroxase, a new metalloproteinase from *B. atrox* snake venom with strong fibrinolytic activity. *Toxicon* **2012**, *60*, 70–82. [[CrossRef](#)] [[PubMed](#)]
24. Malinda, K.M.; Kleinman, H.K. The laminins. *Int. J. Biochem. Cell Biol.* **1996**, *28*, 957–959. [[CrossRef](#)]
25. Freitas, V.M.; Jaeger, R.G. The effect of laminin and its peptide SIKVAV on a human salivary gland adenoid cystic carcinoma cell line. *Virchows Arch.* **2002**, *441*, 569–576. [[CrossRef](#)]
26. Siqueira, A.S.; Pinto, M.P.; Cruz, M.C.; Smuczek, B.; Cruz, K.S.; Barbuto, J.A.; Hoshino, D.; Weaver, A.M.; Freitas, V.M.; Jaeger, R.G. Laminin-111 peptide C16 regulates invadopodia activity of malignant cells through $\beta 1$ integrin, Src and ERK 1/2. *Oncotarget* **2016**, *7*, 47904–47917. [[CrossRef](#)]
27. Rucavado, A.; Nicolau, C.A.; Escalante, T.; Kim, J.; Herrera, C.; Gutiérrez, J.M.; Fox, J.W. Viperid Envenomation Wound Exudate Contributes to Increased Vascular Permeability via a DAMPs/TLR-4 Mediated Pathway. *Toxins* **2016**, *8*, 349. [[CrossRef](#)]
28. Escalante, T.; Shannon, J.; Moura-da-Silva, A.M.; Gutiérrez, J.M.; Fox, J.W. Novel insights into capillary vessel basement membrane damage by snake venom hemorrhagic metalloproteinases: A biochemical and immunohistochemical study. *Arch. Biochem. Biophys.* **2006**, *455*, 144–153. [[CrossRef](#)]
29. Paes Leme, A.F.; Sherman, N.E.; Smalley, D.M.; Sizukusa, L.O.; Oliveira, A.K.; Menezes, M.C.; Fox, J.W.; Serrano, S.M. Hemorrhagic activity of HF3, a snake venom metalloproteinase: Insights from the proteomic analysis of mouse skin and blood plasma. *J. Proteome Res.* **2012**, *11*, 279–291. [[CrossRef](#)]
30. Dale, C.S.; Gonçalves, L.R.; Juliano, L.; Juliano, M.A.; da Silva, A.M.; Giorgi, R. The C-terminus of murine S100A9 inhibits hyperalgesia and edema induced by jararhagin. *Peptides* **2004**, *25*, 81–89. [[CrossRef](#)]

31. Bernardes, C.P.; Menaldo, D.L.; Mamede, C.C.; Zoccal, K.F.; Cintra, A.C.; Faccioli, L.H.; Stanziola, L.; de Oliveira, F.; Sampaio, S.V. Evaluation of the local inflammatory events induced by BpirMP, a metalloproteinase from *Bothrops pirajai* venom. *Mol. Immunol.* **2015**, *68*, 456–464. [[CrossRef](#)] [[PubMed](#)]
32. Kimura, L.F.; Prezotto-Neto, J.P.; Távora, B.C.; Faquim-Mauro, E.L.; Pereira, N.A.; Antoniazzi, M.M.; Jared, S.G.; Teixeira, C.F.; Santoro, M.L.; Barbaro, K.C. Mast cells and histamine play an important role in edema and leukocyte recruitment induced by *Potamotrygon motoro* stingray venom in mice. *Toxicon* **2015**, *103*, 65–73. [[CrossRef](#)] [[PubMed](#)]
33. Ricciotti, E.; FitzGerald, G.A. Prostaglandins and inflammation. *Arter. Thromb. Vasc. Biol.* **2011**, *31*, 986–1000. [[CrossRef](#)]
34. De Toni, L.G.; Menaldo, D.L.; Cintra, A.C.; Figueiredo, M.J.; de Souza, A.R.; Maximiano, W.M.; Jamur, M.C.; Souza, G.E.; Sampaio, S.V. Inflammatory mediators involved in the paw edema and hyperalgesia induced by Batroxase, a metalloproteinase isolated from *Bothrops atrox* snake venom. *Int. Immunopharmacol.* **2015**, *28*, 199–207. [[CrossRef](#)]
35. Fernandes, C.M.; Zamuner, S.R.; Zuliani, J.P.; Rucavado, A.; Gutiérrez, J.M.; Teixeira, C.e.F. Inflammatory effects of BaP1 a metalloproteinase isolated from *Bothrops asper* snake venom: Leukocyte recruitment and release of cytokines. *Toxicon* **2006**, *47*, 549–559. [[CrossRef](#)]
36. Farsky, S.H.; Gonçalves, L.R.; Gutiérrez, J.M.; Correa, A.P.; Rucavado, A.; Gasque, P.; Tambourgi, D.V. *Bothrops asper* snake venom and its metalloproteinase BaP-1 activate the complement system. Role in leucocyte recruitment. *Mediat. Inflamm.* **2000**, *9*, 213–221. [[CrossRef](#)]
37. Preciado, L.M.; Pereañez, J.A.; Comer, J. Potential of Matrix Metalloproteinase Inhibitors for the Treatment of Local Tissue Damage Induced by a Type P-I Snake Venom Metalloproteinase. *Toxins* **2019**, *12*, 8. [[CrossRef](#)]
38. Moura-da-Silva, A.M.; Ramos, O.H.P.; Baldo, C.; Niland, S.; Hansen, U.; Ventura, J.S.; Furlan, S.; Butera, D.; Della-Casa, M.S.; Tanjoni, I.; et al. Collagen binding is a key factor for the hemorrhagic activity of snake venom metalloproteinases. *Biochimie* **2008**, *90*, 484–492. [[CrossRef](#)]
39. Menezes, M.C.; Leme, A.F.P.; Melo, R.L.; Silva, C.A.; Della Casa, M.; Bruni, F.M.; Lima, C.; Lopes-Ferreira, M.; Camargo, A.C.M.; Fox, J.W.; et al. Activation of leukocyte rolling by the cysteine-rich domain and the hyper-variable region of HF3, a snake venom hemorrhagic metalloproteinase. *Febs Lett.* **2008**, *582*, 3915–3921. [[CrossRef](#)]
40. Moreira, V.; Teixeira, C.; da Silva, H.B.; Lima, M.R.D.; Dos-Santos, M.C. The role of TLR2 in the acute inflammatory response induced by *Bothrops atrox* snake venom. *Toxicon* **2016**, *118*, 121–128. [[CrossRef](#)]
41. Delgado-Rizo, V.; Martínez-Guzmán, M.A.; Iñiguez-Gutierrez, L.; García-Orozco, A.; Alvarado-Navarro, A.; Fafutis-Morris, M. Neutrophil Extracellular Traps and Its Implications in Inflammation: An Overview. *Front. Immunol.* **2017**, *8*, 81. [[CrossRef](#)]
42. Rucavado, A.; Escalante, T.; Teixeira, C.F.; Fernandes, C.M.; Diaz, C.; Gutiérrez, J.M. Increments in cytokines and matrix metalloproteinases in skeletal muscle after injection of tissue-damaging toxins from the venom of the snake *Bothrops asper*. *Mediat. Inflamm* **2002**, *11*, 121–128. [[CrossRef](#)]
43. Fasshauer, M.; Klein, J.; Lossner, U.; Paschke, R. Interleukin (IL)-6 mRNA expression is stimulated by insulin, isoproterenol, tumour necrosis factor alpha, growth hormone, and IL-6 in 3T3-L1 adipocytes. *Horm. Metab. Res.* **2003**, *35*, 147–152. [[CrossRef](#)]
44. Tanaka, T.; Narazaki, M.; Kishimoto, T. IL-6 in inflammation, immunity, and disease. *Cold Spring Harb Perspect. Biol.* **2014**, *6*, a016295. [[CrossRef](#)]
45. Lopes, D.S.; Baldo, C.; Oliveira, C.e.F.; de Alcântara, T.M.; Oliveira, J.D.; Goullart, L.R.; Hamaguchi, A.; Homs-Brandeburgo, M.I.; Moura-da-Silva, A.M.; Clissa, P.B.; et al. Characterization of inflammatory reaction induced by neuwiedase, a P-I metalloproteinase isolated from *Bothrops neuwiedi* venom. *Toxicon* **2009**, *54*, 42–49. [[CrossRef](#)]
46. Gutiérrez, J.M.; Escalante, T.; Rucavado, A.; Herrera, C.; Fox, J.W. A Comprehensive View of the Structural and Functional Alterations of Extracellular Matrix by Snake Venom Metalloproteinases (SVMPs): Novel Perspectives on the Pathophysiology of Envenoming. *Toxins* **2016**, *8*, 304. [[CrossRef](#)]
47. Baldo, C.; Jamora, C.; Yamanouye, N.; Zorn, T.M.; Moura-da-Silva, A.M. Mechanisms of vascular damage by hemorrhagic snake venom metalloproteinases: Tissue distribution and in situ hydrolysis. *PLoS Negl. Trop. Dis.* **2010**, *4*, e727. [[CrossRef](#)]

48. Baldo, C.; Lopes, D.S.; Faquim-Mauro, E.L.; Jacysyn, J.F.; Niland, S.; Eble, J.A.; Clissa, P.B.; Moura-da-Silva, A.M. Jararhagin disruption of endothelial cell anchorage is enhanced in collagen enriched matrices. *Toxicon* **2015**, *108*, 240–248. [[CrossRef](#)]
49. Taylor, K.R.; Gallo, R.L. Glycosaminoglycans and their proteoglycans: Host-associated molecular patterns for initiation and modulation of inflammation. *Faseb. J.* **2006**, *20*, 9–22. [[CrossRef](#)]
50. Parish, C.R. Heparan sulfate and inflammation. *Nat. Immunol.* **2005**, *6*, 861–862. [[CrossRef](#)]
51. Frevert, C.W.; Felgenhauer, J.; Wygrecka, M.; Nastase, M.V.; Schaefer, L. Danger-Associated Molecular Patterns Derived From the Extracellular Matrix Provide Temporal Control of Innate Immunity. *J. Histochem. Cytochem.* **2018**, *66*, 213–227. [[CrossRef](#)] [[PubMed](#)]
52. Newton, K.; Dixit, V.M. Signaling in innate immunity and inflammation. *Cold Spring Harb. Perspect. Biol.* **2012**, *4*. [[CrossRef](#)] [[PubMed](#)]
53. Anders, H.J.; Schaefer, L. Beyond tissue injury-damage-associated molecular patterns, toll-like receptors, and inflammasomes also drive regeneration and fibrosis. *J. Am. Soc. Nephrol.* **2014**, *25*, 1387–1400. [[CrossRef](#)] [[PubMed](#)]
54. Sorokin, L. The impact of the extracellular matrix on inflammation. *Nat. Rev. Immunol.* **2010**, *10*, 712–723. [[CrossRef](#)] [[PubMed](#)]
55. Hughes, C.S.; Postovit, L.M.; Lajoie, G.A. Matrigel: A complex protein mixture required for optimal growth of cell culture. *Proteomics* **2010**, *10*, 1886–1890. [[CrossRef](#)] [[PubMed](#)]
56. Kleinman, H.K.; Martin, G.R. Matrigel: Basement membrane matrix with biological activity. *Semin. Cancer Biol.* **2005**, *15*, 378–386. [[CrossRef](#)]
57. Talbot, N.C.; Caperna, T.J. Proteome array identification of bioactive soluble proteins/peptides in Matrigel: Relevance to stem cell responses. *Cytotechnology* **2015**, *67*, 873–883. [[CrossRef](#)]
58. Herrera, C.; Macêdo, J.K.; Feoli, A.; Escalante, T.; Rucavado, A.; Gutiérrez, J.M.; Fox, J.W. Muscle Tissue Damage Induced by the Venom of *Bothrops asper*: Identification of Early and Late Pathological Events through Proteomic Analysis. *Plos Negl. Trop. Dis.* **2016**, *10*, e0004599. [[CrossRef](#)]
59. Laemmli, U.K. Cleavage of structural proteins during the assembly of the head of bacteriophage T4. *Nature* **1970**, *227*, 680–685. [[CrossRef](#)]
60. Távora, B.C.; Kimura, L.F.; Antoniazzi, M.M.; Chiariello, T.M.; Faquim-Mauro, E.L.; Barbaro, K.C. Involvement of mast cells and histamine in edema induced in mice by *Scolopendra viridicornis* centipede venom. *Toxicon* **2016**, *121*, 51–60. [[CrossRef](#)]



© 2020 by the authors. Licensee MDPI, Basel, Switzerland. This article is an open access article distributed under the terms and conditions of the Creative Commons Attribution (CC BY) license (<http://creativecommons.org/licenses/by/4.0/>).

APÊNDICE B - Processing of Snake Venom Metalloproteinases: generation of toxin diversity and enzyme inactivation.

Review

Processing of Snake Venom Metalloproteinases: Generation of Toxin Diversity and Enzyme Inactivation

Ana M. Moura-da-Silva ^{1,*}, Michelle T. Almeida ¹, José A. Portes-Junior ¹, Carolina A. Nicolau ², Francisco Gomes-Neto ² and Richard H. Valente ²

¹ Laboratório de Imunopatologia, Instituto Butantan, São Paulo CEP 05503-900, Brazil; michelle.almeida@butantan.gov.br (M.T.A.); portes.junior@butantan.gov.br (J.A.P.-J.)

² Laboratório de Toxinologia, Instituto Oswaldo Cruz, Rio de Janeiro CEP 21040-360, Brazil; carolnicolau.bio@gmail.com (C.A.N.); gomes.netof@gmail.com (F.G.-N.); richardhemmi@gmail.com (R.H.V.)

* Correspondence: ana.moura@butantan.gov.br; Tel.: +55-11-2627-9779

Academic Editors: Jay Fox and José María Gutiérrez

Received: 4 May 2016; Accepted: 3 June 2016; Published: 9 June 2016

Abstract: Snake venom metalloproteinases (SVMPs) are abundant in the venoms of vipers and rattlesnakes, playing important roles for the snake adaptation to different environments, and are related to most of the pathological effects of these venoms in human victims. The effectiveness of SVMPs is greatly due to their functional diversity, targeting important physiological proteins or receptors in different tissues and in the coagulation system. Functional diversity is often related to the genetic diversification of the snake venom. In this review, we discuss some published evidence that posit that processing and post-translational modifications are great contributors for the generation of functional diversity and for maintaining latency or inactivation of enzymes belonging to this relevant family of venom toxins.

Keywords: snake venom; metalloproteinase; post-translational processing; enzyme inhibitor; hemorrhage

1. Introduction

Generation of diversity is a very important feature in the evolution of different species of animals, especially in systems in which fast adaptation to the environment is required. The most relevant system in which the generation of diversity plays a key role is the immune system. A large repertoire of antibody molecules, T cell receptors, and MHC antigens are mostly generated by intrinsic mechanisms of genetic recombination, together with post-transcriptional and post-translational processing [1–7], generating molecules responsible for host protection against aggressors and for self-maintenance. Although such a large repertoire is not necessary for many other systems, generation of diversity is also used as mechanism for fitness enhancement in most venomous animals, from cone snails [8] to advanced snakes [9], generating a toxin array that interacts with functionally-relevant receptors of different species [10], enabling capture of a greater diversity of prey, or evasion from different predators. In advanced snakes, generation of diversity of venom components was a great adaptive advantage that allowed the radiation of several taxa after the appearance of the venom glands, recruitment and neofunctionalization of toxin genes, and development of the venom injection system [9,10]. A few gene families have been recruited for snake venom production [11]. However, these genes are under accelerated evolution and undergo a number of duplications followed by distinct genetic modification mechanisms as accumulation of substitutive mutations, domain loss, recombination, and neofunctionalization that result in the large diversity within venom toxin gene families [12–17].

Snake venom metalloproteinases (SVMPs) are particularly important for the adaptation of snakes to different environments. In the venoms of most species of viper snakes, SVMPs are the most abundant component [18,19] and, as discussed above, the evolutionary mechanisms of this gene family allowed the structural and functional diversity of SVMPs in viper venoms. SVMPs are able to interact with different targets that control hemostasis or relevant tissues related to essential physiological functions in prey and predators [20,21]. The most evident effect of SVMPs is hemorrhage, as a result of a combined disruption of capillary vessels integrity and impairment of the blood coagulation system, resulting in consumption of coagulation plasma factors [20]. The mechanisms of action of distinct SVMPs involve different targets as, for example, activation of coagulation Factor X [22], activation of Factor II [23], fibrino(gen)olytic activity [24], binding and damage of capillary vessels [25–27], among others. SVMPs interacting with distinct hemostatic targets may be found in the same pool of venom from a single species [21] and, together, these different enzymes interfere with the whole hemostatic system, subduing prey usually by shock [28].

The structural diversity of SVMPs is well known [29–31] and three classes (P-I, P-II, and P-III), further subdivided into at least 11 subclasses, have been described based on their domain structure [31]. This classification is based on the presence of different domains in the zymogens predicted by the mRNA sequences and the mature form of the enzymes. They are synthesized as pro-enzymes with pre- and prodomains responsible for directing the nascent proteins to the endoplasmic reticulum and for maintaining the latency of the enzyme before secretion, respectively [32,33]. The mechanism involved in the activation of SVMPs (step of biosynthesis involving the removal of the prodomain) is still understudied. Furthermore, an eventual role played by the free prodomain (or its fragments) in enzyme activity after secretion is elusive. In addition to pre- and prodomains, a catalytic domain is present in P-I, P-II, and P-III classes at the C-terminus of the prodomain and is the only domain present in mature class P-I SVMPs. P-II and P-III SVMP classes differ from the former by the presence of non-catalytic domains included at the C-terminus of the catalytic domain: the disintegrin domain in P-II class and disintegrin-like plus cysteine-rich domains in the P-III class [31].

Genes coding for P-III class SVMPs appear to have been the first recruited to the snake venom while P-II and P-I SVMP genes appeared in viperids later, mostly by domain loss [16]. However, genetic mechanisms are not the only ones responsible for generating diversity in SVMPs. Due to the recent increase of data generated by venom proteomes and transcriptomes, it has also become evident that post-transcriptional [34] and post-translational [35] modifications represent additional sources of diversity generation in venom composition, increasing the possibilities of mechanisms of predation and resulting in an adaptive advantage for snakes. In this review, we will focus on the role of processing of nascent SVMPs in the generation of diversity and in the inactivation of these enzymes during and after their biosynthesis.

2. Biosynthesis and Post-Translational Processing of SVMPs

SVMP transcripts predict proteins with multi-domain structure that undergo different post-translational processing generating distinct mature proteins (Figure 1). As other secreted proteins, SVMPs include a signal-peptide/prodomain (p) responsible for driving the nascent SVMP to the endoplasmic reticulum where most of the protein modifications take place. In the endoplasmic reticulum, the pre-domain is removed by signal peptidases (Figure 1-①) resulting in zymogens that are subjected to further modifications [36]. Activation of the enzymes occurs by hydrolysis of the prodomain (Figure 1-②) [37] and, after this step, disintegrin or disintegrin-like/cysteine-rich domains can also be released by proteolysis (Figure 1-③) [38]. Mature forms may present other modifications such as cyclization of amino-terminal glutamyl residues to pyro-glutamate (Figure 1-④), glycosylation (Figure 1-⑤), addition of new domains (Figure 1-⑥), or dimerization of protein chains (Figure 1-⑦) [36]. These steps occur to different extents depending on the primary structure of the precursors predicted by the paralogue genes that originate the transcripts. As a result, different biological activities are associated to each particular isoform. Therefore, post-translational modifications are essential for

activity and stability of the proteins, and also for diversifying their specific targets. Some of the issues related to each of these processing steps will be discussed below.

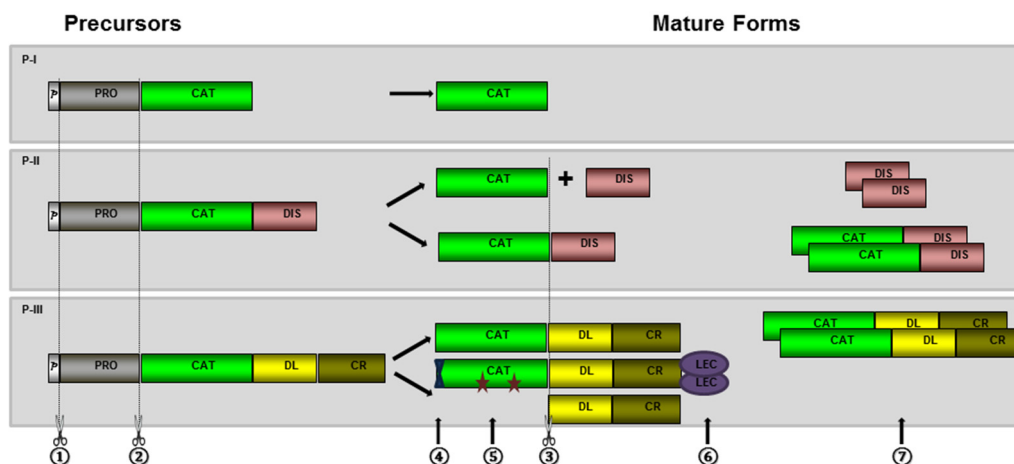


Figure 1. Schematic representation of the most typical post-translational modification steps occurring during the maturation of nascent SVMPs: SVMP precursors are composed of signal-peptide/pre-(p), pro- (PRO), catalytic or metalloproteinase (CAT), disintegrin (DIS), disintegrin-like (DL), cysteine-rich (CR), and lectin-like (LEC) domains. Processing of nascent SVMP involves removal of signal-peptide/pre-domain (①) hydrolysis of the prodomain (②) and disintegrin or disintegrin-like/cysteine-rich domains (③), cyclization of amino-terminal glutamyl residues to pyro-glutamate (④), glycosylation (represented by stars—⑤), addition of new domains (⑥) or dimerization of protein chains (⑦).

2.1. Hydrolysis of the Prodomain

Activation of SVMPs is regulated by hydrolysis of their prodomains, as happens with matrix metalloproteinases (MMPs) and disintegrin and metalloproteinase (ADAM) proteins. Prodomains of SVMPs include a conserved motif (PKMCGVT), also found in ADAM and MMP precursors [33]. In this motif, a free cysteine residue is a key factor for maintaining enzyme latency via a cysteine-switch mechanism. This process controls the activation state of enzymes by blocking the catalytic site (inactivated state) before the proteolytic processing of the prodomain (active state) [33,39].

In MMPs, activation generally occurs at the extracellular space catalyzed by members of the plasminogen/plasmin cascade, by other MMPs or by chemical modification of the conserved cysteine residue in the cysteine switch motif [40–42]. A different mechanism of activation is verified in ADAMs, as the prodomain is generally removed intracellularly by pro-protein convertases [43], or by autocatalytic mechanisms [31,44,45]. In SVMPs, only a few studies attempted to explain enzyme activation and/or hydrolysis of their prodomains. However, studying the activation of recombinant pro-atrolysin-E, Shimokawa and collaborators [38] suggested that chemical modifications are not efficient for activation, which probably occurs by proteolysis by metalloproteinase present on the crude venom. In a recent study from our group [46], we used antibodies specific to jararhagin prodomain to search for the presence of prodomains in different compartments of snake venom glands, either as zymogens or in the processed form. Using gland extracts obtained at different times of the venom production cycle, we immunodetected electrophoretic bands matching to the SVMP zymogen molecular mass (in high abundance), and only faint bands with molecular masses corresponding to different forms of cleaved prodomain. However, the presence of zymogens in the venom was rare, detected only as faint bands in samples collected from the lumen of venom gland at the peak of venom production. In milked venom, only weak bands corresponding to free prodomain were detected in samples collected at the peak of venom production, suggesting that most of the prodomain molecules promptly undergo further hydrolysis, generating diverse peptides that are

not immunoreactive with anti-PD-Jar (Figure 2). In agreement to this suggestion, SVMP prodomain peptides are very rare in proteomes of viper venoms, with a few exceptions [47], but they were recently found in the proteopeptidome of *B. jararaca* venom [48], and in proteomes of *B. jararaca* gland extracts [49], which is consistent with our hypothesis.

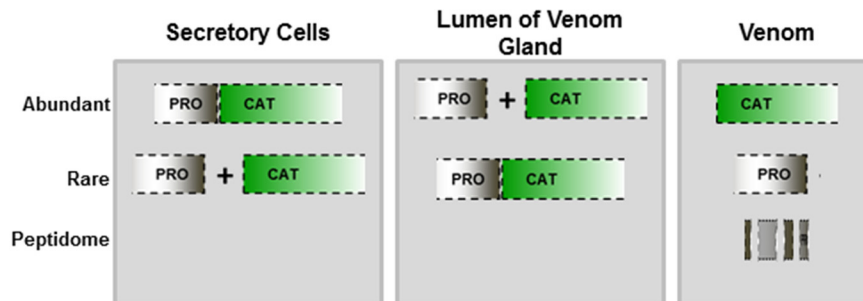


Figure 2. Schematic representation of prodomain processing: Antibodies against jararhagin prodomain detected predominantly bands of zymogen molecular mass in secretory cells and processed form in the lumen of the venom gland. Prodomain was poorly detected in the venom, suggesting that SVMPs are mostly in the active form.

Using immunohistochemistry and immunogold electromicroscopy, prodomain detection was concentrated in secretory vesicles of secretory cells (Figure 3). According to these images, we suggested that SVMPs are stored at secretory cell vesicles mostly as zymogens; the processing of prodomains starts within the secretory vesicles but reaches its maximal level during secretion or as soon as it reaches the lumen of the venom gland.

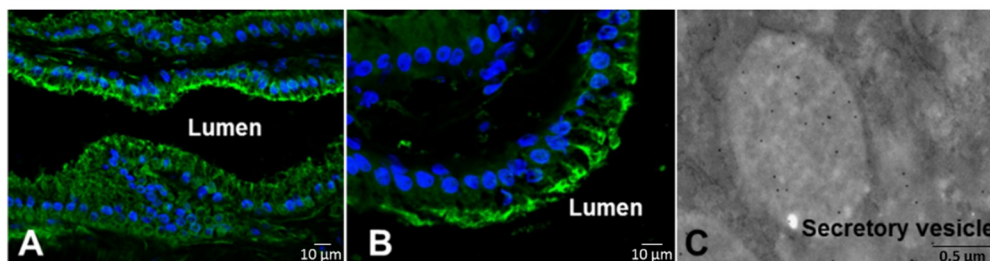


Figure 3. Cellular localization of prodomains. Venom glands collected before (A) or seven days after (B, C) venom extraction were sectioned and subjected to immunofluorescence (A, B) stained with DAPI (blue) and mouse anti-PD-Jar serum (green), which concentrated in the apical region of secretory cells, or electron microscopy (C) after staining with anti-PD-Jar serum, which highlighted spots in the secretory vesicles [46].

According to these data, processing and activation of SVMPs undergo distinct routes than MMPs or ADAMs. MMPs are critical enzymes for remodeling the extracellular matrix in a series of physiological and pathological processes as angiogenesis, wound healing, inflammation, cancer, and infections [40,50]. The regulatory role of MMPs in such processes requires a well-controlled mechanism of activation for which the secretion of latent enzymes is of great advantage. On the other hand, most ADAMs are transmembrane proteins that regulate mostly cell migration, adhesion, signaling and, eventually, proteolysis. In this case, processing of ADAMs through the secretion pathway by furins and other processing enzymes is the most common processing route [43,51]. SVMPs apparently undergo different processing routes since the release of the prodomain is very likely to occur during the secretion of vesicle contents. The enzymes responsible for the processing have not yet been identified, but it can be speculated that venom serine proteinases or even metalloproteinases could be involved. Moreover,

a series of convertases have been detected in proteomic and transcriptomic studies [49]. One issue that remains unsolved and will be discussed below is whether SVMPs are maintained in the lumen of the venom gland in the active form or are kept inactivated by peptides liberated by prodomain hydrolysis or by other inhibitory factors present in the venom as the acidic pH environment, high citrate concentrations and tripeptides containing pyroglutamate.

2.2. Generation of Disintegrin and Disintegrin-Like Domains

Disintegrins are generated by proteolysis of SVMPs originated from class P-II transcripts. These small molecules are abundant in venoms of viper snakes that usually contain the RGD or a related (XGD) motif in a surface exposed loop that binds to RGD-dependent integrins, such as $\alpha_{IIb}\beta_3$, $\alpha_5\beta_1$, and $\alpha_v\beta_3$ or, in a few cases, they may display a MLD motif, targeting $\alpha_4\beta_1$, $\alpha_4\beta_7$, and $\alpha_9\beta_1$, or a K/RTS motif that is very selective for binding to $\alpha_1\beta_1$ integrin [52]. These are important receptors of different cell types, particularly platelets, inflammatory, and vascular endothelial cells, in which they are responsible for inhibition of platelet aggregation or endothelial cell adhesion, migration, and angiogenesis [53,54]. For these reasons, the inclusion of disintegrins in the venom of viper snakes conferred a great adaptive advantage for using hemostatic targets to surrender prey.

Genes coding for class P-II SVMPs have evolved from P-III ancestor genes by a single loss of the cysteine-rich domain followed by convergent losses of the disintegrin domain at different phylogenetic branches that were further responsible for the generation of distinct P-I SVMP structures [16]. After the cysteine-rich domain loss, evolution of P-II genes was continued by gene duplication and neofunctionalization of the disintegrin domain in some of the duplicated copies [16,55]. Other genetic mechanisms of recombination as exon shuffling or pre- or post-transcriptional recombination could also play a role in the diversification of class P-II SVMP structures. The first draft of the genomic organization of a P-III-SVMP gene revealed a series of nuclear retroelements and transposons within introns that could provide genomic explanations for the emergence of distinct class P-II messengers [56]. Evidence for post-transcriptional modification arose when *B. neuwiedi* SVMP cDNA sequences were analyzed: three distinct types of P-II sequences were noted including a typical transcript of class P-II SVMP and other transcripts that presented clear indications of recombination between P-II disintegrin domain coding regions with either P-I or P-III catalytic domain coding regions [34]. The data suggest that recombination between genes encoding SVMPs might have occurred after the emergence of the primary gene copies coding for each scaffold. Moreover, it has also been reported by different authors the occurrence of SVMP structures that might have been assembled by the P-III catalytic domain with the P-II disintegrin domain [57] or even by P-II catalytic domains with the P-III disintegrin-like domains lacking the cysteine-rich domain [58]. Unfortunately, these mechanisms of recombination are still speculative since, up to now, genomic sequences coding for SVMPs were not completely disclosed and the exon/intron distribution at catalytic domain is still unknown.

In viper venoms, the products of P-II genes are diverse and the precursors undergo proteolytic steps depending on the structure predicted by the paralogue gene coding for each different toxin. Most P-II precursors are hydrolyzed at the spacer region, located between catalytic and disintegrin domains [31] generating free disintegrins and catalytic domains that are frequently found in venoms, and also recognized as classical disintegrins and P-I class SVMPs, respectively. However, some P-II precursors are not hydrolyzed and are expressed in the venom as single chained molecules, containing catalytic and disintegrin domains. The enzymes involved in the cleavage of P-II precursors to generate free disintegrins are still unrecognized and the mechanisms by which different P-II precursors are processed (or not) are still speculative. A mainstream hypothesis, postulated by Serrano and Fox [31], suggests that the presence of cysteinyl residues, particularly at the spacer region and at the N-terminus of the disintegrin domain, would confer more resistance to hydrolysis, acting in favor of maintenance of P-II SVMPs in the catalytic form. A few of these enzymes have been characterized [53,59–61] and recent reports indicate potent hemorrhagic activity in catalytic P-II SVMPs that may be achieved by

their capability to cleave ECM proteins combined to their potential to inhibit platelet aggregation and/or to bind to basal lamina [62].

Some P-III class SVMPs are also cleaved generating fragments which correspond to the disintegrin-like/cysteine-rich domains [31]. However, cleavage mechanisms and the fate of the domains after cleavage are apparently different than the ones observed in P-II SVMPs. Most P-III SVMPs are found in venoms in their multi-domain form, containing catalytic, disintegrin-like and cysteine-rich domains, although examples of autolysis at the spacer region of isolated P-III SVMPs have been reported for jararhagin, from *Bothrops jararaca* [63], HR1A and HR1B from *Trimeresurus flavoviridis* [64], HT-1 from *Crotalus ruber ruber* [64], brevilysin H6, from *Gloydius halys brevicaudus* [65], alternagin, from *Bothrops alternatus* [66], batroxhagin, from *Bothrops atrox* [67,68], and catrocollastatin, from *Crotalus atrox* [69]. Autolysis of these proteins usually results in combined disintegrin-like/cysteine-rich domain fragments, known as “C” proteins, which are characterized as inhibitors of collagen-induced platelet-aggregation [63], but may also display pro-inflammatory activity [70] or stimulate endothelial cells to release pro-angiogenic mediators [71]. On the other hand, the free catalytic domain that results from this autolytic process has never been found in venoms, suggesting that a fast hydrolysis of the catalytic domain to small peptides occurs after autolysis. In *B. jararaca* venom, the presence of both intact jararhagin and processed jararhagin-C is currently detected [63,72]. Moreover, a third form of processed protein was detected that comprised a processed form of jararhagin-C linked to the catalytic domain by disulfide bonds [73]. This evidence suggests that at least three different proteoforms of jararhagin may exist and they probably display distinct pairing of cysteinyl residues that will drive to three different autolytic pathways. The three possibilities of autolysis appear to occur in venoms of other snakes. We recently reported the same three forms of processed batroxhagin, a P-III SVMP isolated from the venom of *B. atrox* [67]. The presence of these different forms of P-III SVMPs in venoms contributes to greater structural and functional complexity of the venom, and may be a common feature among other class P-III SVMPs.

2.3. Dimerization and Inclusion of Other Domains

The position and pairing of cysteinyl residues certainly play a role in the liberation of disintegrins, but they are also very important in generating multimeric structures of some nascent SVMPs, increasing their structural and functional diversity. One example is the linkage of lectin-like domains to the cysteine-rich domain of class P-III SVMPs generating very active pro-coagulant toxins as RVV-X, from *Vipera russelli* [32–34], classified as a PIIIId, or previously as a P-IV SVMP [30]. However, homodimers or heterodimers of homologous domains are most commonly found in the venoms and dimerization apparently contributes to the enhancement of the toxin activity. Class P-III SVMPs VAP1 and VAP2 from *Crotalus atrox* have been crystallized in their dimeric form [74,75] exerting potent pro-apoptotic activity in endothelial cell cultures [76]. Bilitoxin and BlatH1 are also examples of non-processed P-II SVMP homodimers [77,78]. Interestingly, in both cases the RGD sequence displayed in the disintegrin domain is replaced by MGD and TDN, respectively, resulting in toxins that are unable to block the platelet fibrinogen receptor; however, both dimeric P-II SVMPs are potent hemorrhagins with activity levels comparable to those of class P-III SVMPs [62,77].

The most common dimers of SVMPs present in venoms are undoubtedly homo- and heterodimeric disintegrins. For example, contortrostatin, a homodimeric disintegrin that displays RGD motifs in both chains, has been produced in a recombinant form [79] and presented substantial anti-angiogenic and anti-cancer effects [79] with some efficacy as an adjuvant in chemotherapy for melanoma [80] and for viral infections [81]. Heterodimers composed of distinct disintegrin domains have also been isolated. Usually, one chain contains the conserved RGD motif and the other chain displays alternative motifs that modulate specificity and selectivity. The first heterodimeric disintegrin group identified included EMF-10 and CC-8 disintegrins, with a RGD motif in one chain and a WGD in the other [82]. As a result, the heterodimer is the strongest blocker of the fibrinogen receptor and effective to modulate megakaryocyte activity [83]. Other interesting group of heterodimeric

disintegrins includes EC3, VLO5, and EO5 with V/RGD motif in one chain and the MLD motif in the other [84]. These toxins target mainly $\alpha_4\beta_1$, $\alpha_4\beta_7$, and $\alpha_9\beta_1$ integrins, mostly related to inflammatory cell receptors [85]. Heterodimeric disintegrins are common in venoms of *Viperinae* subfamily of vipers, and the substitution of the RGD motif at least in one chain may decrease the effect of these toxins on platelets related to impairment of hemostasis. Although this is an apparent disadvantage for the snakes, the non-RGD disintegrins are undoubtedly good leading molecules for drug development or for producing biotechnological tools to address the mechanisms of action of integrin receptors.

2.4. Other Post-Translational Modifications

Most of snake venom proteins undergo glycosylation during their biosynthesis pathway. In eukaryotic cells, glycosylation influences important biochemical properties of the proteins, such as folding, stability, solubility, and ligand binding. In spite of the importance of glycosylation for eukaryotic-secreted proteins, very little is known about the carbohydrate structures present in venom glycoproteins.

In SVMPs, primary structures predict several putative *N*-glycosylation sites [31], and important functions have already been correlated to glycan moieties. However, glycosylation sites identified in the available crystal structures of SVMPs indicate a significant variability, and suggest that the presence of glycan moieties is not predictable based on primary structure information only [86]. Studying the cobra venom glycome, Huang and co-authors [86] identified four major *N*-glycan moieties on the biantennary glycan core, and a high variability of *N*-glycan composition in SVMPs from individual snake specimens. In the same study, the authors reported that these glycoproteins elicit much higher antibody response in antiserum when compared to other high-abundance cobra venom toxins, such as small molecular mass CTXs. The higher immunogenicity of SVMPs compared to other venom components has been also shown by our group [18], and it can be at least partially attributed to the glycan moieties present on these molecules. Moreover, *Bothrops jararaca* SVMPs bothropasin, BJ-PI, and HF3 were subjected to *N*-deglycosylation that induced loss of structural stability of bothropasin and BJ-PI. Although HF3 remained apparently intact, its hemorrhagic and fibrinogenolytic activities were partially impaired, suggesting the importance of glycans for stability, and also for the interaction with substrates [87].

The role of glycosylation in the generation of toxin diversity has been recently addressed in a few studies approaching ontogenetic or gender-related venom variability. The *N*-glycan composition of newborn and adult venoms did not vary significantly [88], but gender-based variations contributed to different glycosylation levels in toxins [35]. The studies demonstrated a complexity of carbohydrate moieties found in glycoproteins, indicating another level of complexity in snake venoms that could be related to the diversification of biological activities.

Another form of post-translational modification observed in many SVMPs is the cyclization of amino-terminal glutamyl residues to pyro-glutamate. The cyclization of glutamyl residues by the acyltransferase glutamyl cyclase is a common occurrence in many organisms. For many bioactive peptides, cyclization of amino-terminal glutamyl residues renders the peptide resistant to proteolytic processing by exopeptidases, thus protecting their biological activities [89]. Glutamyl cyclase has been identified in the venom of viperid snakes [90] particularly in venoms collected at the seventh and tenth days after venom extraction [46]. Most class P-III SVMPs possess, in their mature form, a pyroglutamic acid as the *N*-terminus [31], and this modification provides protection to these enzymes from further digestion by aminopeptidases, or even further processing steps resulting in the release of disintegrin domains.

3. The Role of Prodomains for Enzyme Inactivation

One still-unsolved issue is the maintenance of mature enzymes in the lumen of the venom gland. Since SVMPs degrade extracellular matrix components [91,92] and can lead to loss of viability of different cell types [20] (including epithelial cells [93]), they can be considered a potential risk for the

maintenance of venom gland integrity. It is currently accepted that the acidic pH environment in the lumen of the venom gland could limit proteolytic activity of SVMPs [94]. Additionally, high citrate concentrations and tripeptides containing pyroglutamate found in venoms could inhibit SVMPs that would be activated after venom injection due to dilution factors [95,96]. Previously, secretion of SVMPs into the lumen of the gland as zymogens was also considered as a mechanism for maintaining the latency of these enzymes. However, we have recently shown that the activation of SVMPs mainly occurs during the secretion to the lumen of the venom gland, and cleaved prodomains undergo further hydrolysis to small peptides [46].

The potential of peptides containing the cysteine-switch motif for the inactivation of SVMPs has already been shown [37]. This work led us to test if processed prodomain or prodomain degradation peptides could play a role in the inhibition of activated SVMPs, within the gland environment. To test this hypothesis, we produced jararhagin recombinant prodomain (PD-Jar) as described [46], and synthesized a 14-mer C-terminally amidated peptide (SynPep), based on a naturally-occurring prodomain peptide fragment that was abundantly detected in *Bothrops jararaca* peptidome [48]. Interestingly, our preliminary data show that both recombinant PD-Jar and SynPep inhibited jararhagin catalytic activity, and also toxic activities such as induction of fibrinolysis and hemorrhage (Table 1).

Table 1. Inhibition of jararhagin activities by its recombinant prodomain (PD-Jar) or a prodomain degradation peptide (SynPep).

Activity	PD-Jar ¹		SynPep ¹	
	Molar Ratio	% Inhibition	Molar Ratio	% Inhibition
Catalytic ²	1:10	98	1:5000	90
Fibrinolytic ³	1:14	100	1:200	100
Hemorrhagic ⁴	1:9	100	1:500	100

¹ Values correspond to enzyme to PD-Jar/SynPep molar ratios that resulted in inhibition of jararhagin activity; ² Inhibition of enzymatic activity was tested by incubation with Abz-A-G-L-A-EDDnp as fluorescence quenched metalloproteinase substrate and compared according to the relative fluorescence units (RFU/min/ μ g) of each reaction [97]; ³ Inhibition of jararhagin fibrinolytic activity was calculated by measuring the hydrolysis halo in fibrin-containing agarose plates [98]; ⁴ Hemorrhage levels were calculated by measuring the hemorrhagic area 30 min after intradermal injection in the dorsal region of four mice [98].

Inhibition of metalloproteinase activity by isolated prodomains has been recently addressed in the search for specific therapeutic tools for pathologies involving these enzymes. The cleaved prodomain of certain ADAMs can act as a selective inhibitor of the catalytic activity of the enzyme. Moss and coworkers [99] and Gonzales *et al.* [100] produced the recombinant prodomains of ADAM-9 and TACE, respectively, for the purpose of understanding their mechanism of inhibition and selectivity against these proteinases. In these studies, ADAM-9 prodomain was highly specific and the inhibition of ADAM-9, by its recombinant prodomain, regulated ADAM-10 activity controlling the release of soluble α -secretase enzyme, which is an important task in the therapy Alzheimer's disease [99]. Additionally, TACE prodomain was also specific for this enzyme and could be used as a potential inhibitor of TNF- α release in inflammatory diseases [100]. Considering the high selectivity of prodomains as metalloproteinase inhibitors, we are currently testing more accurately the selectivity and kinetics parameters of SVMPs' inhibition by PD-Jar and SynPep, and their effects on neutralization of local effects induced by viper venoms. These experiments may increase our understanding about the maintenance of inactivated SVMPs inside the venom glands, and could also lead to therapeutic alternatives to minimize local damage induced by snake venoms.

The animal protocols used in this work were evaluated and approved by the Animal Use and Ethic Committee (CEUAIB) of the Institute Butantan (Protocol 1271/14). They are in accordance with COBEA guidelines and the National law for Laboratory Animal Experimentation (Law no. 11.794, 8 October 2008).

4. Conclusions

The contribution of post-translational processing to the generation of venom diversity has been a recent issue offering important insights for understanding the complexity of animal venom arsenals. In this review, we present some current data that support the participation of post-translational processing for generation of diversity of snake venom metalloproteinases. Furthermore, there are other snake venom toxin families (serine proteinases, phospholipases, and C-type lectin-like proteins) represented by several proteoforms, and we predict that similar features discussed here for SVMPs could also be applicable to account, at least in part, for their diversity, and that the same would hold true for venom components from different animal species. Indeed, in a very elegant study, Dutertre and collaborators [101] explained the expanded peptide diversity in the cone snail *Conus marmoreus* revealing how a limited set of approximately 100 transcripts could generate thousands of conopeptides in the venom of a single species. More recently, Zhang and collaborators [102] working with peptide toxins from the tarantula *Haplopelma hainanum* went further into this aspect by showing the role of post-translational modifications in the generation of venom diversity and also in diversifying the functional venom arsenal. In this review, we addressed this issue for snake venom metalloproteinases. Although genetic mechanisms are essential for generating a great number of SVMP paralogue genes, post-translational processing appears as an important contributor for diversifying the SVMP arsenal able to interact with a greater number of physiological targets present in different prey. The articles revised in this paper may represent only the tip of the iceberg explaining SVMPs diversity. With analytical methods improvements, such as top-down proteomic approaches, characterization of proteoforms of complex molecules may present a larger number of possibilities for post-translational modification in SVMPs, supporting the role of processing for the stability, maintenance and functional diversification of this important toxin family present in snake venoms.

Acknowledgments: AMMS is a CNPq fellow (CNPq 304025/2014-3) and is supported by CAPES (AuxPE 1209/2011 and 1519/2011) and FAPESP (2014/26058-8). MTA was sponsored by a CNPq fellowship (131820/2014-1) and JAPR by a CAPES fellowship (AuxPE 1206/2011). RHV is supported by a CAPES grant, which also supports CAN as a post-doctoral fellow (AUXPE 1224/2011).

Author Contributions: A.M.M.-S., J.A.P.-J., and R.H.V. wrote the main body of this review, with contributions from C.A.N and F.G.-N. Regarding the original data displayed in Table 1, the experiments were conceived by A.M.M.-S. and J.A.P.-J., while performed by M.T.A. and J.A.P.-J.

Conflicts of Interest: The authors declare no conflict of interest.

Abbreviations

The following abbreviations are used in this manuscript:

SVMP	Snake Venom Metalloproteinase
ADAM	A Disintegrin and Metalloproteinase
MMP	Matrix Metalloproteinase
PD-Jar	Recombinant prodomain of Jararhagin
MHC	Major Histocompatibility Complex
ECM	Extracellular Matrix
TACE	Tumor Necrosis Factor-alpha Converting Enzyme
DAPI	4',6-diamidino-2-phenylindole
SynPep	Synthetic Peptide of a prodomain hydrolysis product found in <i>B. jararaca</i> venom peptidome

References

1. Elhanati, Y.; Sethna, Z.; Marcou, Q.; Callan, C.G.; Mora, T.; Walczak, A.M. Inferring processes underlying b-cell repertoire diversity. *Philos. Trans. R. Soc. Lond. B Biol. Sci.* **2015**, *370*. [[CrossRef](#)] [[PubMed](#)]
2. Hoehn, K.B.; Fowler, A.; Lunter, G.; Pybus, O.G. The diversity and molecular evolution of b cell receptors during infection. *Mol. Biol. Evol.* **2016**, *33*, 1147–1157. [[CrossRef](#)] [[PubMed](#)]

3. Warren, R.L.; Freeman, J.D.; Zeng, T.; Choe, G.; Munro, S.; Moore, R.; Webb, J.R.; Holt, R.A. Exhaustive T-cell repertoire sequencing of human peripheral blood samples reveals signatures of antigen selection and a directly measured repertoire size of at least 1 million clonotypes. *Genome Res.* **2011**, *21*, 790–797. [[CrossRef](#)] [[PubMed](#)]
4. Qi, Q.; Liu, Y.; Cheng, Y.; Glanville, J.; Zhang, D.; Lee, J.Y.; Olshen, R.A.; Weyand, C.M.; Boyd, S.D.; Goronzy, J.J. Diversity and clonal selection in the human T-cell repertoire. *Proc. Natl. Acad. Sci. USA* **2014**, *111*, 13139–13144. [[CrossRef](#)] [[PubMed](#)]
5. Subedi, G.P.; Barb, A.W. The structural role of antibody N-glycosylation in receptor interactions. *Structure* **2015**, *23*, 1573–1583. [[CrossRef](#)] [[PubMed](#)]
6. Liu, L. Antibody glycosylation and its impact on the pharmacokinetics and pharmacodynamics of monoclonal antibodies and fc-fusion proteins. *J. Pharm. Sci.* **2015**, *104*, 1866–1884. [[CrossRef](#)] [[PubMed](#)]
7. Nikolich-Zugich, J.; Slifka, M.K.; Messaoudi, I. The many important facets of T-cell repertoire diversity. *Nat. Rev. Immunol.* **2004**, *4*, 123–132. [[CrossRef](#)]
8. Olivera, B.M.; Teichert, R.W. Diversity of the neurotoxic conus peptides: A model for concerted pharmacological discovery. *Mol. Interv.* **2007**, *7*, 251–260. [[CrossRef](#)] [[PubMed](#)]
9. Fry, B.G.; Vidal, N.; van der Weerd, L.; Kochva, E.; Renjifo, C. Evolution and diversification of the toxicofera reptile venom system. *J. Proteom.* **2009**, *72*, 127–136. [[CrossRef](#)]
10. Casewell, N.R.; Wüster, W.; Vonk, F.J.; Harrison, R.A.; Fry, B.G. Complex cocktails: The evolutionary novelty of venoms. *Trends Ecol. Evol.* **2013**, *28*, 219–229. [[CrossRef](#)] [[PubMed](#)]
11. Calvete, J.J.; Juárez, P.; Sanz, L. Snake venomomics. Strategy and applications. *J. Mass Spectrom.* **2007**, *42*, 1405–1414. [[CrossRef](#)] [[PubMed](#)]
12. Ogawa, T.; Nakashima, K.; Nobuhisa, I.; Deshimaru, M.; Shimohigashi, Y.; Fukumaki, Y.; Sakaki, Y.; Hattori, S.; Ohno, M. Accelerated evolution of snake venom phospholipase A2 isozymes for acquisition of diverse physiological functions. *Toxicon* **1996**, *34*, 1229–1236. [[CrossRef](#)]
13. Ohno, M.; Ménez, R.; Ogawa, T.; Danse, J.M.; Shimohigashi, Y.; Fromen, C.; Ducancel, F.; Zinn-Justin, S.; Le Du, M.H.; Boulain, J.C.; *et al.* Molecular evolution of snake toxins: Is the functional diversity of snake toxins associated with a mechanism of accelerated evolution? *Prog. Nucleic Acid Res. Mol. Biol.* **1998**, *59*, 307–364. [[PubMed](#)]
14. Moura-da-Silva, A.M.; Theakston, R.D.G.; Crampton, J.M. Evolution of disintegrin cysteine-rich and mammalian matrix-degrading metalloproteinases: Gene duplication and divergence of a common ancestor rather than convergent evolution. *J. Mol. Evol.* **1996**, *43*, 263–269. [[CrossRef](#)] [[PubMed](#)]
15. Brust, A.; Sunagar, K.; Undheim, E.A.; Vetter, I.; Yang, D.C.; Casewell, N.R.; Jackson, T.N.; Koludarov, I.; Alewood, P.F.; Hodgson, W.C.; *et al.* Differential evolution and neofunctionalization of snake venom metalloprotease domains. *Mol. Cell. Proteom.* **2013**, *12*, 651–663. [[CrossRef](#)] [[PubMed](#)]
16. Casewell, N.R.; Wagstaff, S.C.; Harrison, R.A.; Renjifo, C.; Wüster, W. Domain loss facilitates accelerated evolution and neofunctionalization of duplicate snake venom metalloproteinase toxin genes. *Mol. Biol. Evol.* **2011**, *28*, 2637–2649. [[CrossRef](#)] [[PubMed](#)]
17. Casewell, N.R.; Wagstaff, S.C.; Wüster, W.; Cook, D.A.; Bolton, F.M.; King, S.I.; Pla, D.; Sanz, L.; Calvete, J.J.; Harrison, R.A. Medically important differences in snake venom composition are dictated by distinct postgenomic mechanisms. *Proc. Natl. Acad. Sci. USA* **2014**, *111*, 9205–9210. [[CrossRef](#)] [[PubMed](#)]
18. Sousa, L.F.; Nicolau, C.A.; Peixoto, P.S.; Bernardoni, J.L.; Oliveira, S.S.; Portes-Junior, J.A.; Mourão, R.H.; Lima-dos-Santos, I.; Sano-Martins, I.S.; Chalkidis, H.M.; *et al.* Comparison of phylogeny, venom composition and neutralization by antivenom in diverse species of bothrops complex. *PLoS Negl. Trop. Dis.* **2013**, *7*. [[CrossRef](#)] [[PubMed](#)]
19. Calvete, J.J.; Sanz, L.; Angulo, Y.; Lomonte, B.; Gutiérrez, J.M. Venoms, venomomics, antivenomics. *FEBS Lett.* **2009**, *583*, 1736–1743. [[CrossRef](#)] [[PubMed](#)]
20. Moura-da-Silva, A.M.; Butera, D.; Tanjoni, I. Importance of snake venom metalloproteinases in cell biology: Effects on platelets, inflammatory and endothelial cells. *Curr. Pharm. Des.* **2007**, *13*, 2893–2905. [[CrossRef](#)] [[PubMed](#)]
21. Bernardoni, J.L.; Sousa, L.F.; Wermelinger, L.S.; Lopes, A.S.; Prezoto, B.C.; Serrano, S.M.T.; Zingali, R.B.; Moura-da-Silva, A.M. Functional variability of snake venom metalloproteinases: Adaptive advantages in targeting different prey and implications for human envenomation. *PLoS ONE* **2014**, *9*. [[CrossRef](#)]

22. Siigur, E.; Tõnismägi, K.; Trummal, K.; Samel, M.; Vija, H.; Subbi, J.; Siigur, J. Factor X activator from viper a lebetina snake venom, molecular characterization and substrate specificity. *Biochim. Biophys. Acta* **2001**, *1568*, 90–98. [[CrossRef](#)]
23. Modesto, J.C.; Junqueira-de-Azevedo, I.L.; Neves-Ferreira, A.G.; Fritzen, M.; Oliva, M.L.; Ho, P.L.; Perales, J.; Chudzinski-Tavassi, A.M. Insularinase A, a prothrombin activator from *Bothrops insularis* venom, is a metalloprotease derived from a gene encoding protease and disintegrin domains. *Biol. Chem.* **2005**, *386*, 589–600. [[PubMed](#)]
24. Kamiguti, A.S.; Slupsky, J.R.; Zuzel, M.; Hay, C.R. Properties of fibrinogen cleaved by jararhagin, a metalloproteinase from the venom of *Bothrops jararaca*. *Thromb. Haemost.* **1994**, *72*, 244–249. [[PubMed](#)]
25. Baldo, C.; Jamora, C.; Yamanouye, N.; Zorn, T.M.; Moura-da-Silva, A.M. Mechanisms of vascular damage by hemorrhagic snake venom metalloproteinases: Tissue distribution and *in situ* hydrolysis. *PLoS Negl. Trop. Dis.* **2010**, *4*. [[CrossRef](#)] [[PubMed](#)]
26. Escalante, T.; Shannon, J.; Moura-da-Silva, A.M.; Gutiérrez, J.M.; Fox, J.W. Novel insights into capillary vessel basement membrane damage by snake venom hemorrhagic metalloproteinases: A biochemical and immunohistochemical study. *Arch. Biochem. Biophys.* **2006**, *455*, 144–153. [[CrossRef](#)] [[PubMed](#)]
27. Escalante, T.; Rucavado, A.; Fox, J.W.; Gutiérrez, J.M. Key events in microvascular damage induced by snake venom hemorrhagic metalloproteinases. *J. Proteom.* **2011**, *74*, 1781–1794. [[CrossRef](#)] [[PubMed](#)]
28. Kamiguti, A.S.; Cardoso, J.L.; Theakston, R.D.; Sano-Martins, I.S.; Hutton, R.A.; Rugman, F.P.; Warrell, D.A.; Hay, C.R. Coagulopathy and haemorrhage in human victims of *Bothrops jararaca* envenoming in Brazil. *Toxicon* **1991**, *29*, 961–972. [[CrossRef](#)]
29. Bjarnason, J.B.; Fox, J.W. Snake venom metalloendopeptidases: Reprolysins. *Methods Enzymol.* **1995**, *248*, 345–368. [[PubMed](#)]
30. Fox, J.W.; Serrano, S.M.T. Structural considerations of the snake venom metalloproteinases, key members of the M12 reprolysin family of metalloproteinases. *Toxicon* **2005**, *45*, 969–985. [[CrossRef](#)] [[PubMed](#)]
31. Fox, J.W.; Serrano, S.M.T. Insights into and speculations about snake venom metalloproteinase (SVMP) synthesis, folding and disulfide bond formation and their contribution to venom complexity. *FEBS J.* **2008**, *275*, 3016–3030. [[CrossRef](#)] [[PubMed](#)]
32. Gomis-Rüth, F.X. Structural aspects of the metzincin clan of metalloendopeptidases. *Mol. Biotechnol.* **2003**, *24*, 157–202. [[CrossRef](#)]
33. Stöcker, W.; Grams, F.; Baumann, U.; Reinemer, P.; Gomis-Rüth, F.X.; McKay, D.B.; Bode, W. The metzincins—Topological and sequential relations between the astacins, adamalysins, serralysins, and matrixins (collagenases) define a superfamily of zinc-peptidases. *Protein Sci.* **1995**, *4*, 823–840. [[CrossRef](#)] [[PubMed](#)]
34. Moura-da-Silva, A.M.; Furlan, M.S.; Caporrino, M.C.; Grego, K.F.; Portes-Junior, J.A.; Clissa, P.B.; Valente, R.H.; Magalhães, G.S. Diversity of metalloproteinases in *Bothrops neuwiedi* snake venom transcripts: Evidences for recombination between different classes of SVMPs. *BMC Genet.* **2011**, *12*. [[CrossRef](#)] [[PubMed](#)]
35. Zelanis, A.; Menezes, M.C.; Kitano, E.S.; Liberato, T.; Tashima, A.K.; Pinto, A.F.; Sherman, N.E.; Ho, P.L.; Fox, J.W.; Serrano, S.M. Proteomic identification of gender molecular markers in *Bothrops jararaca* venom. *J. Proteom.* **2016**, *139*, 26–37. [[CrossRef](#)] [[PubMed](#)]
36. Moura-da-Silva, A.M.; Serrano, S.M.T.; Fox, J.W.; Gutiérrez, J.M. Snake venom metalloproteinases: Structure, function and effects on snake bite pathology. In *Animal Toxins: State of the Art*; Lima, M.H., Pimenta, A.M.C., Martin-Euclaire, M.F., Zingali, R.B., Eds.; UFMG: Belo Horizonte, Brazil, 2009; pp. 525–546.
37. Grams, F.; Huber, R.; Kress, L.F.; Moroder, L.; Bode, W. Activation of snake venom metalloproteinases by a cysteine switch-like mechanism. *FEBS Lett.* **1993**, *335*, 76–80. [[CrossRef](#)]
38. Shimokawa, K.; Jia, L.G.; Wang, X.M.; Fox, J.W. Expression, activation, and processing of the recombinant snake venom metalloproteinase, pro-atrolysin e. *Arch. Biochem. Biophys.* **1996**, *335*, 283–294. [[CrossRef](#)] [[PubMed](#)]
39. Bode, W.; Gomis-Rüth, F.X.; Stöckler, W. Astacins, serralysins, snake venom and matrix metalloproteinases exhibit identical zinc-binding environments (HEXXHXXGXXH and Met-turn) and topologies and should be grouped into a common family, ‘the metzincins’. *FEBS Lett.* **1993**, *331*, 134–140. [[CrossRef](#)]
40. Okamoto, T.; Akuta, T.; Tamura, F.; van der Vliet, A.; Akaike, T. Molecular mechanism for activation and regulation of matrix metalloproteinases during bacterial infections and respiratory inflammation. *Biol. Chem.* **2004**, *385*, 997–1006. [[CrossRef](#)] [[PubMed](#)]

41. Van Wart, H.E.; Birkedal-Hansen, H. The cysteine switch: A principle of regulation of metalloproteinase activity with potential applicability to the entire matrix metalloproteinase gene family. *Proc. Natl. Acad. Sci. USA* **1990**, *87*, 5578–5582. [[CrossRef](#)] [[PubMed](#)]
42. Tallant, C.; Marrero, A.; Gomis-Rüth, F.X. Matrix metalloproteinases: Fold and function of their catalytic domains. *Biochim. Biophys. Acta* **2010**, *1803*, 20–28. [[CrossRef](#)] [[PubMed](#)]
43. Lum, L.; Reid, M.S.; Blobel, C.P. Intracellular maturation of the mouse metalloprotease disintegrin MDC15. *J. Biol. Chem.* **1998**, *273*, 26236–26247. [[CrossRef](#)] [[PubMed](#)]
44. Howard, L.; Maciewicz, R.A.; Blobel, C.P. Cloning and characterization of ADAM28: Evidence for autocatalytic pro-domain removal and for cell surface localization of mature ADAM28. *Biochem. J.* **2000**, *348*, 21–27. [[CrossRef](#)] [[PubMed](#)]
45. Schlomann, U.; Wildeboer, D.; Webster, A.; Antropova, O.; Zeuschner, D.; Knight, C.G.; Docherty, A.J.; Lambert, M.; Skelton, L.; Jockusch, H.; *et al.* The metalloprotease disintegrin ADAM8. Processing by autocatalysis is required for proteolytic activity and cell adhesion. *J. Biol. Chem.* **2002**, *277*, 48210–48219. [[CrossRef](#)] [[PubMed](#)]
46. Portes-Junior, J.A.; Yamanouye, N.; Carneiro, S.M.; Knittel, P.S.; Sant’Anna, S.S.; Nogueira, F.C.; Junqueira, M.; Magalhães, G.S.; Domont, G.B.; Moura-da-Silva, A.M. Unraveling the processing and activation of snake venom metalloproteinases. *J. Proteom. Res.* **2014**, *13*, 3338–3348. [[CrossRef](#)] [[PubMed](#)]
47. Valente, R.H.; Guimarães, P.R.; Junqueira, M.; Neves-Ferreira, A.G.; Soares, M.R.; Chapeaurouge, A.; Trugilho, M.R.; León, I.R.; Rocha, S.L.; Oliveira-Carvalho, A.L.; *et al.* *Bothrops insularis* venomics: A proteomic analysis supported by transcriptomic-generated sequence data. *J. Proteom.* **2009**, *72*, 241–255. [[CrossRef](#)] [[PubMed](#)]
48. Nicolau, C.A.; Carvalho, P.C.; Junqueira-de-Azevedo, I.L.M.; Teixeira-Ferreira, A.; Junqueira, M.; Perales, J.; Neves-Ferreira, A.G.C.; Valente, R.H. An in-depth snake venom proteopeptidome characterization: Benchmarking *Bothrops jararaca*. *J. Proteom.* submitted for publication. 2016.
49. Luna, M.S.; Valente, R.H.; Perales, J.; Vieira, M.L.; Yamanouye, N. Activation of *Bothrops jararaca* snake venom gland and venom production: A proteomic approach. *J. Proteom.* **2013**, *94*, 460–472. [[CrossRef](#)] [[PubMed](#)]
50. Murphy, G.; Nagase, H. Progress in matrix metalloproteinase research. *Mol. Asp. Med.* **2008**, *29*, 290–308. [[CrossRef](#)] [[PubMed](#)]
51. Wewer, U.M.; Mörgelin, M.; Holck, P.; Jacobsen, J.; Lydolph, M.C.; Johnsen, A.H.; Kveiborg, M.; Albrechtsen, R. ADAM12 is a four-leafed clover: The excised prodomain remains bound to the mature enzyme. *J. Biol. Chem.* **2006**, *281*, 9418–9422. [[CrossRef](#)] [[PubMed](#)]
52. Marcinkiewicz, C. Applications of snake venom components to modulate integrin activities in cell-matrix interactions. *Int. J. Biochem. Cell Biol.* **2013**, *45*, 1974–1986. [[CrossRef](#)] [[PubMed](#)]
53. Calvete, J.J. The continuing saga of snake venom disintegrins. *Toxicon* **2013**, *62*, 40–49. [[CrossRef](#)] [[PubMed](#)]
54. Huang, T.F.; Yeh, C.H.; Wu, W.B. Viper venom components affecting angiogenesis. *Haemostasis* **2001**, *31*, 192–206. [[CrossRef](#)] [[PubMed](#)]
55. Juárez, P.; Comas, I.; González-Candelas, F.; Calvete, J.J. Evolution of snake venom disintegrins by positive Darwinian selection. *Mol. Biol. Evol.* **2008**, *25*, 2391–2407. [[CrossRef](#)] [[PubMed](#)]
56. Sanz, L.; Harrison, R.A.; Calvete, J.J. First draft of the genomic organization of a PIII-SVMP gene. *Toxicon* **2012**, *60*, 455–469. [[CrossRef](#)] [[PubMed](#)]
57. Mazzi, M.V.; Magro, A.J.; Amui, S.F.; Oliveira, C.Z.; Ticli, F.K.; Stábeli, R.G.; Fuly, A.L.; Rosa, J.C.; Braz, A.S.; Fontes, M.R.; *et al.* Molecular characterization and phylogenetic analysis of JussuMP-I: A RGD-P-III class hemorrhagic metalloprotease from *Bothrops jararacussu* snake venom. *J. Mol. Graph. Model.* **2007**, *26*, 69–85. [[CrossRef](#)] [[PubMed](#)]
58. Cidade, D.A.P.; Wermelinger, L.S.; Lobo-Hajdu, G.; Davila, A.M.R.; Bon, C.; Zingali, R.B.; Albano, R.M. Molecular diversity of disintegrin-like domains within metalloproteinase precursors of *Bothrops jararaca*. *Toxicon* **2006**, *48*, 590–599. [[CrossRef](#)] [[PubMed](#)]
59. Singhamatr, P.; Rojnuckarin, P. Molecular cloning of albolatin, a novel snake venom metalloprotease from green pit viper (*Trimeresurus albolabris*), and expression of its disintegrin domain. *Toxicon* **2007**, *50*, 1192–1200. [[CrossRef](#)] [[PubMed](#)]
60. Suntravat, M.; Jia, Y.; Lucena, S.E.; Sánchez, E.E.; Pérez, J.C. cDNA cloning of a snake venom metalloproteinase from the eastern diamondback rattlesnake (*Crotalus adamanteus*), and the expression of its disintegrin domain with anti-platelet effects. *Toxicon* **2013**, *64*, 43–54. [[CrossRef](#)] [[PubMed](#)]

61. Zhu, L.; Yuan, C.; Chen, Z.; Wang, W.; Huang, M. Expression, purification and characterization of recombinant jerdonitin, a P-II class snake venom metalloproteinase comprising metalloproteinase and disintegrin domains. *Toxicon* **2010**, *55*, 375–380. [[CrossRef](#)] [[PubMed](#)]
62. Herrera, C.; Escalante, T.; Voisin, M.B.; Rucavado, A.; Morazán, D.; Macêdo, J.K.; Calvete, J.J.; Sanz, L.; Nourshargh, S.; Gutiérrez, J.M.; *et al.* Tissue localization and extracellular matrix degradation by PI, PII and PIII snake venom metalloproteinases: Clues on the mechanisms of venom-induced hemorrhage. *PLoS Negl. Trop. Dis.* **2015**, *9*. [[CrossRef](#)] [[PubMed](#)]
63. Usami, Y.; Fujimura, Y.; Miura, S.; Shima, H.; Yoshida, E.; Yoshioka, A.; Hirano, K.; Suzuki, M.; Titani, K. A 28 kDa-protein with disintegrin-like structure (jararhagin-C) purified from *Bothrops jararaca* venom inhibits collagen- and adp-induced platelet aggregation. *Biochem. Biophys. Res. Commun.* **1994**, *201*, 331–339. [[CrossRef](#)] [[PubMed](#)]
64. Takeya, H.; Nishida, S.; Nishino, N.; Makinose, Y.; Omori-Satoh, T.; Nikai, T.; Sugihara, H.; Iwanaga, S. Primary structures of platelet aggregation inhibitors (disintegrins) autoproteolytically released from snake venom hemorrhagic metalloproteinases and new fluorogenic peptide substrates for these enzymes. *J. Biochem.* **1993**, *113*, 473–483. [[PubMed](#)]
65. Fujimura, S.; Oshikawa, K.; Terada, S.; Kimoto, E. Primary structure and autoproteolysis of brevilysin h6 from the venom of *Gloydius halys brevicaudus*. *J. Biochem.* **2000**, *128*, 167–173. [[CrossRef](#)] [[PubMed](#)]
66. Souza, D.H.F.; Iemma, M.R.C.; Ferreira, L.L.; Faria, J.P.; Oliva, M.L.V.; Zingali, R.B.; Niewiarowski, S.; Selistre-de-Araujo, H.S. The disintegrin-like domain of the snake venom metalloprotease alternagin inhibits $\alpha 2\beta 1$ integrin-mediated cell adhesion. *Arch. Biochem. Biophys.* **2000**, *384*, 341–350. [[CrossRef](#)] [[PubMed](#)]
67. Freitas-de-Sousa, L.A.; Amazonas, D.R.; Sousa, L.F.; Sant’Anna, S.S.; Nishiyama, M.Y., Jr.; Serrano, S.M.T.; Junqueira-de-Azevedo, I.L.M.; Chalkidis, H.M.; Moura-da-Silva, A.M.; Mourao, R.H.V. Comparison of venoms from wild and long-term captive bothrops atrox snakes and characterization of batroxrhagin, the predominant class piii metalloproteinase from the venom of this species. *Biochimie* **2015**, *118*, 60–70. [[CrossRef](#)] [[PubMed](#)]
68. Petretski, J.H.; Kanashiro, M.M.; Rodrigues, F.R.; Alves, E.W.; Machado, O.L.T.; Kipnis, T.L. Edema induction by the disintegrin-like/cysteine-rich domains from a *Bothrops atrox* hemorrhagin. *Biochem. Biophys. Res. Commun.* **2000**, *276*, 29–34. [[CrossRef](#)] [[PubMed](#)]
69. Shimokawa, K.; Shannon, J.D.; Jia, L.G.; Fox, J.W. Sequence and biological activity of catrocollastatin-c: A disintegrin-like/cysteine-rich two-domain protein from *Crotalus atrox* venom. *Arch. Biochem. Biophys.* **1997**, *343*, 35–43. [[CrossRef](#)] [[PubMed](#)]
70. Clissa, P.B.; Lopes-Ferreira, M.; Della-Casa, M.S.; Farsky, S.; Moura-da-Silva, A.M. Importance of jararhagin disintegrin-like and cysteine-rich domains in the early events of local inflammatory response. *Toxicon* **2006**, *47*, 591–596. [[CrossRef](#)] [[PubMed](#)]
71. Cominetti, M.; Terruggi, C.H.B.; Ramos, O.H.P.; Fox, J.W.; Mariano-Oliveira, A.; de Freitas, M.S.; Figueiredo, C.C.; Morandi, V.; Selistre-de-Araujo, H.S. Alternagin-C, a disintegrin-like protein, induces vascular endothelial cell growth factor (VEGF) expression and endothelial cell proliferation *in vitro*. *J. Biol. Chem.* **2004**, *279*, 18247–18255. [[CrossRef](#)] [[PubMed](#)]
72. Paine, M.J.; Desmond, H.P.; Theakston, R.D.; Crampton, J.M. Purification, cloning, and molecular characterization of a high molecular weight hemorrhagic metalloprotease, jararhagin, from *Bothrops jararaca* venom. Insights into the disintegrin gene family. *J. Biol. Chem.* **1992**, *267*, 22869–22876. [[PubMed](#)]
73. Moura-da-Silva, A.M.; Della-Casa, M.S.; David, A.S.; Assakura, M.T.; Butera, D.; Lebrun, I.; Shannon, J.D.; Serrano, S.M.T.; Fox, J.W. Evidence for heterogeneous forms of the snake venom metalloproteinase jararhagin: A factor contributing to snake venom variability. *Arch. Biochem. Biophys.* **2003**, *409*, 395–401. [[CrossRef](#)]
74. Igarashi, T.; Araki, S.; Mori, H.; Takeda, S. Crystal structures of catrocollastatin/VAP2B reveal a dynamic, modular architecture of adam/adamalsin/reprolysin family proteins. *FEBS Lett.* **2007**, *581*, 2416–2422. [[CrossRef](#)] [[PubMed](#)]
75. Takeda, S.; Igarashi, T.; Mori, H.; Araki, S. Crystal structures of VAP1 reveal ADAMS’ MDC domain architecture and its unique c-shaped scaffold. *EMBO J.* **2006**, *25*, 2388–2396. [[CrossRef](#)] [[PubMed](#)]
76. Kikushima, E.; Nakamura, S.; Oshima, Y.; Shibuya, T.; Miao, J.Y.; Hayashi, H.; Nikai, T.; Araki, S. Hemorrhagic activity of the vascular apoptosis-inducing proteins VAP1 and VAP2 from *Crotalus atrox*. *Toxicon* **2008**, *52*, 589–593. [[CrossRef](#)] [[PubMed](#)]

77. Nikai, T.; Taniguchi, K.; Komori, Y.; Masuda, K.; Fox, J.W.; Sugihara, H. Primary structure and functional characterization of bilitoxin-1, a novel dimeric p-ii snake venom metalloproteinase from *Agkistrodon bilineatus* venom. *Arch. Biochem. Biophys.* **2000**, *378*, 6–15. [[CrossRef](#)] [[PubMed](#)]
78. Camacho, E.; Villalobos, E.; Sanz, L.; Pérez, A.; Escalante, T.; Lomonte, B.; Calvete, J.J.; Gutiérrez, J.M.; Rucavado, A. Understanding structural and functional aspects of PII snake venom metalloproteinases: Characterization of BlatH1, a hemorrhagic dimeric enzyme from the venom of *Bothriechis lateralis*. *Biochimie* **2014**, *101*, 145–155. [[CrossRef](#)] [[PubMed](#)]
79. Minea, R.; Swenson, S.; Costa, F.; Chen, T.C.; Markland, F.S. Development of a novel recombinant disintegrin, contortrostatin, as an effective anti-tumor and anti-angiogenic agent. *Pathophysiol. Haemost. Thromb.* **2005**, *34*, 177–183. [[CrossRef](#)] [[PubMed](#)]
80. Schwartz, M.A.; McRoberts, K.; Coyner, M.; Andarawewa, K.L.; Frierson, H.F.; Sanders, J.M.; Swenson, S.; Markland, F.; Conaway, M.R.; Theodorescu, D. Integrin agonists as adjuvants in chemotherapy for melanoma. *Clin. Cancer Res.* **2008**, *14*, 6193–6197. [[CrossRef](#)] [[PubMed](#)]
81. Hubbard, S.; Choudhary, S.; Maus, E.; Shukla, D.; Swenson, S.; Markland, F.S.; Tiwari, V. Contortrostatin, a homodimeric disintegrin isolated from snake venom inhibits herpes simplex virus entry and cell fusion. *Antivir. Ther.* **2012**, *17*, 1319–1326. [[CrossRef](#)] [[PubMed](#)]
82. Marcinkiewicz, C.; Calvete, J.J.; Vijay-Kumar, S.; Marcinkiewicz, M.M.; Raida, M.; Schick, P.; Lobb, R.R.; Niewiarowski, S. Structural and functional characterization of EMF10, a heterodimeric disintegrin from *Eristocophis macmahoni* venom that selectively inhibits $\alpha 5\beta 1$ integrin. *Biochemistry* **1999**, *38*, 13302–13309. [[CrossRef](#)] [[PubMed](#)]
83. Calvete, J.J.; Fox, J.W.; Agelan, A.; Niewiarowski, S.; Marcinkiewicz, C. The presence of the WGD motif in CC8 heterodimeric disintegrin increases its inhibitory effect on $\alpha IIb\beta 3$, $\alpha v\beta 3$, and $\alpha 5\beta 1$ integrins. *Biochemistry* **2002**, *41*, 2014–2021. [[CrossRef](#)] [[PubMed](#)]
84. Marcinkiewicz, C.; Calvete, J.J.; Marcinkiewicz, M.M.; Raida, M.; Vijay-Kumar, S.; Huang, Z.; Lobb, R.R.; Niewiarowski, S. EC3, a novel heterodimeric disintegrin from *Echis carinatus* venom, inhibits $\alpha 4$ and $\alpha 5$ integrins in an RGD-independent manner. *J. Biol. Chem.* **1999**, *274*, 12468–12473. [[CrossRef](#)] [[PubMed](#)]
85. Marcinkiewicz, C.; Taooka, Y.; Yokosaki, Y.; Calvete, J.J.; Marcinkiewicz, M.M.; Lobb, R.R.; Niewiarowski, S.; Sheppard, D. Inhibitory effects of MLDG-containing heterodimeric disintegrins reveal distinct structural requirements for interaction of the integrin $\alpha 9\beta 1$ with vcam-1, tenascin-c, and osteopontin. *J. Biol. Chem.* **2000**, *275*, 31930–31937. [[CrossRef](#)] [[PubMed](#)]
86. Huang, H.W.; Liu, B.S.; Chien, K.Y.; Chiang, L.C.; Huang, S.Y.; Sung, W.C.; Wu, W.G. Cobra venom proteome and glycome determined from individual snakes of *Naja atra* reveal medically important dynamic range and systematic geographic variation. *J. Proteom.* **2015**, *128*, 92–104. [[CrossRef](#)] [[PubMed](#)]
87. Oliveira, A.K.; Leme, A.F.P.; Asega, A.F.; Camargo, A.C.M.; Fox, J.W.; Serrano, S.M.T. New insights into the structural elements involved in the skin haemorrhage induced by snake venom metalloproteinases. *Thromb. Haemost.* **2010**, *104*, 485–497. [[CrossRef](#)] [[PubMed](#)]
88. Zelanis, A.; Serrano, S.M.; Reinhold, V.N. N-glycome profiling of *Bothrops jararaca* newborn and adult venoms. *J. Proteom.* **2012**, *75*, 774–782. [[CrossRef](#)] [[PubMed](#)]
89. Fischer, W.H.; Spiess, J. Identification of a mammalian glutaminyl cyclase converting glutaminyl into pyroglutaminyl peptides. *Proc. Natl. Acad. Sci. USA* **1987**, *84*, 3628–3632. [[CrossRef](#)] [[PubMed](#)]
90. Calvete, J.J.; Fasoli, E.; Sanz, L.; Boschetti, E.; Righetti, P.G. Exploring the venom proteome of the western diamondback rattlesnake, *Crotalus atrox*, via snake venomomics and combinatorial peptide ligand library approaches. *J. Proteom. Res.* **2009**, *8*, 3055–3067. [[CrossRef](#)] [[PubMed](#)]
91. Baramova, E.N.; Shannon, J.D.; Bjarnason, J.B.; Fox, J.W. Degradation of extracellular matrix proteins by hemorrhagic metalloproteinases. *Arch. Biochem. Biophys.* **1989**, *275*, 63–71. [[CrossRef](#)]
92. Baramova, E.N.; Shannon, J.D.; Fox, J.W.; Bjarnason, J.B. Proteolytic digestion of non-collagenous basement membrane proteins by the hemorrhagic metalloproteinase Ht-e from *Crotalus atrox* venom. *Biomed. Biochim. Acta* **1991**, *50*, 763–768. [[PubMed](#)]
93. Costa, E.P.; Santos, M.F. Jararhagin, a snake venom metalloproteinase-disintegrin, stimulates epithelial cell migration in an *in vitro* restitution model. *Toxicon* **2004**, *44*, 861–870. [[CrossRef](#)] [[PubMed](#)]
94. Mackessy, S.P. Venom composition in rattlesnakes: Trends and biological significance. In *The Biology of Rattlesnakes*; Hayes, W.K., Beaman, K.R., Cardwell, M.D., Bush, S.P., Eds.; Loma Linda University Press: Loma Linda, CA, USA, 2008; pp. 495–510.

95. Marques-Porto, R.; Lebrun, I.; Pimenta, D.C. Self-proteolysis regulation in the *Bothrops jararaca* venom: The metallopeptidases and their intrinsic peptidic inhibitor. *Comp. Biochem. Physiol. C Toxicol. Pharmacol.* **2008**, *147*, 424–433. [[CrossRef](#)] [[PubMed](#)]
96. Munekiyo, S.M.; Mackessy, S.P. Presence of peptide inhibitors in rattlesnake venoms and their effects on endogenous metalloproteases. *Toxicon* **2005**, *45*, 255–263. [[CrossRef](#)] [[PubMed](#)]
97. Kuniyoshi, A.K.; Rocha, M.; Cajado Carvalho, D.; Juliano, M.A.; Juliano Neto, L.; Tambourgi, D.V.; Portaro, F.C. Angiotensin-degrading serine peptidase: A new chymotrypsin-like activity in the venom of *Bothrops jararaca* partially blocked by the commercial antivenom. *Toxicon* **2012**, *59*, 124–131. [[CrossRef](#)] [[PubMed](#)]
98. Baldo, C.; Tanjoni, I.; León, I.R.; Batista, I.F.C.; Della-Casa, M.S.; Clissa, P.B.; Weinlich, R.; Lopes-Ferreira, M.; Lebrun, I.; Amarante-Mendes, G.; *et al.* BnPI, a novel P-I metalloproteinase from *Bothrops neuwiedi* venom: Biological effects benchmarking relatively to jararhagin, a P-III SVMP. *Toxicon* **2008**, *51*, 54–65. [[CrossRef](#)] [[PubMed](#)]
99. Moss, M.L.; Powell, G.; Miller, M.A.; Edwards, L.; Qi, B.; Sang, Q.X.; de Strooper, B.; Tesseur, I.; Lichtenthaler, S.F.; Taverna, M.; *et al.* ADAM9 inhibition increases membrane activity of ADAM10 and controls α -secretase processing of amyloid precursor protein. *J. Biol. Chem.* **2011**, *286*, 40443–40451. [[CrossRef](#)] [[PubMed](#)]
100. Gonzales, P.E.; Solomon, A.; Miller, A.B.; Leesnitzer, M.A.; Sagi, I.; Milla, M.E. Inhibition of the tumor necrosis factor- α -converting enzyme by its pro domain. *J. Biol. Chem.* **2004**, *279*, 31638–31645. [[CrossRef](#)] [[PubMed](#)]
101. Dutertre, S.; Jin, A.H.; Kaas, Q.; Jones, A.; Alewood, P.F.; Lewis, R.J. Deep venomomics reveals the mechanism for expanded peptide diversity in cone snail venom. *Mol. Cell. Proteom.* **2013**, *12*, 312–329. [[CrossRef](#)] [[PubMed](#)]
102. Zhang, Y.Y.; Huang, Y.; He, Q.Z.; Luo, J.; Zhu, L.; Lu, S.S.; Liu, J.Y.; Huang, P.F.; Zeng, X.Z.; Liang, S.P. Structural and functional diversity of peptide toxins from tarantula *Haplopelma hainanum* (*Ornithoctonus hainana*) venom revealed by transcriptomic, peptidomic, and patch clamp approaches. *J. Biol. Chem.* **2015**, *290*, 26471–26472. [[CrossRef](#)] [[PubMed](#)]



© 2016 by the authors; licensee MDPI, Basel, Switzerland. This article is an open access article distributed under the terms and conditions of the Creative Commons Attribution (CC-BY) license (<http://creativecommons.org/licenses/by/4.0/>).

ANEXOS

Tabela Suplementar A.1: Identification of peptides generated by the incubation of Matrigel with ATXL and BATXH by LC-MS/MS*.

Table S1. Identification of peptides generated by the incubation of Matrigel with ATXL and BATXH by LC-MS/MS*.											
Table S1. I	Charge	Mass	PEP	MS/MS Count	Protein names	Protein IDs	Sequence	Gene names	Leading protein:Leading razor protein	Protein group IDs	
ATXL-R1	2	1718.86	9.51E-03	1	Heat shock cognate 71 kDa protein;Heat	P63017;P1662	IANDGQNRRTTSPYVA	Hspa8;Hspa11H	P63017	P63017	86
ATXL-R1	2	1301.68	7.17E-03	1	Laminin subunit gamma-1	P02468	LKEAEREVTDL	Lamc1	P02468	P02468	15
ATXL-R1	2	1037.55	7.03E-03	1	Laminin subunit alpha-1	P19137	HADIHKNGG	Lama1	P19137	P19137	39
ATXL-R1	1	624.348	6.93E-03	1	SCY1-like protein 2	Q8CFE4	LPFLGP	Scyl2	REV_F2YMG0	REV_F2YMG0	129
ATXL-R1	2	1197.64	6.83E-03	1	ATP synthase subunit alpha, mitochondri	Q03265	LGNAIDKGPVGS	Atp5a1	Q03265	Q03265	100
ATXL-R1	2	943.524	6.60E-03	1	Histone H2A.V;Histone H2A.Z;Histone H2	Q3THW5;P0C0AGLQFPVGR		H2afv;H2afz;Histi	Q3THW5;Q8CGF	Q8CGF	46,27
ATXL-R1	2	1445.79	6.17E-03	1	Calreticulin	P14211	LIVRPDNTYE	Calr	P14211	P14211	35
ATXL-R1	2	1086.58	5.78E-03	1	Tubulin alpha-4A chain;Tubulin alpha-8 ch	P68368;Q9LJZ	QTLNLPYPR	Tuba4a;Tuba8;T	P68368	P68368	18
ATXL-R1	2	1330.71	3.71E-03	1	60S ribosomal protein L18	P35980	TAVVVGTVTDVDR	Rpl18	P35980	P35980	55
ATXL-R1	3	1443.75	2.91E-03	1	Laminin subunit alpha-1	P19137	QTARKDFQPPVSA	Lama1	P19137	P19137	39
ATXL-R1	2	951.441	2.59E-03	1	Vimentin	P20152	FGSGGTSRRP	Vim	P20152	P20152	43
ATXL-R1	2	1222.7	2.40E-03	1	Laminin subunit beta-1	P02469	ANLPGVIVVER	Lamb1	P02469	P02469	16
ATXL-R1	2	1137.51	2.34E-03	1	Vimentin	P20152	SFRQVDVNAS	Vim	P20152	P20152	43
ATXL-R1	2	1257.73	1.83E-03	1	Laminin subunit alpha-1	P19137	LVEHVPGRVPR	Lama1	P19137	P19137	39
ATXL-R1	2	1529.73	1.73E-03	1	Laminin subunit beta-1	P02469	AIKQADEIIQGTGN	Lamb1	P02469	P02469	16
ATXL-R1	2	1653.8	1.39E-03	1	Actin, cytoplasmic 2;Actin, cytoplasmic 2	P63260;P60711	TVLSGGTMYPGIADR	Actg1;Actb	P63260	P63260	70
ATXL-R1	3	1329.63	1.28E-03	1	Prolyl 3-hydroxylase 1	Q3V1T4-3;Q3V	FSSGGTENPHGVKA	Lepre1	Q3V1T4-3	Q3V1T4-3	107
ATXL-R1	2	1028.56	1.25E-03	1	Actin, cytoplasmic 2;Actin, cytoplasmic 2	P63260;P60711	QVITIGNER	Actg1;Actb;Actg	P63260	P63260	70
ATXL-R1	3	1499.75	1.19E-03	1	Heterogeneous nuclear ribonucleoprotein	Q922X1-2;Q92	SVQRPGYDRPRTGA	Hnmpf	Q922X1-2	Q922X1-2	184
ATXL-R1	2	968.456	1.11E-03	1	Nidogen-1	P10493	ASLHGGGEPTT	Nid1	P10493	P10493	29
ATXL-R1	2	1228.64	8.69E-04	1	Laminin subunit gamma-1	P02468	LQNRITTEE	Lamc1	P02468	P02468	15
ATXL-R1	2	1280.69	8.67E-04	1	Fibrinogen beta chain;Fibrinopeptide B;F	Q8K0E8	LRPAPPISGGGY	Fgb	Q8K0E8	Q8K0E8	132
ATXL-R1	2	1132.51	7.86E-04	1	Glyceraldehyde-3-phosphate dehydrogen	P16858	HSSTFDAGAGIA	Gapdh	P16858	P16858	38
ATXL-R1	2	1211.64	6.43E-04	1	40S ribosomal protein S5;40S ribosomal	P97461	ATPAVAETPOIK	Rps5	P97461	P97461	94
ATXL-R1	2	1210.53	6.41E-04	1	Laminin subunit gamma-1	P02468	MVTDAQFEDR	Lamc1	P02468	P02468	15
ATXL-R1	2	970.508	4.71E-04	1	Procollagen-llysine-2-oxoglutarate 5-dioxy	Q9R0B9	VAINMGKPTK	Plocl2	Q9R0B9	Q9R0B9	160
ATXL-R1	2	1338.84	4.36E-04	1	Laminin subunit alpha-1;Laminin subunit a	P19137;Q6067	LINGRPSADPPSP	Lama1;Lama2	P19137	P19137	39
ATXL-R1	2	1270.57	4.04E-04	1	Laminin subunit gamma-1	P02468	HEATDYVWRP	Lamc1	P02468	P02468	15
ATXL-R1	2	1380.75	2.93E-04	1	Heterogeneous nuclear ribonucleoprotein	Q92204-4;Q92	SYPARVPPPPPIA	Hnmpc	Q92204-4	Q92204-4	163
ATXL-R1	2	989.533	2.45E-04	1	Laminin subunit alpha-1	P19137	ISMEVGRKA	Lama1	P19137	P19137	39
ATXL-R1	2	1036.57	2.17E-04	1	Laminin subunit alpha-1	P19137	HADIHKNGG	Lama1	P19137	P19137	39
ATXL-R1	2	1144.61	1.29E-04	1	Laminin subunit gamma-1	P02468	IRNTIETGI	Lamc1	P02468	P02468	15
ATXL-R1	2	1082.54	9.07E-05	1	Transcription intermediary factor 1-beta	Q62318	LTEGPGAEGPR	Trim28	Q62318	Q62318	115
ATXL-R1	2	1038.53	2.18E-05	1	Protein disulfide-isomerase	P09103	ITSNSGVFSK	P4hb	P09103	P09103	24
ATXL-R1	3	1412.72	2.04E-05	1	Heterogeneous nuclear ribonucleoprotein	Q922X1-2;Q92	VQRPGYDRPRTGA	Hnmpf	Q922X1-2	Q922X1-2	184
ATXL-R1	2	1637.81	1.39E-05	1	Actin, cytoplasmic 2;Actin, cytoplasmic 2	P63260;P60711	TVLSGGTMYPGIADR	Actg1;Actb	P63260	P63260	70
ATXL-R1	2	1212.64	7.45E-06	1	60S ribosomal protein L30	P62889	IIDPGDSIIR	Rpl30	P62889	P62889	83
ATXL-R1	3	1579.98	4.51E-06	1	78 kDa glucose-regulated protein	P20029	KLIPRNTVPTKKS	Hspa5	P20029	P20029	42
ATXL-R1	2	1260.72	1.12E-06	1	Elongation factor 1-alpha 1;Elongation fac	P10126;P6263	VILINHPGQISA	Eef1a1;Eef1a2	P10126	P10126	28
ATXL-R1	2	1379.72	7.63E-07	1	Laminin subunit gamma-1	P02468	HKQEADIVRVA	Lamc1	P02468	P02468	15
ATXL-R1	2	1232.59	1.43E-07	1	60 kDa heat shock protein, mitochondrial	P63038;P63031	VGGTSDVEVNEK	Hspd1	P63038	P63038	87
ATXL-R1	2	975.466	7.61E-08	1	Laminin subunit beta-1	P02469	IEDPVSRR	Lamb1	P02469	P02469	16
ATXL-R1	2	1117.48	5.78E-09	1	Tubulin beta-4B chain;Tubulin beta-5 chai	P68372;P9902	HSLGGGTSGSGMGT	Tubb4b;Tubb5;T	P68372	P68372	90
ATXL-R1	2	1036.49	5.76E-16	1	Vimentin	P20152	ANYQDTIGR	Vim	P20152	P20152	43
ATXL-R2	2	1130.56	9.34E-03	1	Laminin subunit gamma-1	P02468	LGNAAADATEAK	Lamc1	P02468	P02468	15
ATXL-R2	2	901.487	7.47E-03	1	40S ribosomal protein S6	P62754	LTDTTVPTR	Rps6	P62754	P62754	79
ATXL-R2	2	1222.7	7.36E-03	1	Laminin subunit beta-1	P02469	ANLPGVIVVER	Lamb1	P02469	P02469	16
ATXL-R2	2	1501.78	7.25E-03	1	Transcription intermediary factor 1-beta	Q62318	AIGAPPAPEGETPK	Trim28	Q62318	Q62318	115
ATXL-R2	3	1205.65	7.03E-03	1	Ubiquitin-1;Ubiquitin-2	Q8R317-2;Q8F	LIVRNPPEISH	Ubqln1;Ubqln2	Q8R317-2	Q8R317-2	136
ATXL-R2	2	1160.63	6.68E-03	1	Hemoglobin subunit beta-1;Hemoglobin s	Q02088;P02081	LVVYVPTQR	Hbb-b1;Hbb-b2;	P02088	P02088	13
ATXL-R2	2	1036.52	6.68E-03	1	Laminin subunit beta-1	P02469	STEGEVIFR	Lamb1	P02469	P02469	16
ATXL-R2	2	1028.56	6.35E-03	1	Actin, cytoplasmic 2;Actin, cytoplasmic 2	P63260;P60711	QVITIGNER	Actg1;Actb;Actg	P63260	P63260	70
ATXL-R2	2	1653.8	6.28E-03	1	Actin, cytoplasmic 2;Actin, cytoplasmic 2	P63260;P60711	TVLSGGTMYPGIADR	Actg1;Actb	P63260	P63260	70
ATXL-R2	2	1028.51	6.20E-03	1	Heat shock cognate 71 kDa protein;Heat	P63017;P1662	LKINSINPDE	Hspa8;Hspa11H	P63017	P63017	86
ATXL-R2	2	1388.78	3.72E-03	1	Elongation factor 1-alpha 1;Elongation fac	P10126;P6263	QVILINHPGQISA	Eef1a1;Eef1a2	P10126	P10126	28
ATXL-R2	2	1036.57	3.57E-03	1	Laminin subunit alpha-1	P19137	HADIHKNGG	Lama1	P19137	P19137	39
ATXL-R2	2	1036.49	3.56E-03	1	Vimentin	P20152	ANYQDTIGR	Vim	P20152	P20152	43
ATXL-R2	2	1529.67	3.45E-03	1	Laminin subunit beta-1	P02469	SRDPYHETLNPD	Lamb1	P02469	P02469	16
ATXL-R2	2	865.466	3.19E-03	1	Laminin subunit alpha-1	P19137	ALLHAPTGS	Lama1	P19137	P19137	39
ATXL-R2	2	1218.62	3.00E-03	1	Calreticulin	P14211	LIVRPDNTYE	Calr	P14211	P14211	35
ATXL-R2	2	943.524	2.83E-03	1	Histone H2A.V;Histone H2A.Z;Histone H2	Q3THW5;P0C0AGLQFPVGR		H2afv;H2afz;Histi	Q3THW5;Q8CGF	Q8CGF	46,27
ATXL-R2	2	911.519	2.73E-03	1	Elongation factor 1-alpha 1;Elongation fac	P10126;P6263	GGIGTVPVGR	Eef1a1;Eef1a2	P10126	P10126	28
ATXL-R2	2	989.533	2.61E-03	1	Laminin subunit alpha-1	P19137	ISMEVGRKA	Lama1	P19137	P19137	39
ATXL-R2	2	1167.62	2.43E-03	1	Lamin-B1	P14733	ASAPATPLSPTR	Lmb1	P14733	P14733	36
ATXL-R2	3	1329.63	2.35E-03	1	Prolyl 3-hydroxylase 1	Q3V1T4-3;Q3V	FSSGGTENPHGVKA	Lepre1	Q3V1T4-3	Q3V1T4-3	107
ATXL-R2	3	1492.79	2.04E-03	1	Laminin subunit alpha-1	P19137	ANAPRPNWILER	Lama1	P19137	P19137	39
ATXL-R2	3	1318.71	1.91E-03	1	Glyceraldehyde-3-phosphate dehydrogen	P16858	LEKPAKYDDIK	Gapdh	P16858	P16858	38
ATXL-R2	2	1257.73	1.83E-03	1	Laminin subunit alpha-1	P19137	LVEHVPGRVPR	Lama1	P19137	P19137	39
ATXL-R2	2	1115.58	1.51E-03	1	60S ribosomal protein L3	P27659	IQVNGGTVAEK	Rpl3	P27659	P27659	83
ATXL-R2	2	1751.85	1.07E-03	1	Actin, cytoplasmic 2;Actin, cytoplasmic 2	P63260;P60711	INTVLSGGTMYPGIADI	Actg1;Actb	P63260	P63260	70
ATXL-R2	2	1144.61	7.09E-04	1	Laminin subunit gamma-1	P02468	IRNTIETGI	Lamc1	P02468	P02468	15
ATXL-R2	2	1109.55	6.69E-04	1	Fibrinogen alpha chain;Fibrinopeptide A;F	E9PV24-2;E9P	LSEHRPDLGS	Fga	E9PV24-2	E9PV24-2	4
ATXL-R2	2	1082.54	5.02E-04	1	Transcription intermediary factor 1-beta	Q62318	LTEGPGAEGPR	Trim28	Q62318	Q62318	115
ATXL-R2	2	1338.84	4.36E-04	1	Laminin subunit alpha-1;Laminin subunit a	P19137;Q6067	LINGRPSADPPSP	Lama1;Lama2	P19137	P19137	39
ATXL-R2	3	1257.73	3.96E-04	1	Laminin subunit alpha-1	P19137	LVEHVPGRVPR	Lama1	P19137	P19137	39
ATXL-R2	2	1130.65	3.54E-04	1	Laminin subunit alpha-1	P19137	IKKEIKVAT	Lama1	P19137	P19137	39
ATXL-R2	2	1003.55	2.67E-04	1	Laminin subunit beta-1	P02469	VITTFAPNR	Lamb1	P02469	P02469	16
ATXL-R2	3	1336.69	1.73E-04	1	Laminin subunit beta-1	P02469	LDGELDEKYYK	Lamb1	P02469	P02469	16
ATXL-R2	2	1024.8	1.49E-04	1	Elongation factor 1-alpha 1;Elongation fac	P10126;P6263	IGGIGTVPVGR	Eef1a1;Eef1a2	P10126	P10126	28
ATXL-R2	2	975.466	1.31E-04	1	Laminin subunit beta-1	P02469	IEDPVSRR	Lamb1	P02469	P02469	16
ATXL-R2	2	1189.62	1.16E-04	1	Laminin subunit beta-1	P02469	QVEVLKTDAS	Lamb1	P02469	P02469	16
ATXL-R2	3	1499.75	9.98E-05	1	Heterogeneous nuclear ribonucleoprotein	Q922X1-2;Q92	SVQRPGYDRPRTGA	Hnmpf	Q922X1-2	Q922X1-2	184
ATXL-R2	2	1280.69	6.67E-05	1	Fibrinogen beta chain;Fibrinopeptide B;F	Q8K0E8	LRPAPPISGGGY	Fgb	Q8K0E8	Q8K0E8	132
ATXL-R2	2	1232.59	5.22E-05	1	60 kDa heat shock protein, mitochondrial	P63038;P63031	VGGTSDVEVNEK	Hspd1	P63038	P63038	87
ATXL-R2	2	1212.64	4.41E-05	1	60S ribosomal protein L30	P62889	IIDPGDSIIR	Rpl30	P62889	P62889	83
ATXL-R2	3	1944.05	2.15E-05	1	Claithrin heavy chain 1	Q68FD5	LHIEVGTPTPTGNQFPFI	Ctce	Q68FD5	Q68FD5	118
ATXL-R2	2	1529.73	6.86E-06	1	Laminin subunit beta-1	P02469</					

Tabela Suplementar A.1: Identification of peptides generated by the incubation of Matrigel with ATXL and BATXH by LC-MS/MS*.

Table S1. Identification of peptides generated by the incubation of Matrigel with ATXL and BATXH by LC-MS/MS*.											
Table S1.	I Charge	Mass	PEP	MS/MS Count	Protein names	Protein IDs	Sequence	Gene names	Leading protein:	Leading razor protein	Protein group IDs
BATXH-R1	3	1590.8	9.42E-03	1	78 kDa glucose-regulated protein	P20029	LTSNPENTVDAKRF	Hspa5	P20029	P20029	42
BATXH-R1	2	1322.65	9.23E-03	1	60 kDa heat shock protein, mitochondrial	P63038;P63031	LNLEDVQAHLG	Hspd1	P63038	P63038	87
BATXH-R1	2	1160.63	7.33E-03	1	Hemoglobin subunit beta-1;Hemoglobin subunit beta-1	P02088;P02081	LVVYPWTQR	Hbb-b1;Hbb-b2	P02088	P02088	13
BATXH-R1	2	1060.49	6.57E-03	1	Heat shock protein HSP 90-alpha	P07901	HLEINPDHS	Hsp90aa1	P07901	P07901	20
BATXH-R1	2	1086.61	6.57E-03	1	40S ribosomal protein S4, X isoform	P62702	TIRYPDPLI	Rps4x	P62702	P62702	78
BATXH-R1	2	865.466	6.56E-03	1	Laminin subunit alpha-1	P19137	ALLHAPTGS	Lama1	P19137	P19137	39
BATXH-R1	2	1030.53	6.48E-03	1	Laminin subunit gamma-1	P02468	ISQDLEKQA	Lamc1	P02468	P02468	15
BATXH-R1	3	1359.71	5.91E-03	1	Glyceraldehyde-3-phosphate dehydrogenase	P16858	IFQERDPTNIK	Gapdh	P16858	P16858	38
BATXH-R1	2	1200.63	5.91E-03	1	Plasminogen;Plasmin heavy chain A;Activator	P20918	IFTPTNPRAG	Plg	P20918	P20918	45
BATXH-R1	2	1024.6	5.91E-03	1	Elongation factor 1-alpha 1;Elongation factor 1-alpha	P10126;P6263	GGIGTVPVGR	Eff1a1;Eef1a2	P10126	P10126	28
BATXH-R1	2	1090.54	5.44E-03	1	Laminin subunit alpha-1	P19137	LWDLGSGSTR	Lama1	P19137	P19137	39
BATXH-R1	2	900.503	4.96E-03	1	Actin, cytoplasmic 2;Actin, cytoplasmic 2	P63260;P60711	VITIGNER	Actg1;Actb;Actg	P63260	P63260	70
BATXH-R1	2	1451.69	4.91E-03	1	Protein disulfide-isomerase	P09103	TMIDYNGERTLDG	P4hb	P09103	P09103	24
BATXH-R1	2	1338.64	4.11E-03	1	Laminin subunit alpha-1;Laminin subunit alpha-1	P19137;Q6067	LINGRPSADDPSP	Lama1;Lama2	P19137	P19137	39
BATXH-R1	2	1066.55	3.95E-03	1	Transcription intermediary factor 1-beta	Q62318	LTEGPGAEGR	Trim28	Q62318	Q62318	115
BATXH-R1	2	1012.52	2.98E-03	1	Citrate synthase, mitochondrial	Q9CZU6	VLDPEGR	Cs	Q9CZU6	Q9CZU6	149
BATXH-R1	2	1240.62	1.73E-03	1	Nidogen-1	P10493	AGGADAQRPTLQG	Nid1	P10493	P10493	29
BATXH-R1	2	1498.87	1.07E-03	1	Laminin subunit gamma-1	P02468	LIEIASRELEKAK	Lamc1	P02468	P02468	15
BATXH-R1	2	1548.75	1.05E-03	1	Heat shock cognate 71 kDa protein;Heat shock cognate 71 kDa protein	P63017;P1662	IANDQGNRTTPSY	Hspa8;Hspa11H	P63017	P63017	86
BATXH-R1	2	1233.65	6.87E-04	1	Tubulin alpha-4A chain;Tubulin alpha-8 chain	P68368;Q9JJZ	FQTNLVYPR	Tube4a;Tube8	P68368	P68368	18
BATXH-R1	2	1166.55	6.71E-04	1	Protein disulfide-isomerase A6	Q922R8	LTDQDFKVV	Pdia6	Q922R8	Q922R8	141
BATXH-R1	2	1038.53	6.41E-04	1	Protein disulfide-isomerase	P09103	ITSNSGVFSK	P4hb	P09103	P09103	24
BATXH-R1	2	1055.54	5.61E-04	1	Nidogen-1	P10493	ADAQRPTLQG	Nid1	P10493	P10493	29
BATXH-R1	2	1210.53	4.77E-04	1	Laminin subunit gamma-1	P02468	MVTDQAFEDR	Lamc1	P02468	P02468	15
BATXH-R1	2	1004.49	4.17E-04	1	78 kDa glucose-regulated protein	P20029	VAFTPEGER	Hspa5	P20029	P20029	42
BATXH-R1	4	2039.19	3.15E-04	1	78 kDa glucose-regulated protein	P20029	VMTKLPRNTVPTKKS	Hspa5	P20029	P20029	42
BATXH-R1	3	1364.73	2.70E-04	1	Laminin subunit alpha-1	P19137	IRSQQDLVGGHR	Lama1	P19137	P19137	39
BATXH-R1	2	1339.63	7.15E-05	1	Tubulin beta-4B chain;Tubulin beta-5 chain	P68372;P9902	VISDEHIDPTGT	Tubb4b;Tubb5	P68372	P68372	90
BATXH-R1	3	1286.73	2.35E-05	1	40S ribosomal protein S3	P62908	IGPKKPLPDHVS	Rps3	P62908	P62908	84
BATXH-R1	2	1573.85	6.69E-06	1	Glyceraldehyde-3-phosphate dehydrogenase	P16858	ITIFQERDPTNIK	Gapdh	P16858	P16858	38
BATXH-R1	2	981.478	3.92E-06	1	Laminin subunit alpha-1	P19137	ANAPRPGNW	Lama1	P19137	P19137	39
BATXH-R1	2	1073.55	3.27E-07	1	78 kDa glucose-regulated protein	P20029	ITITNDQNR	Hspa5	P20029	P20029	42
BATXH-R2	3	1286.73	9.67E-03	1	40S ribosomal protein S3	P62908	IGPKKPLPDHVS	Rps3	P62908	P62908	84
BATXH-R2	2	1305.66	9.20E-03	1	Peptidyl-prolyl cis-trans isomerase FKBP	Q61576	LVSREDGLPTGY	Fkbp10	Q61576	Q61576	114
BATXH-R2	2	1160.63	9.17E-03	1	Hemoglobin subunit beta-1;Hemoglobin subunit beta-1	P02088;P02081	LVVYPWTQR	Hbb-b1;Hbb-b2	P02088	P02088	13
BATXH-R2	2	1038.53	7.25E-03	1	Protein disulfide-isomerase	P09103	ITSNSGVFSK	P4hb	P09103	P09103	24
BATXH-R2	3	1405.72	6.86E-03	1	Nesprin-2	Q6ZWQ0	LROYQNIKNL	Syne2	Q6ZWQ0	Q6ZWQ0	120
BATXH-R2	2	1004.49	6.68E-03	1	78 kDa glucose-regulated protein	P20029	VAFTPEGER	Hspa5	P20029	P20029	42
BATXH-R2	2	1083.6	6.64E-03	1	Laminin subunit alpha-1	P19137	DLDPVTRR	Lama1	P19137	P19137	39
BATXH-R2	2	1089.58	6.30E-03	1	Clathrin heavy chain 1	Q68FD5	VLESNPYR	Cltc	Q68FD5	Q68FD5	118
BATXH-R2	2	1086.61	6.13E-03	1	40S ribosomal protein S4, X isoform	P62702	TIRYPDPLI	Rps4x	P62702	P62702	78
BATXH-R2	2	1075.59	5.66E-03	1	10 kDa heat shock protein, mitochondrial	Q64433	VLLPEYGGTK	Hspe1	Q64433	Q64433	117
BATXH-R2	2	998.515	4.98E-03	1	Nidogen-1	P10493	ADAQRPTLQG	Nid1	P10493	P10493	29
BATXH-R2	3	1573.85	4.84E-03	1	Glyceraldehyde-3-phosphate dehydrogenase	P16858	ITIFQERDPTNIK	Gapdh	P16858	P16858	38
BATXH-R2	2	865.466	4.68E-03	1	Laminin subunit alpha-1	P19137	ALLHAPTGS	Lama1	P19137	P19137	39
BATXH-R2	2	1536.76	3.98E-03	1	Actin, cytoplasmic 2;Actin, cytoplasmic 2	P63260;P60711	VLSGGTTMVGAIADR	Actg1;Actb;Actg	P63260	P63260	70
BATXH-R2	3	1865.97	3.42E-03	1	Laminin subunit alpha-1	P19137	LIAGKREWDAAAGTHI	Lama1	P19137	P19137	39
BATXH-R2	2	1338.64	2.09E-03	1	Laminin subunit alpha-1;Laminin subunit alpha-1	P19137;Q6067	LINGRPSADDPSP	Lama1;Lama2	P19137	P19137	39
BATXH-R2	2	1024.6	1.53E-03	1	Elongation factor 1-alpha 1;Elongation factor 1-alpha	P10126;P6263	GGIGTVPVGR	Eff1a1;Eef1a2	P10126	P10126	28
BATXH-R2	2	1280.69	9.06E-04	1	Fibrinogen beta chain;Fibrinopeptide B;Fibrinopeptide B	Q8K0E8	LRPAPPPISSGGY	Fgb	Q8K0E8	Q8K0E8	132
BATXH-R2	2	988.571	6.81E-04	1	Histone H4	Q62806	VLENVIR	Hist1H4a	Q62806	Q62806	80
BATXH-R2	2	1211.52	6.50E-04	1	Laminin subunit beta-1	P02469	YHETLNPDHS	Lamb1	P02469	P02469	16
BATXH-R2	3	1364.73	2.70E-04	1	Laminin subunit alpha-1	P19137	IRSQQDLVGGHR	Lama1	P19137	P19137	39
BATXH-R2	2	1193.55	2.46E-04	1	Calreticulin	P14211	FLDGDAWTRN	Calr	P14211	P14211	35
BATXH-R2	3	1314.61	1.85E-04	1	Hemoglobin subunit alpha	P01942	SHHPADFTPAVH	Hba	P01942	P01942	12
BATXH-R2	2	1272.69	3.37E-05	1	Laminin subunit beta-1	P02469	LDKTVKELAEQ	Lamb1	P02469	P02469	16
BATXH-R2	2	1332.67	1.51E-06	1	Glyceraldehyde-3-phosphate dehydrogenase	P16858	ITIFQERDPTNIK	Gapdh	P16858	P16858	38
BATXH-R2	2	1090.54	5.35E-07	1	Laminin subunit alpha-1	P19137	LWDLGSGSTR	Lama1	P19137	P19137	39
BATXH-R2	3	1492.79	9.98E-08	1	Laminin subunit alpha-1	P19137	IRSQQDLVGGHRQ	Lama1	P19137	P19137	39
BATXH-R2	2	1573.85	3.35E-08	1	Glyceraldehyde-3-phosphate dehydrogenase	P16858	ITIFQERDPTNIK	Gapdh	P16858	P16858	38
BATXH-R2	3	1482.74	1.83E-09	1	Laminin subunit alpha-1	P19137	IEVHVNSGDGTSLR	Lama1	P19137	P19137	39
BATXH-R2	2	1359.71	1.48E-09	1	Glyceraldehyde-3-phosphate dehydrogenase	P16858	IFQERDPTNIK	Gapdh	P16858	P16858	38
Control-R1	3	1647.86	9.91E-03	1	40S ribosomal protein S20	P60867	DTGKTPVEVEAIHR	Rps20	P60867	P60867	71
Control-R1	3	1241.69	9.42E-03	1	Histone H2A.V;Histone H2A.Z	Q3THW5;P0CC	ATIAGGGVPIHIH	H2afv;H2afz	Q3THW5	Q3THW5	27
Control-R1	2	988.571	7.71E-03	1	Histone H4	P62806	VLENVIR	Hist1H4a	P62806	P62806	80
Control-R1	3	1248.65	7.03E-03	1	Prolyl 4-hydroxylase subunit alpha-1	Q60715-2;Q60	LLELDEPHQR	P4ha1	Q60715-2	Q60715-2	110
Control-R1	2	1038.53	6.57E-03	1	Serpin H1	P19324	VIEVTHDLQ	Serpinh1	P19324	P19324	41
Control-R1	2	1146.59	5.92E-03	1	60S ribosomal protein L18	P35980	FDQLAESPK	Rpl18	P35980	P35980	55
Control-R1	2	1779.83	5.57E-03	1	Protein disulfide-isomerase	P09103	VDATESDLAQYGVPR	P4hb	P09103	P09103	24
Control-R1	2	1269.73	5.57E-03	1	Aspartate aminotransferase, mitochondrial	P05202	IAATILTSPDLR	Got2	P05202	P05202	17
Control-R1	2	1481.67	5.30E-03	1	60S ribosomal protein L8	P62918	GVAMNPVEHPFGGG	Rpl8	P62918	P62918	85
Control-R1	2	975.466	4.96E-03	1	Laminin subunit beta-1	P02469	IEDPYSR	Lamb1	P02469	P02469	16
Control-R1	3	1380.85	4.65E-03	1	40S ribosomal protein S13	P62301	KGLTPSQIGVILR	Rps13	P62301	P62301	77
Control-R1	3	1208.63	4.16E-03	1	Laminin subunit alpha-1	P19137	IRSQQDLVGGH	Lama1	P19137	P19137	39
Control-R1	3	1777.86	3.91E-03	1	Heterogeneous nuclear ribonucleoprotein	Q922X1-2;Q92	FMSVQRPQPYDRPQT	Hnmpf	Q922X1-2	Q922X1-2	164
Control-R1	2	1182.54	3.75E-03	1	Hemoglobin subunit alpha	P01942	HFDVSHGSAQV	Hba	P01942	P01942	12
Control-R1	2	1428.71	3.45E-03	1	40S ribosomal protein S14	P62264	IEDVTPIPSDDTR	Rps14	P62264	P62264	75
Control-R1	2	1328.74	3.11E-03	1	Elongation factor 1-alpha 1	P10126	VETGVLPKPMVVT	Eff1a1	P10126	P10126	28
Control-R1	3	1373.69	2.85E-03	1	Histone H4	Q62806	VIRDAVTEYHSA	Hist1H4a	Q62806	Q62806	80
Control-R1	2	1029.54	2.83E-03	1	Tubulin beta-4B chain;Tubulin beta-5 chain	P68372;P9902	AVNMVPPFR	Tubb4b;Tubb5	P68372	P68372	90
Control-R1	2	1338.68	1.67E-03	1	Vimentin	P20152	TYSLGSLARPSTS	Vim	P20152	P20152	43
Control-R1	3	1311.71	1.51E-03	1	Laminin subunit alpha-1	P19137	DLRDLPIVTR	Lama1	P19137	P19137	39
Control-R1	2	1113.84	1.47E-03	1	Tubulin beta-4B chain;Tubulin beta-5 chain	P68372;P9902	LVDSDVLDVWR	Tubb4b;Tubb5	P68372	P68372	90
Control-R1	2	1284.74	9.54E-04	1	10 kDa heat shock protein, mitochondrial	Q64433	VLAQTAVVAVGSGGK	Hspe1	Q64433	Q64433	117
Control-R1	2	1083.6	8.64E-04	1	Laminin subunit alpha-1	P19137	DLDPVTRR	Lama1	P19137	P19137	39

Continua

Tabela Suplementar A.1: Identification of peptides generated by the incubation of Matrigel with ATXL and BATXH by LC-MS/MS*.

Table S1. Identification of peptides generated by the incubation of Matrigel with ATXL and BATXH by LC-MS/MS*.											
Table S1.	I Charge	Mass	PEP	MS/MS Count	Protein names	Protein IDs	Sequence	Gene names	Leading protein:Leading razor protein	Protein group IDs	
Control-R1	3	1599.95	8.54E-04	1	Histone H3.3,Histone H3.2,Histone H3.1	P84244,P84221	STELLIRKLPFQR	H3f3a,Hist1h3b	P84244	P84244	14
Control-R1	2	1082.64	7.63E-04	1	40S ribosomal protein S13	P62301	TPSQGVILR	Rps13	P62301	P62301	77
Control-R1	3	1627.88	7.30E-04	1	Malate dehydrogenase, mitochondrial	P08249	GLDPAVNVVPGGHA	Mdh2	P08249	P08249	23
Control-R1	2	1467.77	5.81E-04	1	Apolipoprotein A-I;Proapolipoprotein A-I	T000623	VAPLGAELQESARQ	Apoa1	Q00623	Q00623	97
Control-R1	2	1429.68	4.56E-04	1	78 kDa glucose-regulated protein	P20029	TWNQPSVQDDIK	Hspa5	P20029	P20029	42
Control-R1	2	1953.06	3.91E-04	1	Actin, cytoplasmic 2;Actin, cytoplasmic 2	P63260,P60711	VAPEEHPVLLTEAPLN	Actg1;Actb	P63260	P63260	70
Control-R1	2	1393.68	3.84E-04	1	Eukaryotic initiation factor 4A-I;Eukaryotic	P60843,P10631	GYDVIAQAQSGTGK	Eif4a1;Eif4a2	P60843	P60843	30
Control-R1	3	1364.73	3.65E-04	1	Laminin subunit alpha-1	P19137	IRSQDDVLGGHR	Lama1	P19137	P19137	39
Control-R1	4	1853.08	2.83E-04	1	40S ribosomal protein S3	P62908	IGPKPLPDHVSIVPEK	Rps3	P62908	P62908	84
Control-R1	2	1485.67	1.91E-04	1	Fibrinogen alpha chain;Fibrinopeptide A;F	E9PV24-2,E9PV	VFSEFGDSSSPATR	Fga	E9PV24-2	E9PV24-2	4
Control-R1	2	1014.57	1.24E-04	1	GTP-binding nuclear protein Ran	P62827	LVLVGGGGTGK	Ran	P62827	P62827	8
Control-R1	2	1024.6	8.85E-05	1	Elongation factor 1-alpha 1;Elongation fac	P10126,P6263	IGGITVVPVGR	Eef1a1;Eef1a2	P10126	P10126	28
Control-R1	2	1330.71	7.29E-05	1	60S ribosomal protein L18	P35980	TAVVGTVDVDR	Rpl18	P35980	P35980	55
Control-R1	3	1953.06	4.65E-05	1	Actin, cytoplasmic 2;Actin, cytoplasmic 2	P63260,P60711	VAPEEHPVLLTEAPLN	Actg1;Actb	P63260	P63260	70
Control-R1	3	1842.93	2.01E-05	1	Tubulin beta-4B chain	P68372	INVVYNEATGGKYVPR	Tubb4b	P68372	P68372	90
Control-R1	3	1433.76	3.38E-06	1	Nidogen-1	P10493	LGSPEGLDLHGR	Nid1	P10493	P10493	29
Control-R1	3	1886.96	1.25E-06	1	78 kDa glucose-regulated protein	P20029	VTHAVVTPVAFNDAQI	Hspa5	P20029	P20029	42
Control-R1	2	1528.73	1.02E-06	1	Hemoglobin subunit alpha	P01942	IGHGGAEGAEALER	Hba	P01942	P01942	12
Control-R1	2	1095.56	5.47E-07	1	Serpin H1	P19324	GVVEVTHDLQ	Serpinh1	P19324	P19324	41
Control-R1	3	1352.7	4.46E-07	1	Laminin subunit beta-1	P02469	LHTLGDNLDSR	Lamb1	P02469	P02469	16
Control-R1	2	1336.74	4.18E-08	1	Serpin H1	P19324	HLAAGLGLTEAIDK	Serpinh1	P19324	P19324	41
Control-R1	3	1968.92	2.87E-08	1	Laminin subunit alpha-1	P19137	ALLHAPTQGSYSDGQEH	Lama1	P19137	P19137	39
Control-R1	3	1806.93	2.80E-08	1	3-ketoadyl-CoA thiolase, mitochondrial	Q88W11	TNVSGGAIAGHPGGI	Acaa2	Q88W11	Q88W11	127
Control-R1	2	1199.59	7.98E-10	1	Hemoglobin subunit beta-1	P02088	VITAFNDGLNH	Hbb-b1	P02088	P02088	13
Control-R1	2	1179.61	4.33E-11	1	Histone H4	P62806	ISGLIYEETR	Hist1h4a	P62806	P62806	80
Control-R1	2	1202.64	5.23E-12	1	40S ribosomal protein S4	P14206	FAAATGATPIAGR	Rpsa	P14206	P14206	34
Control-R1	3	1528.73	1.28E-19	1	Hemoglobin subunit alpha	P01942	IGHGGAEGAEALER	Hba	P01942	P01942	12
Control-R1	2	1324.75	6.22E-20	1	Histone H4	P62806	DNIQGITKPAIR	Hist1h4a	P62806	P62806	80
Control-R1	2	1082.52	3.75E-22	1	Vimentin	P20152	FADLSEANR	Vim	P20152	P20152	43
Control-R1	3	1815.93	2.42E-26	1	Protein disulfide-isomerase A6	Q922R8	HQSLGGQYGVQGFPT	Pdia6	Q922R8	Q922R8	141
Control-R1	2	1311.71	1.30E-29	1	Laminin subunit alpha-1	P19137	DLRDLPIVTR	Lama1	P19137	P19137	39
Control-R2	3	1554.76	9.70E-03	1	Hemoglobin subunit alpha	P01942	FFHFVDSHGSAQVK	Hba	P01942	P01942	12
Control-R2	2	1165.68	9.68E-03	1	T-complex protein 1 subunit gamma	R80318	AVAQAEVLEIPR	Ct3	R80318	R80318	92
Control-R2	2	799.35	8.81E-03	1	60S ribosomal protein L14	Q9CR57	TDFDRF	Rpl14	Q9CR57	Q9CR57	148
Control-R2	2	1485.67	8.40E-03	1	Fibrinogen alpha chain;Fibrinopeptide A;F	E9PV24-2,E9PV	VFSEFGDSSSPATR	Fga	E9PV24-2	E9PV24-2	4
Control-R2	2	999.517	7.31E-03	1	60S ribosomal protein L13	P47963	TGPVMPIRN	Rpl13	P47963	P47963	62
Control-R2	2	1251.65	6.86E-03	1	Vimentin	P20152	TYSLSGALRPST	Vim	P20152	P20152	43
Control-R2	2	1478.75	6.83E-03	1	78 kDa glucose-regulated protein	P20029	VVTPAYFVNDAGR	Hspa5	P20029	P20029	42
Control-R2	2	1271.68	6.83E-03	1	Protein disulfide-isomerase A6	Q922R8	VDATVNVQLASR	Pdia6	Q922R8	Q922R8	141
Control-R2	2	911.58	6.47E-03	1	60 kDa heat shock protein, mitochondrial	P63038	VGLQVAVK	Hspd1	P63038	P63038	87
Control-R2	2	1122.46	6.36E-03	1	40S ribosomal protein S2	P25444	SPYQEFTDH	Rps2	P25444	P25444	48
Control-R2	2	958.534	6.34E-03	1	Serpin H1	P19324	LGLTEAIDK	Serpinh1	P19324	P19324	41
Control-R2	2	1146.59	5.92E-03	1	60S ribosomal protein L18	P35980	FDQLALESKP	Rpl18	P35980	P35980	55
Control-R2	2	1199.59	5.91E-03	1	Hemoglobin subunit beta-1	P02088	VITAFNDGLNH	Hbb-b1	P02088	P02088	13
Control-R2	3	1690.77	5.27E-03	1	Hemoglobin subunit alpha	P01942	TYFFHFDVSHGSAQV	Hba	P01942	P01942	12
Control-R2	3	1380.85	4.65E-03	1	40S ribosomal protein S13	P62301	KGLTPSQGVILR	Rps13	P62301	P62301	77
Control-R2	3	1340.66	4.21E-03	1	Alpha-2-HS-glycoprotein	P29699	VESASGETLHSPK	Ahsg	P29699	P29699	52
Control-R2	3	1270.66	4.12E-03	1	Calreticulin	P14211	SDFGKFLVSSGK	Calr	P14211	P14211	35
Control-R2	2	1169.61	3.62E-03	1	Laminin subunit alpha-1	P19137	DLIYVGLPHS	Lama1	P19137	P19137	39
Control-R2	2	1075.59	3.00E-03	1	10 kDa heat shock protein, mitochondrial	Q64433	VLLPEYGGTK	Hspe1	Q64433	Q64433	117
Control-R2	3	1244.65	2.89E-03	1	ATP synthase subunit alpha, mitochondrial	Q03265	SVREPMQTGK	Atp5a1	Q03265	Q03265	100
Control-R2	3	1599.95	2.81E-03	1	Histone H3.3,Histone H3.2,Histone H3.1	P84244,P84221	STELLIRKLPFQR	H3f3a,Hist1h3b	P84244	P84244	14
Control-R2	2	1214.65	2.71E-03	1	60 kDa heat shock protein, mitochondrial	P63038,P63031	NAGVQESLIVEK	Hspd1	P63038	P63038	87
Control-R2	3	1336.74	2.09E-03	1	Serpin H1	P19324	HLAAGLGLTEAIDK	Serpinh1	P19324	P19324	41
Control-R2	2	957.488	1.97E-03	1	Stress-70 protein, mitochondrial	P38647	VLENAEAGR	Hspa9	P38647	P38647	56
Control-R2	2	1338.68	1.86E-03	1	Vimentin	P20152	TYSLSGALRPST	Vim	P20152	P20152	43
Control-R2	3	1777.86	1.71E-03	1	Heterogeneous nuclear ribonucleoprotein	Q922X1-2,Q92	FMSVQRPGYDRPGT	Hnmpf	Q922X1-2	Q922X1-2	24
Control-R2	3	1343.68	1.58E-03	1	Protein disulfide-isomerase	P09103	KSNFEALAAK	P4hb	P09103	P09103	164
Control-R2	3	1627.88	1.27E-03	1	Malate dehydrogenase, mitochondrial	P08249	GLDPAVNVVPGGHA	Mdh2	P08249	P08249	23
Control-R2	3	1842.93	1.06E-03	1	Tubulin beta-4B chain	P68372	INVVYNEATGGKYVPR	Tubb4b	P68372	P68372	90
Control-R2	3	1914.89	8.72E-04	1	ATP synthase subunit beta, mitochondrial	P56480	IMDPNIVGMNEYDVARC	Atp5b	P56480	P56480	65
Control-R2	2	1001.48	7.64E-04	1	Histone H2A type 1-H;Histone H2A;J;Hist	Q8CGP6,Q8R1	IRNDEELN	Hist1h2ah,H2ajf	Q8CGP6	Q8CGP6	46
Control-R2	2	1429.68	7.00E-04	1	78 kDa glucose-regulated protein	P20029	TWNQPSVQDDIK	Hspa5	P20029	P20029	42
Control-R2	2	1246.55	6.89E-04	1	Endoplasmic reticulum resident protein 2c	P57759	FDTQYPYGEK	Erp29	P57759	P57759	67
Control-R2	3	1364.73	6.33E-04	1	Laminin subunit alpha-1	P19137	IRSQDDVLGGHR	Lama1	P19137	P19137	39
Control-R2	2	1553.76	5.83E-04	1	Vimentin	P20152	ETNLESLPLVDTHS	Vim	P20152	P20152	43
Control-R2	3	1739.91	4.61E-04	1	Phosphoglycerate kinase 1;Phosphoglyce	P09411,P0904	VSHVSTGGASLELLE	Pgk1;Pgk2	P09411	P09411	25
Control-R2	3	1352.7	2.70E-04	1	Laminin subunit beta-1	P02469	LHTLGDNLDSR	Lamb1	P02469	P02469	16
Control-R2	2	1186.67	1.24E-04	1	Endoplasmic	P08113	SILVPTSAPR	Hsp90b1	P08113	P08113	21
Control-R2	2	1327.64	9.89E-05	1	Laminin subunit alpha-1	P19137	EASAAENPPVRTS	Lama1	P19137	P19137	39
Control-R2	2	1428.71	8.87E-05	1	40S ribosomal protein S14	P62264	IEDVTPISDSTR	Rps14	P62264	P62264	75
Control-R2	2	1179.61	8.04E-05	1	Histone H4	P62806	ISGLIYEETR	Hist1h4a	P62806	P62806	80
Control-R2	2	1024.6	5.60E-05	1	Elongation factor 1-alpha 1;Elongation fac	P10126,P6263	IGGITVVPVGR	Eef1a1;Eef1a2	P10126	P10126	28
Control-R2	3	1311.71	5.29E-05	1	Laminin subunit alpha-1	P19137	DLRDLPIVTR	Lama1	P19137	P19137	39
Control-R2	3	1953.06	3.82E-05	1	Actin, cytoplasmic 2;Actin, cytoplasmic 2	P63260,P60711	VAPEEHPVLLTEAPLN	Actg1;Actb	P63260	P63260	70
Control-R2	3	1755.97	1.75E-05	1	Malate dehydrogenase, mitochondrial	P08249	GLDPAVNVVPGGHA	Mdh2	P08249	P08249	23
Control-R2	3	1886.96	3.02E-06	1	78 kDa glucose-regulated protein	P20029	VTHAVVTPVAFNDAQI	Hspa5	P20029	P20029	42
Control-R2	2	1481.67	2.81E-06	1	60S ribosomal protein L8	P62918	GVAMNPEVHPFGGHN	Rpl8	P62918	P62918	85
Control-R2	3	1815.93	1.31E-06	1	Protein disulfide-isomerase A6	Q922R8	HQSLGGQYGVQGFPT	Pdia6	Q922R8	Q922R8	141
Control-R2	2	1038.51	6.23E-07	1	Histone H2B type 1-P;Histone H2B type	Q8CGP2,Q8CF	VUNDFIR	Hist1h2bp,Hist11	Q8CGP2	Q8CGP2	31
Control-R2	2	1328.74	1.39E-07	1	Elongation factor 1-alpha 1	P10126	VETGLVKPMGVVT	Eef1a1	P10126	P10126	28
Control-R2	2	1330.71	1.15E-07	1	60S ribosomal protein L18	P35980	TAVVGTVDVDR	Rpl18	P35980	P35980	55
Control-R2	2	1311.71	2.21E-08	1	Laminin subunit alpha-1	P19137	DLRDLPIVTR	Lama1	P19137	P19137	39
Control-R2	2	1509.83	2.14E-09	1	60S ribosomal protein L13	P47963	LATQLTGPVMPIRN	Rpl13	P47963	P47963	62
Control-R2	2	1343.71	1.79E-09	1	60 kDa heat shock protein, mitochondrial	P63038	TVIIQSWGSPK	Hspd1	P63038	P63038	87
Control-R2	2	1284.74	1.38E-09	1	10 kDa heat shock protein, mitochondrial	Q64433	VLOATVAVVGGGK	Hspe1	Q64433	Q64433	117
Control-R2	2	1779.83	5.81E-10	1	Protein disulfide-isomerase	P09103	VDATVNVQLASR	Pdia6	P09103	P09103	24
Control-R2	2	1114.56	3.95E-10	1	Vimentin;Desmin	P20152,P3100	VELQELNDR	Vim;Des	P20152	P20152	43
Control-R2	2	1324.75	2.18E-10	1	Histone H4	P62806	DNIQGITKPAIR	Hist1h4a	P62806	P62806	

Tabela Suplementar A.2: Proteins present in Matrigel and identified as cleaved by ATXL and BATXH by LC-MS/MS*.

Table S2. Proteins present in Matrigel and identified as cleaved by ATXL and BATXH by LC-MS/MS*.

Protein names	Protein ID	Peptide Sequences	MS/MS Count								Identification/Sample			
			ATXL-R1	ATXL-R2	BATXH-R1	BATXH-R2	Control-R1	Control-R2	ATXL-R1	ATXL-R2	BATXH-R1	BATXH-R2	Control-R1	Control-R2
10 kDa heat shock protein, mitochondrial	Q64433	VLLPEYGGTK	0	0	0	1	0	1	-	-	-	+	-	+
3-ketoadipyl-CoA thioesterase, mitochondrial	Q8BW71	VLSQTYVAAGSGGK	0	0	0	0	1	1	-	-	-	-	+	+
40S ribosomal protein S13	P82301	TWSSGAAALGHPGGSSGR	0	0	0	0	1	0	-	-	-	-	+	+
40S ribosomal protein S14	P82284	KGLYFSQIVLIR	0	0	0	0	1	1	-	-	-	-	+	+
40S ribosomal protein S2	P25444	TPSQIVLIR	0	0	0	0	1	0	-	-	-	-	+	+
40S ribosomal protein S20	P60887	EDVTPFISOSTR	0	0	0	0	1	1	-	-	-	-	+	+
40S ribosomal protein S3	P62908	SPYQEFTH	0	0	0	0	0	1	-	-	-	-	-	+
40S ribosomal protein S4, X isoform	P14206	DTAKTPEFEVAIHR	0	0	0	0	1	0	-	-	-	-	-	+
40S ribosomal protein S5	P97461	IGPKKLPDHSVIEPK	0	0	1	1	0	0	-	-	-	+	+	-
40S ribosomal protein S6	P82754	TIRYDPLI	0	0	1	1	0	0	-	-	-	+	+	-
40S ribosomal protein S4	P14206	ATPVAETPDIK	1	0	0	0	0	0	+	-	-	-	-	-
		LDTVPR	0	1	0	0	0	0	-	-	+	-	-	-
		FAAATGATPIAGR	0	0	0	0	1	0	-	-	-	-	-	+
		TVIEQSWGSPK	0	0	0	0	0	1	-	-	-	-	-	+
		VGLQVAVK	0	0	0	0	0	1	-	-	-	-	-	+
		LNLEDVQHDLG	0	0	1	0	0	0	-	-	-	+	-	-
		NAGVGSLSVEK	0	0	0	0	0	1	-	-	-	-	-	+
		VGGTSDVLENK	1	1	0	0	0	0	+	+	-	-	-	-
		LATLDTGPIPIRN	0	0	0	0	0	1	-	-	-	-	-	+
		TGPIPIRN	0	0	0	0	0	1	-	-	-	-	-	+
		IDVIDQNR	0	0	0	0	0	0	-	-	-	-	-	-
		TDPRF	0	0	0	0	0	1	-	-	-	-	-	+
		FQDALESPPK	0	0	0	0	1	1	-	-	-	-	-	+
		TAIVYGVTDVDR	1	0	0	0	1	1	+	-	-	-	-	+
		IQWNGTVAEK	0	1	0	0	0	0	-	-	+	-	-	-
		IDPGDSDIR	1	1	0	0	0	0	+	+	-	-	-	-
		GVAMINVEVFFGGGN	0	0	0	0	1	1	-	-	-	-	-	+
		ITRDQNR	0	0	1	0	0	0	-	-	+	-	-	-
		KLIPNIVPTKKS	1	0	0	0	0	0	+	-	-	-	-	-
		LIGRTWNPFSVQGD	0	0	0	0	0	0	-	-	-	-	-	-
		LTSNPENTVFAK	0	0	1	0	0	0	-	-	-	+	-	-
		TWNPDSVQDK	0	0	0	0	1	1	-	-	-	-	-	+
		VAFTRER	0	0	1	1	0	0	-	-	+	-	-	-
		VMTKLIPNIVPTKKSQ	0	0	1	0	0	0	-	-	-	+	-	-
		VTHAVTVPAYFNAQDR	0	0	0	0	1	1	-	-	-	-	-	+
		VWATNGDTHLGGDFDQR	0	0	0	0	0	0	-	-	-	-	-	-
		VTVFVAFNAQDR	0	0	0	0	0	1	-	-	-	-	-	+
		IVTWIDQMK	0	0	0	0	0	0	-	-	-	-	-	-
		NTVLSGGTMYPGIADR	0	1	0	0	0	0	-	-	-	+	-	-
		TVLSGGTMYPGIADR	2	2	0	0	0	0	+	+	-	-	-	-
		VAFPEEHLLEAPLNP	0	0	0	0	2	1	-	-	-	-	-	+
		VLSGGTMYPGIADR	0	0	0	1	0	0	-	-	-	-	+	-
		FAGDAPRK	0	0	0	0	0	0	-	-	-	-	-	-
		LAGRDLDY	0	0	0	0	0	0	-	-	-	-	-	-
		QVITIGNER	1	1	0	0	0	0	+	+	-	-	-	-
		VITIGNER	0	0	1	0	0	0	-	-	-	+	-	-
		VESASGETLHSPK	0	0	0	0	0	1	-	-	-	-	-	+
		VAKDAGLGSARQ	0	0	0	0	1	0	-	-	-	-	-	+
		IAATLTSPLR	0	0	0	0	1	0	-	-	-	-	-	+
		LGNADIGKPIGS	1	0	0	0	0	0	+	-	-	-	-	-
		SVREPMQTGIK	0	0	0	0	0	1	-	-	-	-	-	+
		MDPNVGEHYDIARG	0	0	0	0	0	1	-	-	-	-	-	+
		VVHIEDGTTIKY	0	0	0	0	0	0	-	-	-	-	-	-
		LIRWVSAQDGA	0	0	0	0	0	0	-	-	-	-	-	-
		FLDGGAWIHR	0	0	0	1	0	0	-	-	-	-	+	-
		LIVRPDNTYE	0	1	0	0	0	0	-	-	-	+	-	-
		LIVRPDNTYEK	1	0	0	0	0	0	+	-	-	-	-	-
		SDRQKPLVLSGK	0	0	0	0	0	1	-	-	-	-	-	+
		VLDPSGDR	0	0	1	0	0	0	-	-	-	+	-	-
		IEVGTPTGQPFPPK	0	0	0	0	0	0	-	-	-	-	-	-
		LHIEVGTPTGQPFPPK	0	1	0	0	0	0	-	-	-	+	-	-
		VLLSNPPIR	0	0	0	1	0	0	-	-	-	-	+	-
		LWVINEEDH	0	0	0	0	0	0	-	-	-	-	-	-
		VGGVDFVSNADR	0	0	0	0	0	0	-	-	-	-	-	-
		ADSTQVDTK	0	0	0	0	0	0	-	-	-	-	-	-
		FSDVPLGR	0	0	0	0	0	0	-	-	-	-	-	-
		VETGVLKPGMVAIT	0	0	0	0	1	1	-	-	-	-	-	+
		GGGTVPVGR	0	1	0	0	0	0	-	-	-	+	-	-
		IGSISTVPIGR	0	1	1	1	1	1	-	-	-	+	-	+
		QVILNHPGQISA	0	1	0	0	0	0	-	-	-	+	-	+
		THINIVGIH	0	0	0	0	0	0	-	-	-	-	-	-
		VILLNHPGQISA	1	0	0	0	0	0	+	-	-	-	-	-
		FDTQVPYGEK	0	0	0	0	0	1	-	-	-	-	-	+
		SILVYTSAPR	0	0	0	0	0	1	-	-	-	-	-	+
		GYDVIQAAGSGTGK	0	0	0	0	1	0	-	-	-	-	-	+
		LSERHPDLSG	0	1	0	0	0	0	-	-	-	+	-	-
		VFSEFGDSSSPATR	0	0	0	0	0	1	-	-	-	-	-	+
		LRAPPFISGGY	1	1	0	1	0	0	+	+	-	-	-	-
		AIQVYVYVNDQPPVFGM	0	0	0	0	0	0	-	-	-	-	-	-
		HSSFDAGAGIA	1	1	0	0	0	0	+	+	-	-	-	-
		IFQERDPTNIK	0	0	1	1	0	0	-	-	-	+	+	-
		ITFQERDPTN	0	0	0	1	0	0	-	-	-	+	+	-
		ITFQERDPTNIK	0	0	1	2	0	0	-	-	-	+	+	-
		LENPAKTDK	0	1	0	0	0	0	-	-	-	+	-	-
		RVISAPSADAP	0	0	0	0	0	0	-	-	-	-	-	-
		LVLVGGDGTGK	0	0	0	0	1	0	-	-	-	-	-	+
		NQVAMNPTVFDKAR	0	0	0	0	0	0	-	-	-	-	-	-
		VAMNPTVFDKAR	0	0	0	0	0	0	-	-	-	-	-	-
		IAKQDQRTTPTSY	0	0	1	0	0	0	-	-	-	+	-	-
		IAKQDQRTTPTSYVA	1	0	0	0	0	0	+	-	-	-	-	-
		LKNSNPDE	0	1	0	0	0	0	-	-	-	+	-	-
		HLEINPDHS	0	0	1	0	0	0	-	-	-	+	-	-
		FHFDFVSHGSAQVK	0	0	0	0	0	1	-	-	-	-	-	+
		HFDVSHGSAQV	0	0	0	0	1	0	-	-	-	-	-	+
		IGGHAEGVGAELER	0	0	0	0	2	0	-	-	-	-	-	+
		SHPADFPAVH	0	0	0	1	0	0	-	-	-	-	+	-
		TYFPHFDVSHGSAQV	0	0	0	0	0	1	-	-	-	-	-	+
		VITAFNDGLNH	0	0	0	0	1	1	-	-	-	-	-	+
		LVVYVITQR	0	1	1	1	0	0	-	-	-	+	+	-
		FMSVDRPGPYDRPGTA	0	0	0	0	1	1	-	-	-	-	-	+
		ITLPIVDEPK	0	0	0	0	0	0	-	-	-	-	-	-
		SVQRPGPYDRPGTA	1	1	0	0	0	0	+	+	-	-	-	-
		VQRPGPYDRPGTA	1	1	0	0	0	1	+	+	-	-	-	+
		FFSPLPVRVH	0	0	0	0	0	0	-	-	-	-	-	-
		VHIEGPDGR	0	0	0	0	0	0	-	-	-	-	-	-

